

# An Expert-based Approach for Grid Peak Demand Curtailment using HVAC Thermostat Setpoint Interventions in Commercial Buildings

**Sneharaj Ramdasalli**

Dissertation submitted to the Faculty of Virginia Polytechnic Institute and State University in partial fulfillment of the requirements for the degree of

**Doctor of Philosophy**

**in**

**Electrical Engineering**

**7th May 2021**

**Arlington, VA**

Saifur Rahman  
Jaime De La Reelopez  
Manisa Pipattanasomporn  
Steve Southward  
Guoqiang Yu

***Keywords:*** Building energy modeling, Commercial buildings, Expert opinion, HVAC thermostat setpoint intervention, Peak demand reduction

© 2021 Sneharaj Ramdasalli  
All Rights Reserved

# An Expert-based Approach for Grid Peak Demand Curtailment using HVAC Thermostat Setpoint Interventions in Commercial Buildings

**Sneharaj Ramdaspathi**

## Abstract

This dissertation explores the idea of inducing grid peak demand curtailment by turning commercial buildings into interactive assets for building owners during the demand control period. The work presented here is useful for both *ab initio* design of new sites and for existing or retrofitted sites.

An analytical hierarchy process (AHP)-based framework is developed to curtail the thermal load effectively across a group of commercial buildings. It gives an insight into the amount of peak demand reduction possible for each building, subject to indoor thermal comfort constraints as per ASHRAE standards. Furthermore, the detailed operation of buildings in communion with the electric grid is illustrated through case studies. This analysis forms an outline for the assessment of transactive energy opportunities for commercial buildings in distribution system operations and lays the foundation for a seamless building-to-grid integration framework.

The contribution of this dissertation is fourfold – (a) an efficient method of developing high-fidelity physics-based building energy models for understanding the realistic operation of commercial buildings, (b) identification of minimal dataset to achieve a target accuracy for the building energy models (c) quantification of building peak demand reduction potential and corresponding energy savings across a stipulated range of thermostat setpoint temperatures and (d) AHP-based demand curtailment scheme.

By careful modeling, it is shown that commercial building models developed using this methodology are both accurate and robust. As a result, the proposed approach can be extended to other commercial buildings of diverse characteristics, independent of the location. The methodology presented here takes a holistic approach towards building energy modeling by accounting for several building parameters and interactions between them. In addition, parametric analysis is done to identify a useful minimal dataset required to achieve a specified accuracy for the building energy models. This thesis describes the concept of commercial buildings as interactive assets in a transactive grid environment and the idea behind its working.

# An Expert-based Approach for Grid Peak Demand Curtailment using HVAC Thermostat Setpoint Interventions in Commercial Buildings

**Sneharaj Ramdasalli**

## General Audience Abstract

This dissertation titled “**An Expert-based Approach for Grid Peak Demand Curtailment using HVAC Thermostat Setpoint Interventions in Commercial Buildings**” tackles two important challenges in the energy management domain: – electric grid peak demand curtailment and energy savings in commercial buildings.

The distinguishing feature of the proposed solution lies in addressing these challenges solely through demand-side management (DSM) strategies, which include HVAC thermostat setpoint interventions and lighting control. We present a methodology for developing highly accurate building energy models that serve as digital twins of actual buildings. These digital replicas can be used to quantify the impact of various interventions and reflect the realistic operation of commercial buildings across varied conditions. This enables building owners to control demand intelligently and transact energy effectively in the electricity market.

The development of Internet of Things (IoT) market and advanced technologies such as smart meters and smart thermostats allows for the design of novel strategies that address traditional challenges faced by electric grid operators. This dissertation elaborates on how smart buildings can leverage IoT-based solutions to participate in the electricity market during demand control periods. We also developed an expert opinion-based demand curtailment allocation scheme resulting in grid peak demand reduction. The numerical results obtained reinforce the effectiveness of the proposed solution across varied climatic conditions.

## *Dedication*

With great reverence, I cordially dedicate this dissertation to

**Dr. Ashok Jhunjhunwala,**

for demonstrating by example, the sincerity and seriousness required in performing one's duties diligently and teaching me how to stick one's neck out for the right reasons, regardless.

## Acknowledgments

### **“It takes a village to raise a child and it takes the whole world to support a Ph.D. student”**

I am honored and humbled by the incredible support I have received on this journey towards developing new technologies in building energy management.

I would like to express my foremost gratitude to Dr. Saifur Rahman, my thesis advisor. I thank him for accepting me as his student and taking me under his wing. Without his unparalleled generosity and unconditional support, this work would have not seen the light of day. I am forever grateful for the pains he took in teaching me modeling and encouraging me to think independently. I would like to express my heartfelt thanks to my defense committee - Dr. Jaime De La Ree, Dr. Manisa Pipattanasomporn, Dr. Steve Southward and Dr. Guoqiang Yu, whose thoughtful suggestions at various stages strengthened the fabric of my dissertation.

The kind words of Dr. Paul Torgersen, Dr. Arun Phadke, Dr. Jaime De La Ree, Dr. Fred C. Lee, and Dr. Virgilio Centeno, during my initial years of stay at Blacksburg, VA, set the tone for the rest of my journey at the Virginia Tech Research Center in Arlington, VA. Blacksburg held the fantastic camaraderie of the Power Engineering and CPES lab student groups and fun-filled experiences like game nights, football games, the ever-active drill field, and more. Gargi Singh, Virginia, Neelima Chavali, Sai Dhiraj Amuru, Apoorva Garg, Chetan Mishra, Sharad Bagri, Nidhi Haryani, Vaishnavi Srinivasaraghavan, Diana Devine Stebner, Hema Retty, Kanika Saini, Anna Moorman, Margaret Appleby, and the Huehns (Lorraine, Barry, Scott, and Andrew) made my stay in Blacksburg extra special.

The Advanced Research Institute (ARI) at VT-Arlington provided a stimulating environment where I met many wonderful people who helped shape my thesis and Ph.D. journey in a unique way. Over the years, Dr. Manisa’s guidance has been invaluable. Dr. Murat Kuzlu has been of great support during my time at ARI. I would like to thank Mr. Yonael Teklu for always being there and watching out for me. Ganchimeg Darambazar made the administrative processes smooth and easy to handle. I thank Dr. Kenneth Wong for his leadership, spirit, and enthusiasm in making graduation so special, especially during such testing times. I would also like to thank Susan Merten and the graduate student association (GSA) for tying us into a close-knit VT-NoVA community. My colleagues at ARI – Shibani, Avijit, Fakeha, Hamideh, Waradom, Desong, Kruthika, Rajendra, Mengmeng, Xiangyu, Abdullah, Massoud, Musaed, Aditya, Zejia, Ashraf, and Nazmul have turned out to be extremely valuable friends. The regular visits by Suha and Zafy added much-needed innocence, fun, and frolic to our lab environment. Similarly, thanks to Lulu Chen and all my friends from St. Ann’s and IITM for having my back through thick and thin. I would also like to thank Alugubelly Deepa Reddy for being such an understanding and caring roommate.

I am forever grateful to Professor Ashok Jhunjunwala, my masters thesis guide at the Indian Institute of Technology, Madras (IITM), for taking me under his wing and eventually

inspiring me to pursue my Ph.D. He ignited a spark and fanned the flames, allowing me to develop a lifelong passion for problem-solving and fabricating solutions using Electrical Engineering tools. I consider it a great honor and a matter of privilege to be associated with him. It was a great pleasure working together with Dr. Bhaskar Ramamurthi, the Director of IIT Madras. His ability to provide analytical insights was awe-inspiring. I am indebted to Professor Shanthi Pavan of IITM for evoking my interest in Electrical Engineering via “Analog circuits course and lab”. He explained the importance of investing time in strengthening fundamental concepts and the value and thrill of pursuing an advanced degree in Electrical Engineering. My thanks also go out to Dr. Shanthi Swarup, Dr. K. Sridharan, and Dr. R. Sarathi for their timely support and inspiring words as I transitioned from IIT Madras to Virginia Tech.

I would like to thank my mentor at NREL - Dr. Yingchen Zhang (YC), for his immense faith in me, his incredible support, and valuable advice. Dr. Ben Kroposki was a great support in polishing my work and its presentation during my time at NREL. ESTA International provided me with an opportunity to use my knowledge and skills in designing new data-driven models for Staten Island, NY. Here, I have cherished my time with Mr. Nader Farah and Mrs. Elizabeth Farah, who have nurtured me and helped me get organized across multiple facets. This served as a great opportunity to transition from school into a work environment.

Some incredible angels came forward to support me during the last leg of my Ph.D. journey. Without their timely support, this dissertation work would not have taken shape. I would like to thank Pratyusha Naraparaju for helping me out with Chapter 5 simulations, through long sleepless nights. Jennifer Lawrence, the Director of Writing Center, supported me with her fantastic team of coaches. Together we have invested over 1000 hours in debating, crafting, and polishing every aspect of this dissertation work. It has been a joy working with Madison Storm, Amelia Gay, Aparaj Manuja, Matthew Scopa, Nathan Dragon, Justin Laiti, Mackenzie Williams, Kara Rush, Audrey McGovern, Claire Knowles, Erika Carlson, Katie Grandinetti, Meg Lord, and Brandon Nguyen. My special thanks go to Micheal J. Stamper for helping with the vector illustrated graphics in this dissertation. While I crafted each word in silence, I had a team of angels watch over me. Some of the names include Roxanne Paul, Afroze Mohammed, Kelly McPherson, Tracie Hase, Jessica Mullins, Kristin Sorensen, Mr. Phillip Hernandez de Wright, and Dr. Joseph Simpson. These people offered unconditional support in their own ways toward the end of my Ph.D. experience, something I will forever be grateful for.

At the base of all my work is my family, especially my parents - Mr. Sham Raj Ramdaspathi and Mrs. Sridevi Ramdaspathi, whose loving support, unfathomable sacrifices, and immense faith in my conviction helped me move from strength to strength. Without your loving support, this would have been an impossible feat to achieve. Special thanks to Sreshta Raj Ramdaspathi, who offered the matchless support and understanding only a sister could provide; you are the loveliest present I have ever received, and I am never complete without you. I thank my family for being so understanding and helping me focus on my research during testing times. Above all, I thank God for being the ever-watchful silent senior partner, always showering blessings.

# Table of Contents

<b>1. INTRODUCTION AND THESIS OVERVIEW</b>	
1.1 Background and motivation	1
1.2 Objective and scope of work	3
1.3 Contribution to Building-to-Grid integration research area	4
1.4 Intellectual merit	5
1.5 Hypothesis	6
1.6 Nature of the problem and solution	6
1.7 Broader impacts	9
<b>2. LITERATURE REVIEW</b>	11
2.1 Problem statement	11
2.1.1 Peak demand	11
2.1.1.1 Coincidental peak demand/Grid peak demand	12
2.1.1.2 Non-coincidental peak demand/Building peak demand	12
2.1.2 Automated demand response	12
2.2 Approach	13
2.3 Introduction	14
2.4 Building energy models	16
2.4.1 Building energy modeling - calibration	18
2.5 Model predictive control (MPC)	19
2.6 Demand response (DR)	21
2.7 HVAC thermostat setpoint interventions - thermal modeling/energy flexibility	23
2.8 Peak demand reduction	24
2.9 Energy savings	26
2.10 Demand charge reduction	26
2.11 Analytical Hierarchy Process (AHP): Uses and role in peak demand curtailment applications	28
2.12 Summary	29
<b>3. BUILDING ENERGY MODELING: High Fidelity Models vs Reduced Order Models</b>	
3.1 Modeling commercial buildings in eQUEST	32
3.1.1 Dataset description and model assumptions	35
3.1.2 Building model development	37
3.1.3 Initial building model development	
3.2 The developed eQUEST building model	38

3.3 Model calibration procedure	47
3.4 Model validation	49
3.5 Sensitivity analysis – thermostat setpoint temperature	52
3.6 Reduced order building energy model - minimal dataset model for optimal accuracy	53
<b>4. PEAK DEMAND REDUCTION AND ENERGY SAVINGS USING HVAC THERMOSTAT SETPOINT INTERVENTION</b>	
4.1 Peak demand reduction potential across buildings due to thermostat setpoint interventions	58
4.1.1 Method for thermostat setpoint interventions	59
4.1.2 Calculation of peak demand reduction potential	59
4.1.3 Analysis of peak demand reduction potentials	60
4.1.4 Correlation between peak demand reduction and outdoor temperature across buildings	61
4.1.5 Correlation between peak demand reduction and HVAC-to-Building peak load ratio	62
4.2 Energy savings across buildings due to thermostat setpoint interventions	66
4.2.1 Method for thermostat setpoint interventions	66
4.2.2 Calculation of energy savings potential	66
4.2.3 Analysis of energy savings potential	67
4.2.4 Correlation between energy savings and outdoor temperature across buildings	67
4.2.5 Correlation between average energy savings and HVAC-to-Building peak load ratio	69
4.2.6 Correlation between maximum energy savings and HVAC-to-Building peak load ratio	72
<b>5. AHP-BASED PEAK DEMAND CURTAILMENT ALLOCATION USING HVAC THERMOSTAT SETPOINT INTERVENTIONS</b>	
5.1 Introduction	
5.2 Literature review: Uniqueness of the proposed AHP-based approach	75
5.3 Methodology and model description	
5.3.1 Overall methodology:	84
5.3.2 Methodology of AHP:	86
5.3.2.1 Description of AHP model	86
5.3.2.2 AHP model: inputs and outputs	86
5.3.2.2.1 Inputs	87
5.3.2.2.2 Outputs	87
5.3.2.2.3 AHP process flow: pairwise comparisons and priority vector computations	87
5.3.2.3 Pairwise comparison matrices at each level of the AHP structure in Fig. 21	88

5.3.2.3.1 Level 1 - Pairwise comparison matrix of expert opinions with respect to demand curtailment allocation (overall goal)	88
5.3.2.3.2 Level 2 - Pairwise comparison matrix of the sub-goals with respect to experts	89
5.3.2.3.3 Level 3 - Pairwise comparison matrix of the attributes with respect to each sub-goal:	90
5.3.2.3.4 Level 4 - Pairwise comparison matrix of the alternatives with respect to each attribute:	93
5.3.2.4 Normalized Eigenvectors at each level of the AHP structure in Fig. 21	97
5.3.2.4.1 Level 1 - Normalized Eigenvectors showing weightage of expert opinions:	97
5.3.2.4.2 Level 2 - Normalized Eigenvectors showing weightage of each sub-goal with respect to expert opinions:	98
5.3.2.4.3 Level 3 - Normalized Eigenvectors showing weightage of each attribute with respect to different sub-goals:	99
5.3.2.4.4 Level 4 - Normalized Eigenvectors showing weightage of each alternative with respect to different alternatives:	
5.4 Case studies	102
5.5 Results and discussion	103
5.6 Conclusion	110
<b>6. RESULTS AND DISCUSSION</b>	111
6.1 Key results	112
6.1.1 Expert-based grid peak demand curtailment scheme: results and discussion	113
6.1.2 Building energy modeling results - CH3	114
6.1.3 Peak demand reduction and energy savings results - CH4	
<b>7. CONCLUSION AND FUTURE WORK</b>	
7.1 Conclusion	116
7.2 Future Work	118
<b>REFERENCES</b>	120

# List of Figures

FIG. 1. OVERVIEW OF GRID-CONNECTED BUILDINGS AT DISTRIBUTION LEVEL .....	3
FIG. 2. INPUT DATA SOURCES FOR THE AHP-BASED MODEL .....	7
FIG. 3. BUILDING PEAK DEMAND REDUCTION THROUGH DEMAND RESPONSE.....	13
FIG. 4. VIRGINIA TECH SCHOOL OF PUBLIC AND INTERNATIONAL AFFAIRS BUILDING, 1021 PRINCE ST, ALEXANDRIA, VA .....	33
FIG. 5. BLOCK DIAGRAM OF MODELING PROCEDURE USING EQUEST.....	34
FIG. 6. MODEL OF THE THREE-STORY VIRGINIA TECH SCHOOL OF PUBLIC AND INTERNATIONAL AFFAIRS BUILDING .....	39
FIG. 7. HOURLY SCHEDULE OF OCCUPANTS, LIGHTS, AND EQUIPMENT IN THE BUILDING.....	48
FIG. 8. ACTUAL AND SIMULATED HOURLY BUILDING LOAD (KW) FOR A WEEK.....	49
FIG. 9. ACTUAL AND SIMULATED MONTHLY BUILDING ELECTRICITY CONSUMPTION (MWH) .....	50
FIG. 10. ACTUAL AND SIMULATED HOURLY BUILDING LOAD (KW) FROM JUNE 1, 2017 TO SEPTEMBER 30, 2017 .....	51
FIG. 11. EQUEST BUILDING ENERGY MODELS OF THE SELECTED FIVE COMMERCIAL BUILDINGS .....	57
FIG. 12. OVERALL SCHEME FOR ESTIMATION OF PEAK DEMAND REDUCTION AND ENERGY SAVINGS IN COMMERCIAL BUILDINGS USING EQUEST SOFTWARE .....	58
FIG. 13. PEAK DEMAND REDUCTION ( $\Delta PRDR\%$ ) VS. AVERAGE OUTDOOR TEMPERATURE ( $^{\circ}F$ ) DURING DR PERIOD .....	61
FIG. 14. PEAK DEMAND REDUCTION ( $\Delta PRDR\%$ ) VS. HVAC-TO-BUILDING PEAK LOAD RATIO ACROSS ALL BUILDINGS FOR $5^{\circ}F$ SETPOINT INTERVENTION .....	64
FIG. 15. DAILY LOAD PROFILES OF TWO BUILDINGS WITH DIFFERENT HVAC-TO-BUILDING PEAK LOAD RATIOS ON MAXIMUM PEAK REDUCTION DAYS.....	65
FIG. 16. ENERGY SAVINGS % DUE TO HVAC INTERVENTIONS VS AVERAGE DAILY OUTDOOR TEMPERATURE DURING DR PERIOD .....	68
FIG. 17. AVERAGE ANNUAL ENERGY SAVINGS % VS HVAC-TO-BUILDING PEAK LOAD RATIO ACROSS ALL BUILDINGS FOR $5^{\circ}F$ SETPOINT INTERVENTION .....	70
FIG. 18. LOAD PROFILE OF THE MID-RISE OFFICE BUILDING WITH THERMOSTAT SETPOINT INCREMENTS ON TWO DAYS WITH DIFFERENT OUTDOOR TEMPERATURE CONDITIONS .....	71
FIG. 19. MAXIMUM ENERGY SAVINGS % VS HVAC-TO-BUILDING PEAK LOAD RATIO ACROSS ALL BUILDINGS FOR $5^{\circ}F$ SETPOINT INTERVENTIONS .....	72
FIG. 20. DAILY LOAD PROFILES OF TWO BUILDINGS (STRIP MALL AND MID-RISE OFFICE) WITH DIFFERENT HVAC-TO-BUILDING PEAK LOAD RATIOS DURING RESPECTIVE MAXIMUM ENERGY SAVING DAYS .....	73
FIG. 21. OVERALL OPERATION OF THE AHP-BASED HVAC SETPOINT INTERVENTION SCHEME .....	79
FIG. 22. COMMUNICATION SCHEME FOR THE AHP-BASED DEMAND CURTAILMENT TOOL IN A DAY-AHEAD ELECTRICITY MARKET .....	80
FIG. 23. FLOWCHART ILLUSTRATING THE TWO STEP AHP-BASED DEMAND CURTAILMENT ALGORITHM.....	83
FIG. 24. BLOCK DIAGRAM OF AHP-BASED DEMAND CURTAILMENT PROCEDURE AMONG COMMERCIAL BUILDINGS .....	85
FIG. 25. FOUR-LEVEL HIERARCHICAL AHP STRUCTURE FOR GRID PEAK DEMAND CURTAILMENT.....	86
FIG. 26. PERCENTAGE OF CONTRIBUTION TO SELECTED ELECTRIC GRID PEAK DEMAND CURTAILMENT REQUESTS (100 - 400 KW) .....	107
FIG. 27. INDIVIDUAL DEMAND CURTAILMENT AMOUNT (KW) FOR EACH COMMERCIAL BUILDING.....	108
FIG. 28. MAXIMUM INDOOR TEMPERATURE IN EACH BUILDING ( $^{\circ}F$ ) FOR VARIOUS LEVELS OF DEMAND CURTAILMENT REQUEST.....	109

## List of Tables

TABLE I. DETAILS OF MEDIUM SIZED OFFICE BUILDING	35
TABLE II COEFFICIENTS FOR DEFAULT PERFORMANCE CURVES IN EQUEST	46
TABLE III MONTHLY ENERGY CONSUMPTION OF THE BUILDING DURING SUMMER MONTHS	50
TABLE IV MODELED BUILDING LOAD ERROR	52
TABLE V ACCURACY OF THE BUILDING LOAD MODEL W.R.T. INITIAL HVAC THERMOSTAT SETPOINT TEMPERATURE	52
TABLE VI INFLUENTIAL HVAC AND BUILDING PARAMETERS	54
TABLE VII INPUT DATASET DESCRIPTION – OVERALL BUILDINGS PORTFOLIO	56
TABLE VIII AVERAGE PEAK DEMAND REDUCTION ( $\Delta PR_{DR\%}$ ) ACROSS BUILDINGS AS A RESULT OF THERMOSTAT SETPOINT INTERVENTION	63
TABLE IX AVERAGE ENERGY SAVINGS AS A RESULT OF THERMOSTAT SETPOINT INTERVENTIONS ACROSS ALL BUILDINGS	69
TABLE X AHP SCALE OF PREFERENCE BETWEEN TWO ELEMENTS	88
TABLE XI PAIRWISE COMPARISON MATRIX OF EXPERT OPINIONS	88
TABLE XII PAIRWISE COMPARISON MATRIX OF THE SUB-GOALS WITH RESPECT TO CUSTOMER RELATIONS DEPARTMENT	89
TABLE XIII PAIRWISE COMPARISON MATRIX OF THE SUB-GOALS WITH RESPECT TO SYSTEM OPERATOR	89
TABLE XIV MAXIMIZING ENERGY SAVINGS – PAIRWISE COMPARISON OF ATTRIBUTES	90
TABLE XV MINIMIZING DEMAND CHARGE – PAIRWISE COMPARISON OF ATTRIBUTES	91
TABLE XVI MINIMIZING DISCOMFORT – PAIRWISE COMPARISON OF ATTRIBUTES	92
TABLE XVII AVOID DEMAND RESTRIKE – PAIRWISE COMPARISON OF ATTRIBUTES	93
TABLE XVIII PAIRWISE COMPARISON MATRIX OF BUILDINGS WITH RESPECT TO OCCUPANCY	94
TABLE XIX PAIRWISE COMPARISON MATRIX OF BUILDINGS WITH RESPECT TO INITIAL THERMOSTAT SETPOINT TEMPERATURE ( $T_0$ )	94
TABLE XX PAIRWISE COMPARISON MATRIX OF BUILDINGS WITH RESPECT TO AREA	95
TABLE XXI PAIRWISE COMPARISON MATRIX OF BUILDINGS WITH RESPECT TO CHANGE IN THERMOSTAT SETPOINT TEMPERATURE	95
TABLE XXII PAIRWISE COMPARISON MATRIX OF BUILDINGS WITH RESPECT TO BUILDING ENVELOPE INSULATION	96
TABLE XXIII PAIRWISE COMPARISON MATRIX OF BUILDINGS WITH RESPECT TO HVAC-TO-BUILDING-PEAK LOAD RATIO	96
TABLE XXIV PAIRWISE COMPARISON MATRIX OF BUILDINGS WITH RESPECT TO LIGHTING-TO-BUILDING-PEAK LOAD RATIO	97
TABLE XXV NORMALIZED WEIGHTS AND RANKS SHOWING WEIGHTAGE OF EXPERT OPINIONS	98
TABLE XXVI RESULTING WEIGHTS AND RANKS FOR SUB-GOALS BASED ON EXPERT OPINION	98
TABLE XXVII RESULTING WEIGHTS AND RANKS FOR VARIOUS ATTRIBUTES BASED ON SUB-GOALS	99
TABLE XXVIII RESULTING WEIGHTS AND RANKS FOR VARIOUS ALTERNATIVES BASED ON DIFFERENT ATTRIBUTES	100
TABLE XXIX OVERALL BUILDING DEMAND CURTAILMENT WEIGHTS	101
TABLE XXX EACH BUILDING’S CONTRIBUTION FOR A 100 KW DEMAND CURTAILMENT REQUEST	102
TABLE XXXI DEMAND REDUCTION IN BUILDINGS DUE TO HVAC THERMOSTAT SETPOINT INTERVENTIONS	103
TABLE XXXII DEMAND CURTAILMENT PRIORITY FACTOR AND RANKS FOR VARIOUS BUILDINGS BASED ON DIFFERENT SUB-GOALS	104
TABLE XXXIII DEMAND CURTAILMENT ALLOCATION - ADJUSTED	105
TABLE XXXIV DEMAND CURTAILMENT ALLOCATION - IMPLEMENTATION	106
TABLE XXXV MAXIMUM INDOOR TEMPERATURE DURING THE CONTROL PERIOD [1-5 PM]	109

## List of Abbreviations

HVAC	Heating, Ventilation and Air-conditioning
BEMS	Building Energy Management System
CAGR	Cumulative Annual Growth Rate
CB ECS	Commercial Buildings Energy Consumption Survey
US-DOE	United States Department of Energy
DR	Demand Response
AHP	Analytical Hierarchy Process
DERs	Distributed Energy Resource
PV	Photovoltaics
ADR	Automated Demand Response
PG&E	Pacific Gas and Electric
IP	Internet Protocol
IBC	International Building Code
ASHRAE	American Society of Heating, Refrigerating and Air-Conditioning Engineers
eQUEST	QUick Energy Simulation Tool
RMSE	Root Mean Square Error
MPC	Model Predictive Control
VT SPIA	Virginia Tech School of Public and International Affairs
IEEE	Institute of Electrical and Electronics Engineers
MAPE	Mean Absolute Percentage Error
BIM	Building Information Models
DSM	Demand Side Management
EV	Electric Vehicles
LEED	Leadership in Energy and Environmental Design
DX	Direct Expansion
EER	Energy Efficiency Ratio
TMY	Typical Meteorological Year
PR	Peak Reduction
ES	Energy Savings
NP	Normalized Priorities
ISO	Independent Systems Operator
CR	Consistency Ratio
DC	Demand Curtailment

# 1. INTRODUCTION AND THESIS OVERVIEW

## 1.1 Background and Motivation

Commercial buildings contribute to a significant share of global energy consumption, and thermal load is a substantial part of the total building energy consumption. The thermal load of a commercial building depends upon several factors:

- A. Local weather and climate
- B. Building envelope and energy efficiency features
- C. Directional orientation of the building
- D. Number and orientation of windows
- E. Occupancy of the building
- F. Occupant temperature preferences
- G. Operational timings, etc.

However, heating, ventilation, and air-conditioning (HVAC) system sizing is still done based on ballpark estimates. The consequence is that we now have back-of-the-envelope solutions that are not optimally engineered and are often over-designed to meet unknown future needs without consideration of efficiency. Furthermore, these solutions ignore the benefits that could accrue from an optimal operation of the HVAC system. The financial and environmental implications of such suboptimal designs are significant and hence, this entire problem must be analyzed from a fresh perspective.

Maturity of smart thermostat technology now allows building owners to remotely control and optimize performance of HVAC systems and actively participate in grid operations. Until now, building energy management systems (BEMS) were deployed in a haphazard fashion over the years, for primarily two reasons; (a) they were operated manually and required a flat (ON/OFF) control, and (b) commercial

BEMS solutions were expensive and for the most part meaningful only in case of large commercial buildings. However, to effectively integrate commercial buildings into the fabric of the electric grid, behavior of buildings under different conditions must be studied in detail. Developing building energy models is the first and most important step in addressing this issue.

The building automation systems industry has been the driving force for realizing large scale building-to-grid-integration efforts. It has been growing rapidly in recent years and is expected to grow with a cumulative annual growth rate (CAGR) of 11.5% by 2026 [1]. Commercial buildings account for a significant share of global energy consumption, and this now opens new opportunities for buildings to participate in energy transactions with the electric power grid.

The Commercial Buildings Energy Consumption Survey (CBECS) indicates that there are about 5.6 million commercial buildings in the United States [2]. These buildings together account for 40% of total energy consumption [3]. Hence, improving efficiency of energy utilization in buildings is of prime concern to the United States Department of Energy (US-DOE). One way to do this is by changing the building HVAC thermostat setpoint temperature, which is the subject of this dissertation. Through this work, we propose a method of synergistic thermal load reduction across grid-connected commercial buildings.

[Fig. 1](#) illustrates the operation of smart buildings in a grid-connected environment, emphasizing the requirements of building-to-grid-integration at a distribution grid level.

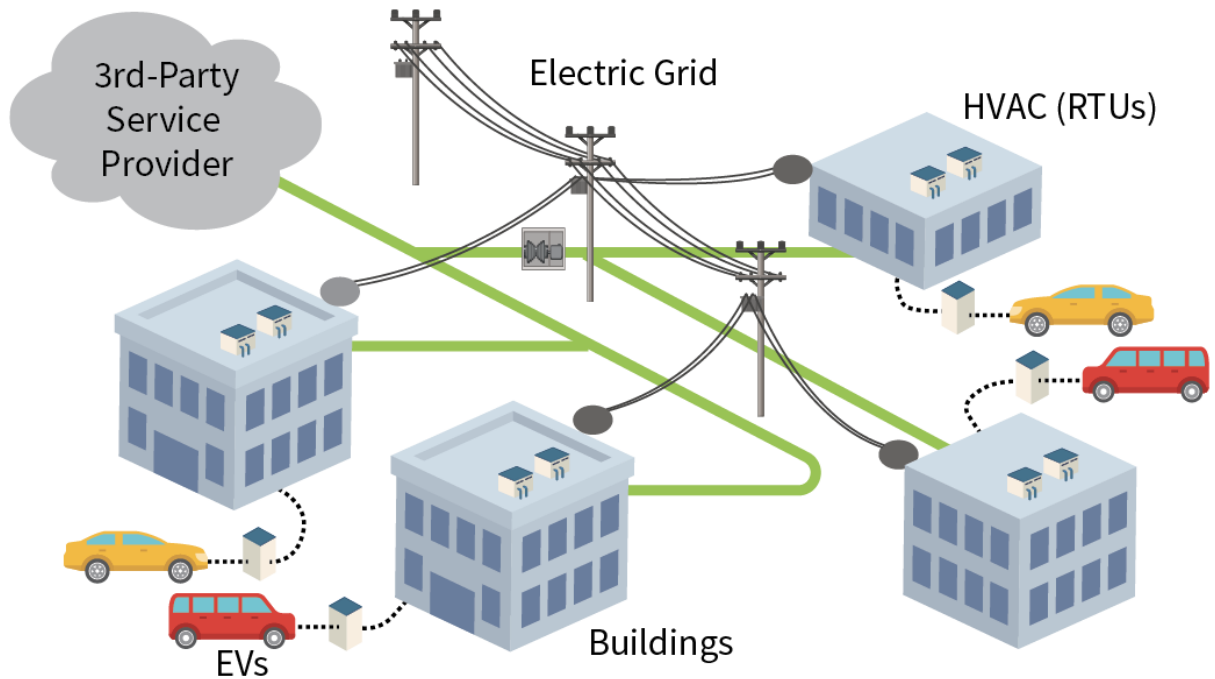


Fig. 1. Overview of grid-connected buildings at distribution level

As shown in [Fig. 1](#), the future distribution grid is envisioned to incorporate a heterogeneous mix of energy sources integrated seamlessly to offer real-time grid support. The bidirectional communication between buildings and electric power grid enables the utility company to interact with buildings during the demand response (DR) period, hence enabling demand control.

## 1.2 Objective and Scope of Work

As intelligent buildings begin to dominate the commercial building landscape, there is a need for a solid and well-engineered building-to-grid integration framework. In this dissertation, we propose a solution that requires multiple commercial buildings to manage their demand synergistically in a decentralized fashion in order to mitigate electric grid peak demand. In order for the commercial buildings to contribute to demand reduction, it is essential to understand their current energy usage. To accomplish this, we need to construct accurate building energy models, which act like digital twins of the actual buildings.

The building energy models developed in this dissertation are quasi-static in nature with an hourly resolution, which means that they are always in thermal equilibrium and hence the indoor temperature changes very slowly, ignoring the transient states. These models are computationally efficient and therefore effective in making predictions about the system behavior. Hence, they find good use in applications requiring planning and control. Therefore, the objective of the first part of this dissertation is to develop accurate high-fidelity, physics-based building energy models.

These models are used to analyze the impact of HVAC thermostat setpoint interventions on building peak demand reduction and quantify the resulting energy savings. The second part deals with developing an expert opinion-based scheme for grid peak demand reduction via HVAC thermostat setpoint interventions in commercial buildings, during the DR period.

### 1.3 Contribution to Building-to-Grid Integration Research Area

This dissertation outlines the operation of grid-connected commercial buildings in the context of a transactive grid. We have designed an analytical hierarchy process (AHP)-based demand curtailment algorithm for grid peak demand reduction by performing HVAC thermostat setpoint interventions in commercial buildings. This algorithm considers the nature and behavior of participating commercial buildings, allocates the required amount of demand curtailment amongst them, and results in the necessary thermostat setpoint intervention required to affect appropriate thermal load curtailment in each building. This work serves as a strong foundation for developing specific guidelines for participation of commercial buildings in a transactive electric power grid. To encourage participation of commercial buildings in the electricity market, a thorough understanding of a building's energy consumption is necessary. It is essential to develop precise building energy models to understand the building's overall performance and gain insights into the impact of parameter variations on total energy consumption.

As a major contribution in this direction, an efficient method of developing high-fidelity building energy models is illustrated in [Chapter 3](#). These models provide a realistic representation of actual building performance and hence serve as digital

twins for the physical commercial buildings. In addition to outlining a procedure to develop high-fidelity building energy models, parametric analysis is done to determine the factors that significantly contribute to the accuracy of the model. Based on the analysis, a minimal input dataset is constructed to provide best accuracy for the given information. This procedure drastically reduces the amount of information required to construct the building energy models while significantly preserving accuracy. These models could further be used to examine the impact of thermostat setpoint interventions on peak demand reduction and quantify the resulting energy savings. The insights obtained from this work are further used to develop an AHP-based scheme for grid peak demand curtailment.

We believe that this is a first, and most important, step in addressing these pressing issues of building-to-grid integration, peak demand reduction, energy efficiency and reducing carbon footprint of commercial buildings, which are a vital part of today's global infrastructure.

#### 1.4 Intellectual Merit

This work illustrates a straightforward way to mitigate local peak demand occurrence via HVAC thermostat setpoint intervention in commercial buildings. The underlying merit of this work lies in: (i) development of accurate high-fidelity building energy models for commercial buildings; (ii) identification of minimum datasets resulting in best accuracy for given information; (iii) analyzing impact of thermostat setpoint interventions on peak demand reduction and energy savings across different commercial buildings; and (iv) development of an integrated demand management tool for demand reduction across different commercial buildings subject to occupant indoor thermal comfort constraints.

In addition, this framework provides a holistic approach optimizing building performance and energy savings by exploiting thermal flexibility of load in commercial buildings during the DR period. This work also investigates the aspect of thermal flexibility in commercial buildings and helps position this new tool in the portfolio of demand management tools in a smart grid environment. This solution gives an insight into thermal behavior of buildings and helps identify candidates that are the most appropriate for thermal load curtailment during DR period. This is done

by considering several attributes of commercial buildings such as their size, location, orientation, operational timings, type of HVAC system, thermostat setpoint temperature, etc. This framework can also be extended to incorporate distributed energy resources (DERs) to operate in conjunction with the proposed demand management tool in a transactive environment.

### 1.5 Hypothesis

The guiding premise of this work is to mitigate grid peak demand by turning commercial buildings into interactive assets for building owners during the demand control period.

Buildings are complex physical objects and are subject to significant variation in occupancy and load usage in real time. Thermal load curtailment in commercial buildings can be used as a load management tool for (a) producing energy savings in each building and (b) reducing the grid peak demand during the DR period. In addition, this thermal load curtailment can also be used as a load-shaping tool [4] in the presence of heterogeneous energy sources and loads.

### 1.6 Nature of the Problem and Solution

The lack of communication between electric grid and commercial buildings often causes energy waste in these buildings, resulting in an unnecessarily high electric bill. By going over the grid's capacity, the assets on the electric grid also suffer, leading to shortened lifetime and frequent replacement of expensive equipment. Therefore, it is important to ensure that the electric power grid and commercial buildings work in reliable coordination.

One of the challenges of starting communication between the electric grid and buildings is that if this communication happens in real time, these buildings cannot make changes quickly enough to react to the grid's command. In addition, the positioning of the AHP-based tool placed between the grid and building causes latency in communication. Considering these aspects, we have proposed a grid peak curtailment solution based on the day-ahead electricity market. For successful implementation, coordination with multiple parties like the electric grid operator, building operator and weather monitoring station is necessary. Furthermore, the type

of information needed from these parties is heterogeneous in nature, making it difficult to integrate multiple sources of data cohesively, as shown in [Fig. 2](#).

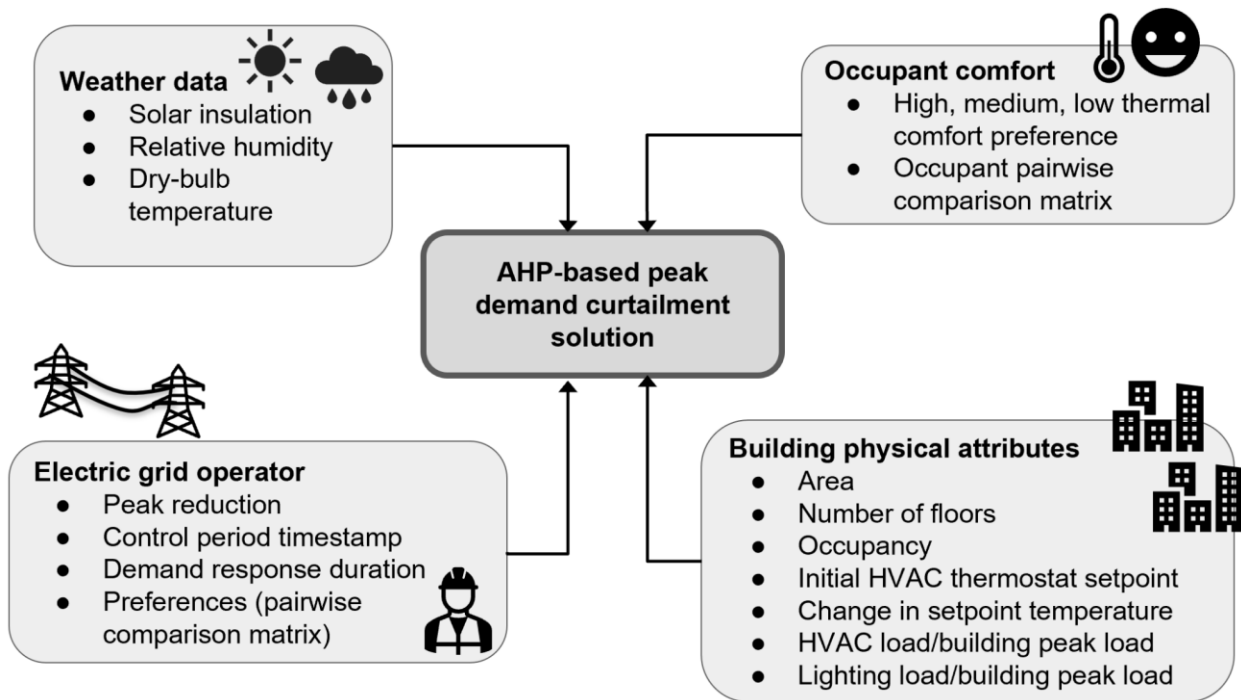


Fig. 2. Input data sources for the AHP-based model

Each occupant is bound to have different comfort level preferences which influences the building's overall load demand. Energy usage of the building also varies based on different weather conditions. This puts a limit on how much demand can be curtailed on a given day. Moreover, these limits have dynamically changing brackets which vary based on attributes such as weather conditions, nature of activity in the buildings, building energy usage profile, occupant comfort, time and length of demand control window, magnitude of demand curtailment, etc. Due to the dynamic nature of this problem, the solution needs to be capable of addressing the changing day-to-day needs of multiple stakeholders.

In order to estimate how much demand could be curtailed in each building, accurate building energy models have to be developed. This requires capturing the interplay between variables such as orientation, building construction, occupancy, operational timings, thermostat setpoints, loads and operating weather conditions. The relation between these variables is complicated and not explicit, with several variables affecting each other in nebulous ways. These highly accurate building

models are difficult to mass-produce as they require a plethora of input data. Contrastingly, the minimum input dataset models that have been subsequently developed are relatively accurate and easier to scale while requiring significantly less input data.

Keeping in mind all these practicalities, an AHP-based framework is developed and positioned to operate in a day-ahead electricity market and conduct end-to-end transactions effectively. This AHP-based tool is useful in running predictive real-time optimization overnight using day-ahead weather forecast data.

Some of the advantages of the proposed approach are:

#### **Electric Utility Operator's Advantages:**

- Introduces novel stakeholders into the electricity market, enhancing grid support during demand reduction period
- Improves longevity of assets deployed in the electrical distribution network
- Provides a reliable way to curtail electric grid peak demand
- Adapts to changing demand patterns of commercial buildings as a result of incorporating solar photovoltaics (PV) and electric vehicles (EV)

#### **Commercial Building Operator's Advantages:**

- Honors occupants' comfort level
- Accurate building energy models serve as digital twins to the physical buildings as they are robust
- Minimal dataset models use significantly less information and hence can be replicated easily
- Estimates both peak demand reduction and energy savings using a single, comprehensive building energy model
- Accommodates the incorporation of new technologies like rooftop solar PV, batteries, EV charging into existing commercial building models

Some of the disadvantages of the proposed approach are:

#### **Electric Utility Operator's Disadvantages:**

- Requires enhanced security to host and analyze sensitive information like thermostat setpoint data, building information, smart meter data, etc.
- Complicates design of protocols due to constant changes in day-to-day operations of electric grid and commercial buildings
- Challenges cohesive integration of disjointed, heterogeneous datasets from multiple sources
- Prohibits real-time control actions as buildings lack swiftness to carry out demand management and promptly update the electric utility operator

#### **Commercial Building Operator's Disadvantages:**

- Building energy model development is resource intensive, tedious and a time-consuming process
- Voids sub-hourly control of load demand in building energy models
- Poses difficulty in understanding the complicated and inexplicit relation between parameters required to create building energy models

### **1.7 Broader Impacts**

This research represents a stepping-stone towards creating a framework integrating buildings into a transactive electric power grid. The proposed solution can be extended to incorporate the addition of rooftop solar PV and EV to commercial buildings in the future. Based on previous research findings, this dissertation rounds out the complexity of power distribution among different buildings allowing for efficient energy use and reliable operation.

As a part of this project, high-fidelity building energy models have been developed. These act as digital twins of the actual buildings, enabling building managers to understand and evaluate different demand management strategies. Additionally, these models help to evaluate the impacts of HVAC setpoint interventions on peak demand reduction and energy savings in the actual commercial buildings. Consequently, the extensive input dataset used to construct the high-fidelity models has been reduced to essentials to create minimum input dataset models. This now allows for the mass-scaling of the AHP-based framework, further extending the potential reach of the proposed solution.

As a first step, it can be used as a preliminary assessment tool to estimate the demand reduction that may be possible for a given set of buildings across different weather conditions. Hence, this work lays a solid foundation and accelerates the transition of a traditional electric power grid into a transactive energy-based framework.

## 2. LITERATURE REVIEW

In order to pursue the proposed solution, this chapter acknowledges the existing literature and poses questions towards successful implementation.

### 2.1 Problem Statement

Some questions we are faced with, in the current situation include:

*How to open the electric power grid for commercial building participation? What are the requirements, benefits, and repercussions in doing so? Specifically, what is the impact of thermostat setpoint interventions on peak demand reduction and energy savings across buildings under different climatic conditions? How can this knowledge be used for the benefit of the building owner? How can it be used to alleviate grid stress conditions?*

To explore possible solutions to the above questions, we must first understand that effective management of the electric power grid depends squarely on the design of an efficient decentralized mode of operation for energy transactions. The heterogeneous nature of current energy portfolios of commercial buildings stems from the adoption of roof-top solar PV, EV, and battery technologies. Efficient energy management schemes can be designed to cater to the needs of commercial buildings and the electric grid in a mutually beneficial way. Realizing the goal of energy self-sufficiency at a distribution level is viable in today's world. This goal seems to be practical when coupled with demand management. Economies of scale, technology-driven price drop, and government subsidies that co-align with the growing conflux of new technologies necessitates a solid and well-engineered solution for building-to-grid integration. Additionally, a multi-faceted problem like this requires outlining the required data infrastructure and designing an end-to-end scheme of data flow.

#### 2.1.1 Peak Demand

Peak demand is the largest instance of power usage in a given time frame, typically a rolling fifteen-minute window. In the context of this problem, there are

two types of peak demand depending on the frame of reference - coincidental peak demand and non-coincidental peak demand.

#### 2.1.1.1 Coincidental Peak Demand/Grid Peak Demand

The highest demand (in kW) of the building during grid on-peak period is called coincidental peak demand. This grid on-peak period varies during summer and winter seasons. The coincidental peak demand charge recovers cost of building out infrastructure like the transmission and distribution substations, lines etc., in support of non-generation related costs necessary to meet peak demands. Coincidental peak reduction is of most value from an electric utility company's perspective [5].

#### 2.1.1.2 Non-coincidental Peak Demand/Building Peak Demand

Typically, the electric utility companies measure power as the average demand over 15 minutes. This is done by summing up the energy consumed in a given time interval and then dividing it by the length of the time interval, giving units of power, in kW. The highest average 15-minute period of demand over a month is the non-coincidental peak demand, which is also referred to as 'building peak demand' or 'peak demand' in this dissertation.

#### 2.1.2 Automated Demand Response

The newly developed open Automated Demand Response (ADR) protocol fully automates the delivery of price and reliability signals to commercial facilities and helps in trimming peak demand effectively [6]. One notable pilot initiative is the ADR program offered by Pacific Gas and Electric (PG&E) [7]. While this program outlines overall strategies for load reduction, there are no specific details or studies provided regarding interventions needed to be made at the customer end. The overall idea discussed in [6] and [7] is depicted in [Fig. 3](#).

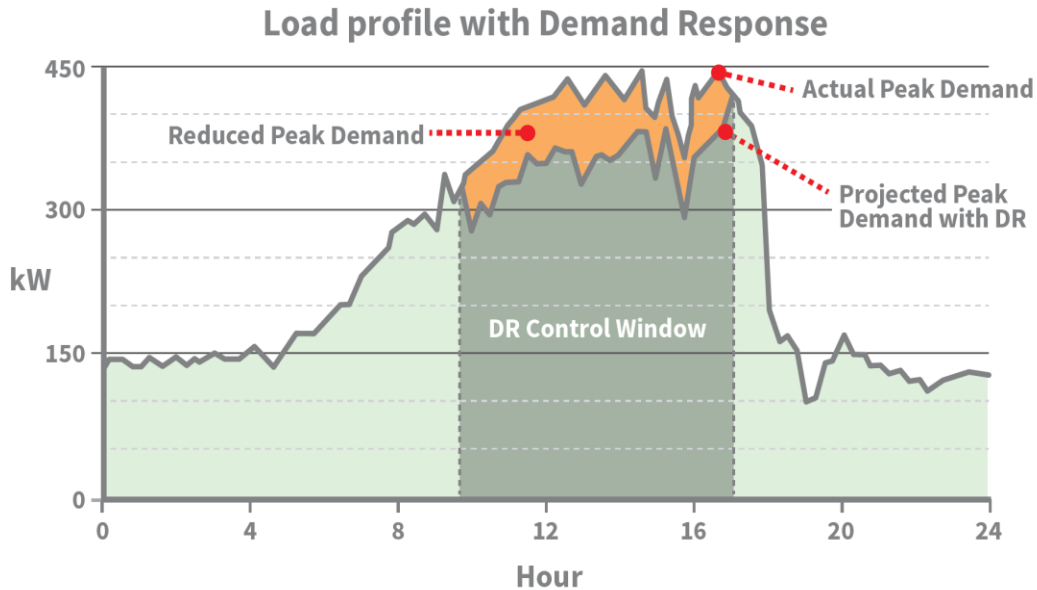


Fig. 3. Building peak demand reduction through demand response

As seen from Fig. 3, in order to quantify the benefits of ADR scheme effectively, establishing a baseline for energy usage in commercial buildings is critical. Once realistic building energy models are created, the impacts of specific interventions can be studied in detail. An overview of the state-of-art practices and research challenges in ADR for smart grids and microgrids is presented in [8]. Recent applications with grid-integrated buildings and microgrids are extending the functionality, by increasing the sophistication of how demand-side load profiles are managed. This paper outlines the architectural models, technology infrastructure, and communication and control protocols that are currently in use. However, the introduction of sensors also introduces concerns of cybersecurity at several access points across the network including BEMS, local area network/wide area network, converged internet protocol (IP) networks and user owned devices [9]. Accurate building energy models can serve as a countermeasure and act as an embedded security system within the building.

## 2.2 Approach

This dissertation is a comprehensive effort to grapple with the issue of demand control in commercial buildings via thermostat setpoint interventions. Commercial

building energy models are developed in a quick energy simulation tool (eQUEST 3.65), a software tool released by the US-DOE. eQUEST makes no *a priori* assumptions about the location, orientation, building envelope, load composition, occupancy, type of HVAC system, nature of activity, or the overall power consumption of the building. All assumptions made throughout this work are referenced to International Building Code (IBC) [10] and American Society of Heating, Refrigeration and Air-conditioning Engineers (ASHRAE) standards [11], [12] and [13]. Hence, this method of building energy modeling is versatile, agnostic to the nature and type of commercial buildings and can be replicated and extended to several other locations.

During the control period, what-if scenarios are run by simulating building energy models with different setpoint temperatures to evaluate and quantify the impact of HVAC thermostat setpoint interventions on peak demand reduction and energy savings in commercial buildings. The initial study focuses on the non-coincidental peak demand at any time during the month, which is more restrictive. This means that the demand restrike must be monitored and it must be ensured that the new peak demand after the setpoint control is less than the initial peak demand being reduced. On-site control for load reduction will have a direct impact on comfort, as it allows customers to make trade-offs between higher electricity costs and comfort. Subsequently, an AHP-based demand curtailment allocation scheme is designed to mitigate grid peak demand by appropriate thermal load curtailment among the participating commercial buildings.

### 2.3 Introduction

The impact of different parameters on building energy consumption must be studied in order to develop strategies to improve energy efficiency. Accurate building energy models accounting for interactions between several components must be developed since buildings are complex dynamic systems. Additionally, the development of control strategies calls for a computationally efficient building energy model.

Authors in [14] presented the capabilities and limitations of standard software tools used in building energy modeling. They indicated that the net energy

consumption must be studied to determine the impacts of increasing HVAC thermostat setpoints, adjusting supply air temperature, and reducing lighting levels. While choice of appropriate software tool is predominantly dictated by the application, eQUEST and EnergyPlus are two prominent software tools which are widely accepted [15]. Another study developed a model of an office building using eQUEST and examined the impacts of varying uncontrolled building parameters like wall construction, glass material and occupancy on building energy consumption [16].

A building energy model of an academic building using EnergyPlus was developed in [17] and a two-step calibration methodology which reduced the root mean square error (RMSE) for monthly energy consumption from 24.48% to 0.37%, is presented. When this model was used to study the impact of modifying the schedule of heat pump (ON/OFF) in an underfloor heating system, monthly energy savings between 20-27% were reported.

In [18], authors investigated energy saving potential obtained by increasing the temperature of chilled water (CHW) supply and have reported a saving of 16% using model predictive control (MPC) strategy with feedforward control structure. While this can be used for estimating ballpark energy savings, the underlying operational pattern of the building remains obscure and thus limits controllability.

It is quintessential to have precise building energy models to understand the building's overall performance and gain insights into the impact of different parameters on total energy consumption. In this work, a bottom-up physics-based method is used to model the Virginia Tech School of Public and International Affairs (VT SPIA) building using eQUEST 3.65. This approach utilizes building physical data and climate condition data along with some assumptions made in compliance with IBC 2018 [10] and ASHRAE Standards [11]-[13]. The rich level of detail involved in modeling makes this approach versatile and highly suitable for modeling existing buildings with great accuracy. The building model developed in eQUEST uses empirical correlations to model interactions between different components and has the engineering muster to accurately predict behavior across a wide range of operating conditions.

Authors in [19] argue that modeling is the most time-consuming and costly part of the automation process based on industrial experience. The intelligent defaults present in eQUEST simplify the modeling process, reduce development time drastically and result in a model that is developed in a relatively shorter time with much lesser effort. Efficacy of the outlined procedure is used to create a digital replica of the building and analyze a broad range of what-if scenarios. This makes producing high-fidelity building energy models an invaluable step in analyzing the overall building performance under different conditions. To study the impact of thermostat setpoint interventions, an equivalent building energy model of the VT SPIA building has been developed in eQUEST. Various categories of inputs required to develop the building energy model in eQUEST are indicated along with the output of the model i.e., hourly building total energy demand. These baseline building energy models have a minimum code compliance with IBC [10] and ASHRAE Standards [11]-[13]. The modeling procedure is further elucidated in [Chapter 3](#). This dissertation also presents a sensitivity analysis by relaxing the HVAC thermostat setpoint temperature assumption from 70°F to see its impact on the accuracy of the model.

Thermostat setpoint interventions are now made on a baseline model to estimate peak demand reduction and corresponding energy savings, closely reflecting the numbers in actual buildings. This study focuses on restricting peak demand in buildings via thermostat setpoint intervention during a 4-hour window encompassing the afternoon building peak. This approach of using a soft DR window centered around the building peak demand eliminated the creation of higher peaks due to demand restrike reported in [20]. The corresponding peak demand reduction and energy saving potential during the DR period have been quantified and tabulated in the [Chapter 4](#). The proposed methodology can be used to quantify peak demand reduction and energy savings in commercial buildings across a wide variety of locations. A summary of relevant literature on building energy modeling is presented in [section 2.4](#).

## 2.4 Building Energy Models

A university building was modeled with real weather data using eQUEST 3.64; the error for annual electricity consumption was within 0.72%, with a range of 4.5-

16% across twelve months [21]. The energy profiles of four residential archetype building models across 12 months captured seasonal variation reasonably well and have thus resulted in an error less than 10% for annual energy consumption [22]. While this serves as a prelude to the development of accurate building energy models, the model presented in [22] has monthly resolution and hence limits controllability. Forecasting annual and monthly energy consumption is relatively easy as the errors average out; however, accurate forecasting for hourly building energy models is more difficult, as it requires the forecast to match well across a much larger sample size.

A review of building energy modeling for control and operation is presented in [23]. Authors classified whole building energy modeling into physics-based, data-driven and hybrid approaches and compared their strengths for DR control applications. They indicated the need for high-frequency data to obtain a good quality building operation model. The authors of [24] discuss top-down and bottom-up approaches for modeling urban building energy use, their strengths and weaknesses in a variety of applications, and integration with geo-spatial techniques. The authors suggest that coupling bottom-up physics-based models with geographic information systems makes for a promising method to predict future urban-scale energy consumption. The issue of performance gap (difference between estimated energy consumption and actual energy consumption) is discussed in [24]. The authors in this paper suggest better information integration, including stochastic aspects of occupants' behavior and installing on-site weather stations to reduce the performance gap.

Furthermore, authors in [25] devised a methodology to identify groups of influential parameters and performed parametric analysis. They outlined a systematic process for developing accurate building energy models. A similar study done on Irish residential dwellings defined the most influential parameters by performing differential sensitivity analysis. A parsimonious hybrid model combining a physics-based model with statistical regression is introduced in [26]. This model is used to estimate energy-saving potential of a building stock due to an energy efficiency upgrade. The parsimonious physics-based model and the hybrid model have average errors of 51.1% and 31.2% respectively. These high values of

errors can be ascribed to fitting a simple multiple linear regression model with building attributes as predictors. Although the hybrid model is an improvement, the resulting error is still significantly large, leaving uncertainty in energy-saving potential in case of an efficiency upgrade. Results presented in [27] indicate that errors up to 40% were observed for hourly peak demand analysis, whereas errors for annual electricity consumption range between 12-55% and 5-99% for regional and urban stocks respectively. This emphasizes the necessity for improving accuracy of building energy models. A critical step in achieving accurate building energy models is the calibration process. Hence, several studies have been done in this area in recent times.

#### 2.4.1 Building Energy Modeling - Calibration

A calibrated simulation model is vital for baselining energy use in measurement and verification projects. Several concepts, proposed procedures, and issues pertinent to building model development processes, are also applicable to the calibration process. In essence, the mathematical formulation of the calibration process is akin to an optimization problem with objective function being the minimization of hour-by-hour mean square errors (between measured and simulated energy use data). The calibration techniques used in literature can be classified into three main categories – manual iterative, statistical, and automated methods as discussed in [16].

A detailed literature review on the calibration of building energy simulation programs along with uses, problems, and procedure is discussed in [28]. This study also touches upon the issue of uncertainty relevant to building simulation programs; further, considerations regarding assessment of uncertainty in building simulations are discussed in [29]. The recent ASHRAE guidelines on measurement of energy savings suggest that the uncertainty declines as the length of the savings reporting period increases [30].

Building model calibration using energy and environmental data is presented in [31]. In this paper, a set of two calibrated environmental sensors together with a weather station are deployed in a 5-storey office building to examine the accuracy of an EnergyPlus virtual building model. The calibrated EnergyPlus model was able

to predict annual hourly space air temperatures with an accuracy of  $\pm 1.5$  °C for 99.5% and an accuracy of  $\pm 1$  °C for 93.2% of the time. Further, a novel framework that can calibrate a building energy model with high accuracies at multiple levels, is introduced in [32]. In this paper, the authors simulated HVAC-related energy consumption at the building level, at an energy conservation measure level, and at the zone level. The simulation results were compared with the measured HVAC-related energy consumption. Findings showed that mean bias error and coefficient of variation of RMSE were below 8.5% and 13.5%, respectively, for all three levels of energy simulation. Similarly, an optimization-based framework to calibrate the whole building energy model is demonstrated in [33]. The optimization algorithm attempts to set the identified parameters to minimize the error between the simulation results and the real-time measurements.

The manual calibration procedure is traditionally used as a wide-spread practice due to its reliability. While the classical iterative manual calibration of whole building energy models using hourly measured data keeps the calibration process evidence-based and systematic [34], it is relatively time-consuming. Alternately, an evaluation of ‘Autotune’ calibration against manual calibration of building energy models is presented in [35]. A bottom-up procedural calibration method based on hourly electricity sub-metering data is presented in [36]. This is coupled with a pragmatic approach of deriving load/occupancy schedules from electricity use data [37] and used as model calibration procedure in the current work.

The building energy models developed using the aforementioned procedure are highly accurate and therefore reflect the actual functioning of the building to a significant degree. These models can now be used to perform DR studies. For the building to actively participate in a DR event, dynamic control models are essential. One such well understood, and widely applied technique is MPC.

## 2.5 Model Predictive Control (MPC)

The number of papers devoted to application of MPC in buildings has been on the rise. In [18], authors highlighted the importance of modeling in the context of predictive control. MPC is a dynamic control strategy where input and output variables can be optimized at each timestep to obtain desired results.

In general, MPC seems to be quite effective for applications involving energy efficiency in buildings. Some of the prominent studies incorporating MPC framework in the domain of building energy modeling are as follows:

In [38], a Stochastic MPC strategy for building climate control is presented. The proposed controller used weather forecasts to compute the required energy and identifies which actuators are needed to keep the indoor temperatures within comfort constraints. Additionally, it was shown that the developed Stochastic MPC technique outperformed traditional rule-based control in both non-renewable primary energy usage and thermal comfort statistics. The Stochastic MPC resulted in much smaller indoor temperature changes, thus exposing occupants to less temperature variation during the day.

Multi-objective optimization of building energy performance and thermal comfort based on MPC is discussed in [39]. In [17], the authors presented a medium size commercial building energy model that is based on simplified MPC. This source develops a lower order system by simplifying the building energy model for an efficient control. Authors in [40] selected controller type as a function of building model uncertainty using MPC. In [41], the authors have presented an iterative two-stage procedure for selection of an appropriate MPC-based building energy model.

To make calculation time as short as possible, an approach of mixed integer linear programming is considered in development of MPC in [42]. For HVAC systems, the practical factors of envelope model setup and their effects on MPC performance is presented in [43]. Several questions on suitability of MPC-based models for building energy management, their integration in smart grids, implementation challenges, market penetration, etc., are addressed in [44]. Furthermore, an MPC framework for prediction and control of energy consumption is developed in [45] based on real-time BEMS data. Nonetheless, using MPC techniques continues to be computationally intensive and cumbersome as it involves linearizing the nonlinear building model and solving the optimization at every timestep. Hence, a high-fidelity physics-based approach is selected for developing building energy models in this dissertation.

The main advantage of the physics-based models is that they provide tremendous insights into the functioning of the actual building. Additionally, high-fidelity models are robust and find utility in a wide variety of applications. One of the drawbacks of physics-based models, however, is that they require significant time, effort, and expertise for development. That said, by making intelligent assumptions and performing parametric analysis, computationally efficient, and accurate, building energy models can be developed with relative ease in a short amount of time. The building energy modeling section ([Chapter 3](#)) presents further details regarding this.

eQUEST is a building energy simulation tool offered by the US-DOE [46]. As depicted in Fig. 5 in reference [47], eQUEST currently tops the category of simulation tools that are suitable but not yet widely applied. This dissertation presents a method of exploiting eQUEST in modeling building energy demand, analyzing peak demand reduction, and energy savings due to HVAC thermostat setpoint interventions.

## 2.6 Demand Response (DR)

Typically, aggregate building load escalates during the hottest or coldest period of the day, contributing to an electric grid system peak. In order to reduce peak demand and support energy savings, electric utilities have several options for engaging customers in DR programs [48]. DR programs have proved to be effective in mitigating many power system challenges, such as high generation cost during peak demand hours, reliability issues and congestion in generation, transmission and distribution. In [49], Jordehi et al., reviewed the recent research work on “DR optimization problem” and classified DR programs into two broad categories – a.) price-based DR programs and b.) incentive-based DR programs. The authors focus on developing optimal DR schemes for commercial customers in this paper. The most commonly used ones are price-based DR programs [50], in which demand reduction can be achieved in response to differing electricity prices during different times of the day. However, from a practicality standpoint a coupon incentive-based DR program is currently used by small and medium size commercial and residential customers [51]. In [52], Luo et al., proposed a data mining driven incentive-based DR scheme. This scheme models electricity trading between virtual power plants

and its participants. Experimental results indicate that the proposed scheme makes intelligent decisions by offering different incentive rate strategies for different consumers. This flexible mechanism induced more consumer load reductions, thus decreasing virtual power plant operation cost further while also improving utilities on the consumer end.

In [53], Davarzani et al., developed and implemented a multi-agent framework for active network management of distribution networks using DR. The proposed algorithm has been tested on a modified Institute of Electrical and Electronics Engineers (IEEE) 69-bus system. The DR implementation resulted in a load reduction of 69.3%, indicating feasibility of the framework. While the source in [53] presented a solution based on multi-agent framework, in [54], a DR framework with competition among utility companies modeled as a non-cooperative game and interaction among residential users as an evolutionary game was proposed. Further, in paper [55], Huang et al., presented a hierarchical coordinated DR control scheme to optimize operations of a group of buildings for aggregate peak demand reduction, using genetic algorithms. With respect to daily peak demand, this scheme showed approximately 5-11% higher reduction and 1-5% more energy savings compared to conventional control.

In [56], Werminski et al., presented a decentralized ADR system for peak demand reduction. The simulation results show a significant reduction in peak power when the decentralized ADR device is used in cooperation with thermostatic devices. Market-based coordination schemes of thermostatically controlled loads based on equivalent thermal parameter models are discussed in [57]-[60]. Currently, there are more than 4.5 million buildings with smart thermostats and the market is expected to rise further in the near future [59],[60],[61]. Deployment of such smart thermostats can make a building demand responsive. A market-based approach for power management and estimation of flexible power reserve in commercial buildings using MPC is discussed in [62]. In [63], Hu et al., investigated the DR potential of air-conditioners under different control strategies using grey-box room thermal models. The model has been validated by comparing the simulated indoor air temperature against measured data and has been found to match with reasonable

accuracy (0.72% mean absolute percentage error (MAPE); indoor temperature measured in °C).

An interdisciplinary investigation of overall building energy consumption and high-performance design using building information models (BIM) is presented in [64]. Further, a controller is designed to manage load usage of each appliance respecting the comfort conditions of each user. This controller is developed using Petri Net framework [65]. Additionally, authors in [66] have discussed a multi-zone HVAC control strategy and combined the advantages of balanced user comfort and energy demand. Moreover, the option of controlling HVAC load and utilizing it for ancillary grid services is explored in PG&E's ancillary service pilot project [67].

In reality, buildings are complex physical objects and are subject to significant variations in occupancy and load usage in real-time. This work presents a clear-cut quantification of peak demand reduction and corresponding energy savings to gain an insight into the impact of HVAC thermostat setpoint interventions in commercial buildings. Towards this end, the VT SPIA building is modeled in eQUEST. Subsequently, HVAC thermostat setpoint is raised in the eQUEST model to quantify and understand the effects of raising thermostat setpoint temperatures on actual building electric energy consumption.

## 2.7 HVAC Thermostat Setpoint Interventions - Thermal Modeling/Energy Flexibility

Thermal load is the largest load in the building. Hence, modeling the thermal load behavior is of interest. Thermal behavior of a building in its environment is described in [68], wherein building models are constructed to estimate indoor temperature, using the SOLENE-microclimate tool [69]. In addition to thermal building modeling, a sensitivity analysis is presented showing that airflow rate, material's properties, blinds' opening ratio, and external weather conditions played a major role. This reveals the vital role played by building envelopes in dictating energy flow in buildings. Authors in [70] developed building models in EnergyPlus and discussed energy retrofit packages involving upgrading the efficiency of window air-conditioners, window glazing and lighting control in high-rise office buildings. The impact of thermostat setpoint temperature variation on building total

energy demand is still missing; however, the thermal load in a building offers greater energy flexibility during the peak demand control period and can be controlled easily as it is a non-critical load.

Authors in [71] reported an annual average thermal peak shifting in the range of 25-78% (from simulation results), due to time-of-day pricing. Further, in [72] the authors presented quantification methodologies – forced time operation and delayed operation to assess energy flexibility in buildings. In [73], authors used DOE reference buildings and focused on quantifying the flexibility of loads in commercial and residential buildings due to thermostat setpoint variation. This is done by constructing hourly piecewise linear regression models quantifying DR potential across a range of outdoor temperatures during the DR period (between 12–6 PM). This approach relies on simulating hundreds of prototype buildings by manipulating building’s parameters, which leads to over-generalizing and makes this process a time-consuming affair.

A tuning methodology consisting of MPC design for energy-efficient building thermal control is presented in [74]. The methodology presented shows that by improving control parameters, a simultaneous reduction in energy consumption and improvement in thermal comfort is possible. Our earlier work [20] on thermostat setpoint interventions in commercial buildings reported a maximum energy savings of about 16% on medium hot days (when average outdoor temperature is between 70-80°F) and about 5% on hot days (when the average outdoor temperature is above 80°F) during a fixed DR period. This study indicates the occurrence of a higher peak due to demand restrike as a repercussion of performing a hard demand control between 12–3 PM. The proposed approach of intervening HVAC thermostat setpoints has two primary outcomes: **peak demand reduction and energy savings.**

## 2.8 Peak Demand Reduction

The ever-increasing energy demand results in elevated grid-stress conditions leading to several perennial problems such as reduction in lifetime of the power grid’s assets, faulty operations, and a myriad of other problems. Because of this, it has been extensively studied by researchers worldwide. Some of the prominent solutions in this area include the following.

Peak demand reduction of building HVAC systems using MPC is discussed in [75]. It is shown that MPC reduced total energy consumption of the HVAC system by 73.2% compared to a flat control where the HVAC runs from 5 AM to 5 PM. Alternately, authors in [76] explored three HVAC scheduling techniques for energy-efficient and cost-effective operation in buildings. They suggested that optimal energy savings are obtained when advanced HVAC scheduling techniques were coupled with predicted mean vote-based approach for reducing zonal HVAC setpoint temperatures [77].

To understand the possible peak demand reduction, a case study using the EnergyPlus model of US-DOE's medium-sized commercial reference office building is presented in [77]. In [78], Zhang et al., suggested a modeling and optimization framework that can be used by building designers and operators to make optimal investment decisions to minimize demand charges. They evaluate measures like installing upgraded energy efficient equipment and applying dynamic building load control strategies to mitigate peak demand in buildings. In [79], Liang et al., proposed a stochastic model co-optimizing operating cost and comfort level in commercial buildings, by presenting piecewise linear models for comfort levels. In [80], Tang et al., developed a game theory-based framework for demand management of a building cluster which allows buildings to manage their own power demands locally. The proposed strategy could reduce aggregate peak demand and electricity cost savings by more than two times compared to individual-level control strategy.

In [81], Saffari et al, presented an optimized technique for demand-side management of peak load by coupling low thermal energy storage and solar PV. It has been shown that higher demand can be reduced by low temperature thermal energy storage as compared to solar PV and that connecting both systems resulted in higher annual electricity cost savings. In [82], Hau et al., designed a spontaneous self-adjusting controller for battery energy storage systems to work in conjunction with on-site solar PV systems. It employs MPC and dynamic programming with anticipatory, preparatory, and recovery actions to achieve a maximum demand reduction of at least 11% over the base case monthly maximum demand.

## 2.9 Energy Savings

An analysis to quantify the expected energy savings associated with ASHRAE Standard 90.1-2016 was published in [83]. In this report, energy savings obtained by enforcing various code sections of Standard 90.1-2016 in 16 EnergyPlus archetype commercial building models across 16 climatic conditions were tabulated. The estimated energy savings range between 1.4-21.2%, with a national average of 7.9%. Authors in [84], developed eQUEST models of three hotel buildings of different sizes and studied the effect of enhancing the wall, roof, glass insulation and upgrading HVAC system type on building energy consumption as per energy conservation building code. While this analysis helps understand the implication of complying with the building codes during design stages, it is unrealistic in the cases of already existing buildings.

A framework for quantifying the impact of occupant behavior on energy savings is presented in [85]. HVAC control as an energy saving measure has been touched upon briefly in [86], wherein it is reported that due to an ON/OFF strategy based on occupancy and user comfort, resulted in energy savings ranging from 8.6% to 22.9% for the whole building. A study of energy savings obtained by adjusting temperature setpoints in retrofitted buildings (US-DOE reference building models in seven different climatic conditions) with different variable air volume boxes is conducted in [87]. Authors in [88] used US-DOE reference building models (EnergyPlus models) for small, medium, and large office buildings and presented a statistical analysis of energy savings concerning different factors, like climate, construction types and dead-band. Relationships between daily optimal setpoints/optimal dead-bands and outdoor temperatures for different climates are also summarized.

## 2.10 Demand Charge Reduction

In [89], Öhrlund et al., presented a causal DR effect evaluation of a mandatory billing demand charge. In summary, this study contributes to the very limited literature on the effects of demand-based tariffs among small and medium sized users and the limited understanding of how demand-side interventions can be evaluated using observational and individual time-series data. In [90], Xu et al.,

developed an adaptive monthly peak demand limiting strategy with an optimal resetting scheme to optimize the limiting threshold for peak power consumption in the building. Using the developed strategy, a 13% reduction in monthly peak demand was achieved for the month of June 2018.

In [91], Malik et al., studied the appliance-level consumption dataset and analyzed the actual contribution of air-conditioners to regional summer demand peaks. Specifically, two demand control strategies have been explored - raising the HVAC thermostat setpoint temperature and widening the control dead band. Increasing the temperature setpoint by 1°C or increasing the temperature dead band by 2°C for longer than an hour resulted in a 25% peak demand reduction. Another study in the same paper showed an aggressive peak demand reduction of around 66% when the temperature set point was increased by 2°C. Findings suggest an aggregate potential peak demand reduction of around 4-9% at a cluster level. However, there are a few limitations to this study. The dataset used for this research is that of New South Wales and has a significant diversity in climatic conditions. It is very likely that residential air-conditioner operation might differ in different NSW regions, particularly inland where temperature extremes are particularly common, and up North where higher humidity and average temperatures are experienced.

In [92], Meinrenken et al., presented a day-ahead demand side management (DSM) framework that optimizes temperature set points and battery dispatch in real time, subject to a time-varying demand-based electricity tariff. The objective is to minimize the total operation cost (tariff charges and battery systems) while still satisfying the occupants' thermal comfort. This concurrent optimization scheme has shown 26% reduction in peak demand and 11% in electricity tariff charges.

All these studies put together point toward a seamless building-to-grid integration framework with multiple stakeholders deriving mutual benefits, subject to indoor thermal comfort constraints.

## 2.11 Analytical Hierarchy Process (AHP): Uses and Role in Peak Demand Curtailment Applications

AHP is a multi-criteria decision-making tool with specified priorities between different input criteria. AHP is used to model a complex decision-making process according to both expert inputs and objective parameters. It is extensively used to incorporate expert opinion in the absence of necessary data. The versatility of AHP as a decision-making tool makes it useful in a wide variety of contexts. Some applications in power system studies include using AHP for assessing equipment health for substation maintenance and upgrade.

For example, in [93], Tanaka et al., have developed a tool for substation asset management measures and visualized the health conditions of substation equipment. In [94], Bernardon et al., presented a methodology to allocate remotely controlled switches in a distribution network, based on AHP. Further, the impact of these switches on the reliability indices was also studied. In [95], Lee et al., presented a unified power quality index based on ideal AHP, which can provide an overall assessment of distribution system performance. The case study presented in the paper demonstrates the process of selecting the best system in terms of improving power quality at low cost. In [96], Fattahi et al., proposed a new AHP-based method for valuation of reactive power in restructured power systems. The effectiveness of the proposed method was verified using IEEE 9-bus system. More recent applications of AHP include allocation of demand curtailment amongst different distribution substations or feeders in an electric utility service area.

In [97], Bian et al., proposed a human expert-based approach to electrical grid peak demand management. The proposed approach helps allocate demand curtailments among distribution substations or feeders in an electric utility service area based on requirements of the central load dispatch center. Results indicated that the proposed scheme handled different amounts of load curtailment effectively. In [98], Shao et al., developed a framework to mitigate grid stress due to electric vehicle penetration. The proposed DR scheme considered dynamic priorities of load based on consumer's real-time needs. The indices proposed in this study can provide electric utilities a better estimate of customer acceptance of a DR program and the capability of a distribution circuit to accommodate EV penetration. These

works strengthen the application of AHP as a useful tool in allocating appropriate demand curtailment.

## 2.12 Summary

This section summarizes research conducted in relevant areas pertaining to the problem statement. Some of the key areas include building energy modeling, model predictive control, demand response, HVAC thermostat setpoint intervention, peak demand reduction, energy savings in buildings, demand charge reduction, and AHP.

In this dissertation, peak demand reduction is affected via thermostat setpoint interventions in commercial buildings. Specifically, the grid peak is addressed using AHP for allocation of demand curtailment among participating commercial buildings. Benefits obtained due to resulting energy savings in each case are also quantified.

Several recent studies include developing accurate building energy models in eQUEST with annual and monthly resolution. Across 12 months, the energy profiles of four residential archetype building models have resulted in an error less than 10% for annual energy consumption [21]. Additionally, a university building was modeled with real weather data using eQUEST 3.64 wherein the error for monthly electricity consumption ranged between 4.5-16% [20]. Whole building energy modeling can be classified into a) physics-based b) data-driven and c) hybrid approaches. Building energy modeling depends on a multitude of diverse parameters, some of which hold higher significance than the others. Efforts have been made to identify the most influential of these parameters by performing differential sensitivity analysis. By making intelligent assumptions and using precise modeling methods, a technique is developed that can construct highly accurate building energy models which serve as digital twins of commercial buildings.

For applications involving energy efficiency in buildings, MPC seems a good candidate. Extensive studies discussing issues like uncertainty in MPC, selection of appropriate building energy models, multi-objective optimization of building energy performance, developing simplified models for efficient MPC control etc., have been conducted in recent times. Other recent studies have also been conducted

wherein MPC strategy has been used for peak demand reduction of building HVAC systems. It is shown that MPC successfully achieved peak demand reduction; the corresponding energy savings from the HVAC system were 73.2% higher compared to a flat control with HVAC system running from 5 AM to 5 PM [75]. Further, a spontaneous self-adjusting controller was developed using MPC and dynamic programming in [82]. This controller enables battery energy storage systems to work in conjunction with on-site solar PV systems. Using this controller reduced monthly peak demand by about 11%.

While MPC-based techniques are widely used, they are computationally intensive and cumbersome. Hence, a high-fidelity physics-based modeling approach is chosen along this line of work. Developing commercial building models using real power consumption data enables us to gain insight into the internal working of the actual building and effectively integrate the buildings into a DR framework.

Today, most of the DR schemes are price, incentive or coupon based. This means they either achieve demand reduction using a tiered price structure across the day or offer bulk incentives for appropriate HVAC cycling schemes. A multi-agent DR framework [53] was tested on a modified IEEE 69-bus system resulting in 69.3% load reduction. Another study designed a game theory-based DR framework with competition among utility companies modeled as a non-cooperative game and interaction among residential users as an evolutionary game [54]. Authors in [55] presented a hierarchical DR control scheme to optimize operations of a group of buildings. This scheme showed approximately 5-11% higher peak demand reduction and 1-5% more energy savings compared to conventional control. This gives an idea of how the overall DR framework pans out with multiple stakeholders dynamically interacting with each other in a transactive market.

Authors in [71] report an annual average thermal peak shifting in the range of 25-78% (from simulation results), due to time-of-day pricing. Studies pertaining to peak demand reduction include development of an adaptive monthly demand limiting strategy resulting in a reduction of 13% [90]. Moreover, increasing HVAC thermostat setpoint temperature and temperature dead band during the summer months resulted in 25% peak reduction for 1°C and 66% for 2°C increment in

HVAC thermostat setpoint temperatures. Findings also suggest an aggregate potential peak demand reduction of around 4-9% at a cluster level [91]. Furthermore, another study showed that adding battery dispatch strategy to HVAC thermostat setpoint interventions resulted in 26% peak demand reduction, while keeping the operational cost of the system and thermal comfort of the occupants in perspective [92].

Energy savings obtained by enforcing various code sections of ASHRAE Standard 90.1-2016 ranged between 1.4-21.2% with a national average of 7.9%, across a diverse set of commercial buildings spread across the United States [83]. In addition, energy savings between 8.6-22.9% was observed using an ON/OFF HVAC control strategy [86].

Traditionally, AHP has been widely used for multi-criteria decision making. Recently, some researchers have used AHP for allocation of peak demand curtailment and designing load reduction schemes in the electric power industry [97]-[98]. Using AHP in this context has the double benefit of performing analysis in an agnostic fashion by considering building attributes like floor area, HVAC-to-building-peak-load%, orientation, number of floors, HVAC type, etc., as well as incorporating inputs of several stakeholders like building operators and utility companies into a holistic decision-making framework. These are the themes explored in this dissertation.

In this dissertation, we propose to apply AHP for allocation of demand curtailment among different commercial buildings and aim to reduce the building thermal load subject to indoor temperature constraints. The implications of overlaying the electric power network with a price signal, with a specific emphasis placed on comfort-to-price sensitivity can also be studied. This work evaluates the potential of peak demand reduction possible in the electric power network under different conditions, with a given number of commercial buildings connected to the network. This research lays the foundation for an active participation of commercial buildings in a transactive energy grid, by considering thermal load curtailment as an energy trading factor. Further details regarding development of state-of-the-art building energy models are presented in Chapter 3.

## 3. BUILDING ENERGY MODELING: High Fidelity Models vs Reduced Order Models

### 3.1 Introduction

This chapter introduces several details that are helpful in developing accurate building energy models. Additionally, it also suggests how to mass-scale the development of accurate building energy models as well as the AHP-based peak demand curtailment scheme proposed in Chapter 5.

### 3.2 Modeling Commercial Buildings in eQUEST

To understand the impact of thermostat setpoint interventions, this study uses an equivalent building energy model of the Virginia Tech - Alexandria campus building: the VT SPIA building. This section discusses the dataset gathered regarding the building and the relevant assumptions made. It also describes the building model development process, calibration, and validation of the developed model.

The building energy models developed in this dissertation are quasi-static in nature with an hourly resolution, which means that they are in thermal equilibrium at all times and hence the indoor temperature changes very slowly. These models are computationally efficient and therefore effective in making predictions about the system behavior. Hence, they find good use in applications requiring planning and control.

The VT SPIA building is located on 1021 Prince Street, Alexandria, VA, USA, as shown in [Fig. 4](#). The corresponding details are given in Table I. This is a three-story medium-sized commercial office building with an area of 25,000 ft<sup>2</sup> and peak load demand of 72.1 kW. This building has brick and glass type fenestration and was constructed in 1981.

## FRONT VIEW



(a). Front view of the building



(b). Side view of the building

Fig. 4. Virginia Tech School of Public and International Affairs building, 1021 Prince St, Alexandria, VA

[Figs. 4\(a\)](#) and [4\(b\)](#) show the front and side view of this building, respectively. Major electrical loads in the building include HVAC, lighting and plug loads (equipment). For this study, information regarding aggregate power consumption is obtained from the smart meter data (30-minute resolution).

This section discusses the dataset gathered from the VT SPIA building and the relevant assumptions made in developing its building energy model using eQUEST 3.65. The procedure for development, calibration and validation of the building model is also elaborated upon. The overall modeling procedure is illustrated in the block diagram shown in [Fig. 5](#).

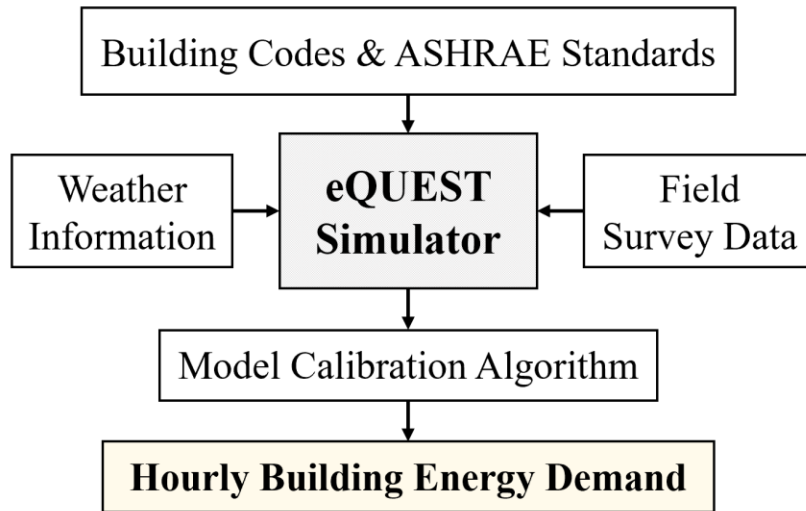


Fig. 5. Block diagram of modeling procedure using eQUEST

Weather information, input data, and building codes/standards (ASHRAE thermal standards, leadership in energy and environmental design (LEED) standards etc.) are given as inputs to eQUEST 3.65. eQUEST uses a weighting factor method wherein it assigns appropriate weights among different parameters, to arrive at an accurate building energy model in a relatively short time span.

Resulting output is then calibrated against data measured by the smart meter installed in the building. The calibrated building energy model is now used to model the building for the rest of the season. The output of the calibrated model (hourly building energy demand) is validated against measured data from the smart meter

that was installed in the building. The description of building’s dataset and relevant model assumptions are presented in [section 3.2.1](#)

### 3.2.1 Dataset Description and Model Assumptions

Summarized in [TABLE I](#) is the data on the VT SPIA building’s physical and operational characteristics from a field survey. It presents details regarding orientation, size, construction material, nature of operation, load composition, and operating schedule. Additionally, this work also relies on the electrical power consumption data from smart meters to derive critical parameters that could not be obtained from the survey, such as load densities, HVAC capacity and fan schedules.

TABLE I. DETAILS OF MEDIUM SIZED OFFICE BUILDING

Attribute	Quantity	Units
<b>General Information</b>		
Building Type	Academic (labs & offices)	
Area	25,000	sq. ft.
Year of construction	1981	-
No. of floors	3	-
Building orientation	South	-
Operating timings	8 AM - 6 PM (Weekends-Closed)	
HVAC system type	Split AC units and gas-fired boilers	
<b>Fenestration details</b>		
Walls	Brick	-
Windows	Glass	-
Doors	Glass	-

In addition to collected data, some assumptions made in building model development, include:

**Weather data:** Alexandria, VA weather data obtained from Weather Underground [99] is used as a reference for constructing the building energy model in eQUEST. The weather data includes hourly information of dry bulb temperature [°F], wet bulb temperature [°F], relative humidity [%], dew point temperature [°F], global solar radiation [BTU/ft<sup>2</sup>] and wind speed [mph].

**Building construction:** eQUEST requires information about building footprint, building layout, construction materials, as well as distribution/types of doors and windows. In addition to the data in [TABLE I](#), additional assumptions are made regarding building fenestration and envelope details. It is typically assumed that the walls are R-19 batt, 2 x 6 metal frame spaced on 24-inch centers, of red masonry brick construction, with a ¾-inch fiberboard sheathing (R-2) exterior insulation. The building has roofing with 3” polyurethane insulation (R-18). The concrete slab clearance is 12 ft. with a floor-to-ceiling clearing space of 9 ft. Walls consist of metal frames with exterior insulation and double glass windows. The assumptions in this category comply with IBC 2015 and ASHRAE standard 90.1 – 2016.

In terms of electrical loads, commercial building loads can be primarily classified into three categories – lighting, plug load and HVAC load. The assumptions made regarding these loads are as follows:

**HVAC system information:** Each floor of the building is served by a packaged multi-zone HVAC system. These HVAC units are of direct expansion (DX) coil type for cooling with dual duct fans, and of gas furnace type for heating. Electrical fans inside the system are driven by a variable speed drive. Determination of HVAC sizes, and fan operation hours of each building is conducted in a model development phase and is discussed in [section 3.2.2](#). Economizers are absent in the building. The HVAC system is configured as per ASHRAE Standard 62.1 – 2016 for ventilation [11] and ASHRAE Standard 55 for thermal environmental conditions [13].

**Building load densities:** Other major loads in buildings are lighting and plug loads such as office equipment, refrigerators, coffee makers, beverage vending machines, etc. The determination of their power densities is also conducted in the model development phase and is discussed in [section 3.2.2](#).

**Seasonal variation in load schedules:** By observing the measured power consumption profiles of the building for one-year, appropriate seasonal breakpoints are derived and given as inputs to the eQUEST model.

**Occupancy Information:** Occupancy in a building varies based on the nature of activity. Typical occupancy is assumed based on the footprint of the building subject

to IBC 2018 [10] and ASHRAE Standard 62.1-2016 [11] and ASHRAE Thermal Standard 55-2013 [13].

After considering these initial assumptions listed above, a model of the VT SPIA building is developed using eQUEST 3.65. The procedure for model development, calibration and validation is described in sections [3.2.2](#), [3.4](#) and [3.5](#) respectively

### 3.2.2 Building Model Development

The VT SPIA building consists of labs and offices and hence is modeled as an open plan office. To develop building energy models, details regarding building layout and construction, load densities, seasonal variation in load schedules and occupancy information are given as inputs to eQUEST.

Then seasons (seasonal breakpoints) are defined, based on power consumption profiles of the buildings. While some buildings demonstrate two discrete seasonal patterns, i.e., Summer and Winter, most buildings also show distinct consumption patterns during shoulder seasons (Autumn and Spring).

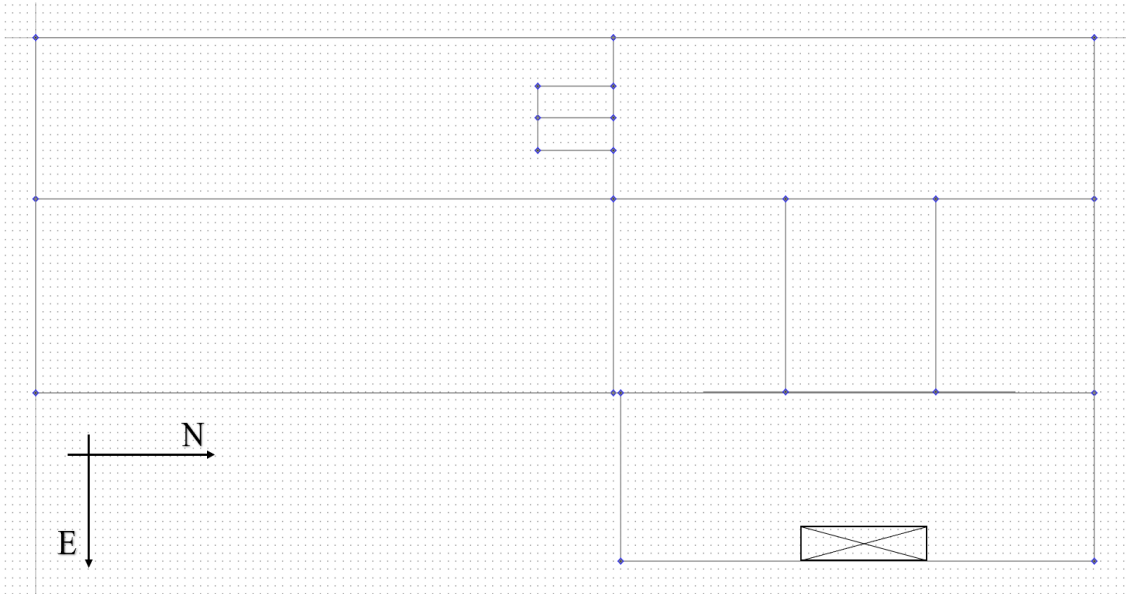
The HVAC system is then configured, with details such as cooling/heating sources, system type, number of systems per floor, and setpoint temperatures for each season, during occupied and unoccupied periods. This also includes cooling and heating design temperatures and air flows. Each floor has a packaged multi zone HVAC system with DX coils and gas furnace to address the cooling and heating requirements. The HVAC system has a total cooling capacity of 63 tons and an energy efficiency ratio (EER) of 8.2. Return air path is ducted. Variable speed drive fans with a flow safety factor of 1.15 are present to modulate the HVAC power consumption. The assumptions regarding initial set-points, design temperatures and air flows are made according to ASHRAE standard 55 [13] which indicates typical HVAC thermostat set-point temperatures in commercial buildings to be between 68-72°F. A mid-range value of 70°F is assumed for the HVAC cooling set-point temperature. Initial fan schedules are set based on the gathered building operation schedules given in [TABLE I](#).

Initial load densities used in the model comply with ASHRAE standard 90.1 – 2016 [12], which indicates a lighting density ranging between 0.6 – 2.03 W/sq.ft.,

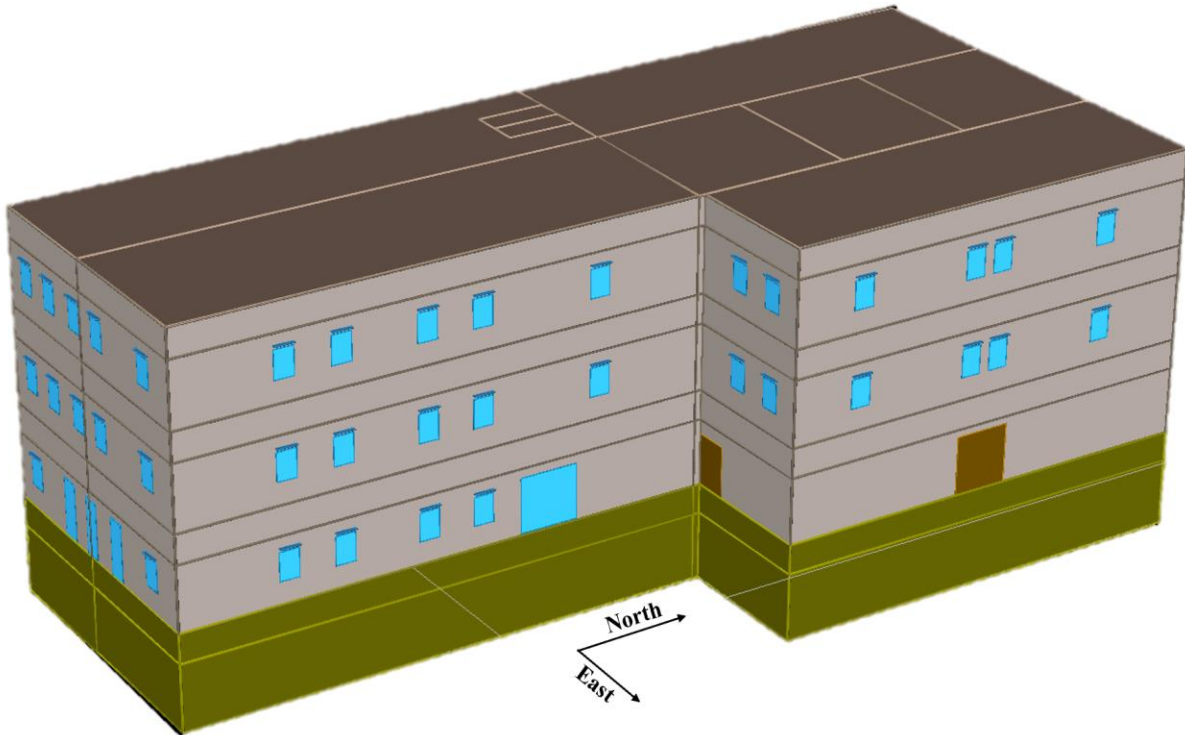
and a typical plug load density between 0.2 – 2.8 W/sq.ft., based on the nature of activity in commercial buildings. Considering these ranges, a lighting load density of 1.1 W/sq.ft., plug load and computer server load densities of 2.4 W/sq.ft. and 2.8 W/sq.ft. respectively, are assumed.

### 3.3 The Developed eQUEST Building Model

By identifying the assumptions made regarding HVAC capacity and lighting, plug load and servers load densities mentioned in [section 3.2.2](#), an eQUEST model of the VT SPIA building has been developed. The building operates between 8AM and 6PM from Monday to Friday and is closed on the weekends. [Fig. 6](#) (a) shows the building’s floor plan, and [Fig. 6](#) (b) shows the 3D model of the VT SPIA building being developed by using eQUEST.



(a). Building floor plan outline



(b). 3D model developed in eQUEST

Fig. 6. Model of the three-story Virginia Tech School of Public and International Affairs building

This building has an east facing door, as can be seen in the building floor plan in [Fig. 6 \(a\)](#). The primary loads in the VT SPIA building during the summer are lighting, plug load, and HVAC cooling load. The HVAC settings for VT SPIA building are as follows:

- The HVAC system runs from 6:00 A.M. to 9:00 P.M.
- Fans operate 2 hours before the building opens and 3 hours after closing time. There is no night cycling for fans.
- The minimum design airflow is 0.5 cfm/sq.ft.
- Supply and cooling design temperatures are 55°F and 68°F respectively.
- Cooling set point is maintained at 70°F during the occupied period and at 82°F for the rest of the day.

Other loads such as coffee maker, refrigerator, domestic water heater etc. are grouped into ‘miscellaneous load’. Therefore, the total load demand in the building at any time instant ‘t’ can be expressed using **equation set A**:

**Equation set A:**

$$P_{total} = P_{lighting} + P_{plug\ load} + P_{misc} + P_{HVAC}$$

$$P_{lighting} = L * A$$

$$P_{plug\ load} = P * A$$

$$P_{misc} = \Sigma P_m$$

where,

$P_{total}$  : total building energy demand kW

$P_{lighting}$  : lighting load demand kW

$P_{plug\ load}$  : plug load demand kW

$P_{misc}$  : total energy demand due to all miscellaneous equipment kW

$L$  : lighting load density W/ft<sup>2</sup>

$P$  : plug load density W/ft<sup>2</sup>

$A$  : occupied area of the building ft<sup>2</sup>

$P_m$  : individual miscellaneous appliance energy demand kW

The calculation of cooling load demand ( $P_{HVAC}$ ) is a bit more involved. [Section 3.3.1](#) presents a summary of HVAC system modeling and gives specific details regarding treatment of HVAC system modeling in eQUEST. Note that the unit conversion between Btu/hr and kW is shown in equation (1).

$$P_{HVAC(Btu/hr)} = 3412.142 * P_{HVAC(kW)} \quad (1)$$

### 3.3.1 HVAC Model Equations

In this section,  $P_{HVAC(Btu/hr)}$  is represented as  $Q_t$  (total cooling load) in **Equation set B**. This equation set gives details regarding HVAC cooling load:

#### **Equation set B:**

$$Q_t = Q_{ext} + Q_{int} + Q_{outside\ air}$$

$$Q_{ext} = Q_{ext\ transmission} + Q_{solar}$$

$$Q_{int} = Q_{lights} + Q_{occupants} + Q_{plug\ load} + Q_{int\ transmission}$$

$$Q_{outside\ air} = Q_{sensible} + Q_{latent}$$

$$Q_{ext\ transmission} = U_1 A_1 * (sa * \Delta t) + U_2 A_2 * (\Delta t)$$

$$Q_{int\ transmission} = U_3 A_3 * (\Delta t)$$

$$Q_{solar} = SHGF * (SF) * A_4$$

$$Q_{sensible} = 1.08 * (\Delta t) * CFM$$

$$Q_{latent} = 0.68 * (M_o - M_i) * CFM$$

$$\Delta t = t_o - t_i$$

where,

$Q_t$	: total simultaneous cooling load	Btu/hr
$Q_{ext}$	: external heat gains	Btu/hr
$Q_{int}$	: internal heat gains	Btu/hr
$Q_{outside\ air}$	: heat load due to outdoor temperature differential	Btu/hr
$Q_{sensible}$	: sensible heat load	Btu/hr

$Q_{latent}$	: latent heat load	Btu/hr
$Q_{solar}$	: load due to solar heat gain	Btu/hr
$Q_{ext\ transmission}$	: heat transmission load from building envelope	Btu/hr
$Q_{int\ transmission}$	: heat transmission load from floors and ceilings	Btu/hr
$Q_{lights}$	: heat load due to lights	Btu/hr
$Q_{occupants}$	: heat load due to occupants	Btu/hr
$Q_{plug\ load}$	: heat load due to plug load	Btu/hr
CFM	: air flow rate	cfm
$t_o$	: outside air design dry bulb temperature	°F
$t_i$	: inside air design dry bulb temperature	°F
$M_o$	: outside moisture content at design wet bulb temperature	g/lb
$M_i$	: inside moisture content at design relative humidity	g/lb
sa	: solar air equivalent temperature differential	-
SHGF	: solar heat gain factor	Btu/(hr.ft <sup>2</sup> )
SF	: shading factor coefficient	-
$U_1$	: heat transfer coefficient of the window glass	Btu/ (hr.ft <sup>2</sup> . °F)
$U_2$	: heat transfer coefficient of the walls	Btu/ (hr.ft <sup>2</sup> . °F)
$U_3$	: heat transfer coefficient of the ceilings	Btu/ (hr.ft <sup>2</sup> . °F)
$A_1$	: area of the windows	ft <sup>2</sup>
$A_2$	: area of the building envelope walls	ft <sup>2</sup>
$A_3$	: area of the ceilings	ft <sup>2</sup>

In eQUEST, design cooling capacity is estimated based on design cooling setpoint, design day outdoor temperature, and solar radiation. The HVAC system

performance curves in eQUEST are constructed based on assumptions and empirical data and can be configured by choosing user-specific coefficients to perform polynomial curve fits. In this dissertation, two types of HVAC systems are used - DX coils for buildings with a footprint less than 100,000 ft<sup>2</sup> and CHW cooling system for buildings with area larger than 100,000 ft<sup>2</sup>. These HVAC models use the coil bypass factor (CBF) modeling method and several performance curves to estimate the relationship between the temperature of air/water leaving the HVAC system and the outdoor air wet bulb temperature. CBF is a function of physical and operational parameters of the coil. It is expressed as a product of design value and two modifier functions, which can be calculated from manufacturers' data. CBF method characterizes the air leaving the coil as being composed of two major streams according to whether the air is cooled by the coil or not. CBF is calculated under the assumption that temperature of the air stream conditioned by the coil is at the apparatus dew point temperature [100]. HVAC model in eQUEST can be summarized using the following three polynomial curves [101], given in **equation set C**:

- CAPFT curve — represents available full load capacity as a function of evaporator and condenser temperatures (bi-quadratic in temperature (T))
- EIRFT curve — represents full-load efficiency (1/COP) as a function of evaporator and condenser temperatures (bi-quadratic in temperature (T))
- EIRFPLR curve — represents efficiency as a function of percentage loading (cubic in part load ratio (PLR))

**Equation set C:**

$$CAPFT = a_1 + b_1 * T_1 + c_1 * T_1^2 + d_1 * T_2 + e_1 * T_2^2 + f_1 * T_1 * T_2$$

$$EIRFT = a_2 + b_2 * T_1 + c_2 * T_1^2 + d_2 * T_2 + e_2 * T_2^2 + f_2 * T_1 * T_2$$

$$Q_{available(T_1, T_2)} = CAPFT * Q_{rated}$$

$$PLR = Q_{operating} / Q_{available(T_1, T_2)}$$

$$Q_{operating} = \dot{m}_{available} * C_p * \Delta T$$

$$EIRFPLR = a_3 + b_3 * PLR + c_3 * PLR^2 + d_3 * PLR^3$$

$$P_{operating} = P_{rated} * EIRFPLR * EIRFT * CAPFT ;$$

where,

Term	DX coils	CHW system	Units
$T_1$	$T_{wb}$	$T_{chws}$	°F
$T_2$	$T_{odb}$	$T_{cws}$	°F
$CAPFT$	: cooling capacity as a function of temperatures ( $T_1, T_2$ )		-
$EIRFT$	: cooling efficiency as a function of temperatures ( $T_1, T_2$ )		-
$EIRFPLR$	: cooling efficiency as a function of part load ratio		-
$PLR$	: part load ratio		-
$Q_{operating}$	: present load on condenser/chiller		Btu/h
$Q_{available(T_1, T_2)}$	: available capacity at present evaporator and condenser conditions		Btu/h
$Q_{rated}$	: rated capacity at AHRI conditions		Btu/h
$C_p$	: specific heat of air/water		J/kgK
$\dot{m}_{available}$	: available mass flow rate		kg/s
$\Delta T$	: $T_1 - T_2$		°F
$P_{operating}$	: power drawn at specified operating conditions		kW
$P_{rated}$	: rated power drawn at AHRI conditions		kW
AHRI	: air-conditioning, heating, and refrigeration institute		-

The CAPFT curve describes how the cooling capacity of the system varies at different inlet temperatures, when compared to cooling capacity at reference conditions, which is normally 44°F and 85°F. The EIRFT curve describes how the full load efficiency (power consumption in kW per ton of cooling) varies with inlet and outlet temperatures; EIRFPLR curve describes how the power consumption varies as a function of part load ratio [102]. Note, that for variable-speed chillers, part-load cooling efficiency curve is a function of both part-load ratio and leaving condenser water temperature. This curve may take the form of EIR-FPLR, which is the fraction of time the unit must run to meet the part-load for that hour. For example, at 40% of full load, the equipment might need to run 50% of the hour (for cycling losses). Note that for small, packaged equipment with SEER ratings (<65,000 Btu/h), the part-load efficiency curve is set to no degradation, since the part-load degradation is built into the DX cooling efficiency temperature adjustment curve. PLR is based on available capacity, not rated capacity. The coefficients for these curves are calculated using the standard least squares linear regression technique [103].

### 3.3.1.1 HVAC System Types: DX Coils and CHW System Models

While both DX coils and CHW broadly operate based on the set of equations listed in [section 3.3.1](#), the corresponding set of equations for DX coils and CHW cooling system with specific adjustments are presented in sections [3.3.1.1](#) and section [3.3.1.2](#) respectively.

#### 3.3.1.1.1 DX Cooling Coils (PSZ-AC)

As shown in [section 3.3.1](#), in a DX cooling system,  $T_1$  corresponds to  $T_{wb}$  and  $T_2$  corresponds to  $T_{odb}$ , where,

$T_{wb}$  : entering coil wet-bulb temperature °F

$T_{odb}$  : outside-air dry-bulb temperature °F

Note: if an air-cooled unit employs an evaporative condenser,  $T_{odb}$  is the effective dry-bulb temperature of the air leaving the evaporative cooling unit. A constant volume fan control method is used in this type of HVAC system.

### 3.3.1.1.2. CHW Cooling System

Similarly, from [section 3.3.1](#) we gather that for a CHW cooling system,  $T_1$  corresponds to  $T_{chws}$  and  $T_2$  corresponds to  $T_{cws}$ , where,

$T_{chws}$  : chilled water supply temperature °F

$T_{cws}$  : condenser water supply temperature °F

### 3.3.1.2 Coefficients of eQUEST Default Performance Curves

This section presents the coefficients of default performance curves used by eQUEST, to model packaged single zone and chilled water HVAC systems.

[TABLE II](#) lists the default coefficients of CAPFT, EIRFT and EIRFPLR curves for DX and CHW type cooling systems [104].

TABLE II COEFFICIENTS FOR DEFAULT PERFORMANCE CURVES IN EQUEST

Coefficient	Air Cooled Direct Expansion (PSZ-AC)			Chilled Water Coils (CHW)		
	CAPFT	EIRFT	EIRFPLR	CAPFT	EIRFT	EIRFPLR
<b>a</b>	0.8740302	-1.0639310	0.2012301	2.5882585	-1.8394760	0.2012301
<b>b</b>	-0.0011416	0.0306584	-0.0312175	-0.2305879	0.0751363	-0.0312175
<b>c</b>	0.0001711	-0.0001269	1.9504979	0.0038359	-0.0005686	1.9504979
<b>d</b>	-0.0029570	0.0154213	-1.1205105	0.1025812	0.0047090	-1.1205105
<b>e</b>	0.0000102	0.0000497	-	0.0005984	0.0000901	-
<b>f</b>	-0.0000592	-0.0002096	-	-0.0028721	-0.0001218	-

Once the initial building model is developed as per details given in [TABLE I](#), aforementioned standards, and approximated performance curves (listed in [TABLE II](#)), output of the model is compared with building power consumption profile for one week (See [Fig. 7](#)). The model is calibrated manually using techniques discussed

in [34], [36] and [37]. The model calibration procedure used in this work is further explained in [section 3.4](#).

### 3.4 Model Calibration Procedure

Some of the best practices in model calibration procedure include partitioning the load profile into categories with similar load patterns and employing a hierarchical calibration method by identifying the most influential input parameters. In this work, the eQUEST model has been calibrated manually by taking an intelligent decision-making approach to estimate the required tuning parameters. The procedure for the required parameter estimation is explained below. In the future, machine learning techniques can be used to make the model calibration procedure automatic.

#### Parameter Estimation:

As the first step in estimating the load densities of lighting and plug loads in the building, the study examines the power consumption of the building during winter. This helps estimate the load densities accurately since the HVAC load is absent. This winter power consumption is further divided into operating hours and non-operating hours, based on the building's operation. During non-operating hours, the lighting load is typically turned off. Hence, dividing power consumption (kW) during non-operational hours by building footprint gives the corresponding plug load density (W/sq.ft.). In this study, it is assumed that all loads other than lighting, such as office equipment, refrigerators, coffee makers, beverage vending machines, hot water heater, etc., are lumped together as plug load in the developed eQUEST model. The perennial constant baseload when present, is modeled as computer server load with appropriate load density in W/sq.ft.

After determining plug load density, lighting load density (W/sq.ft.) is derived by subtracting plug load power consumption from total building power consumption, during building operational hours and dividing the resulting difference by building footprint. Although these loads are temperature independent, there may be a need to adjust them across seasons due to varied usage patterns.

The other major load in buildings is attributed to HVAC, which is fully operational during the summer season. Hence, subtracting lighting and plug load (determined

earlier) from peak power consumption during the operational period in Summer reflects HVAC cooling load information.

Occupancy based hourly operating schedules of various loads on a typical weekday, is shown in [Fig. 7](#).

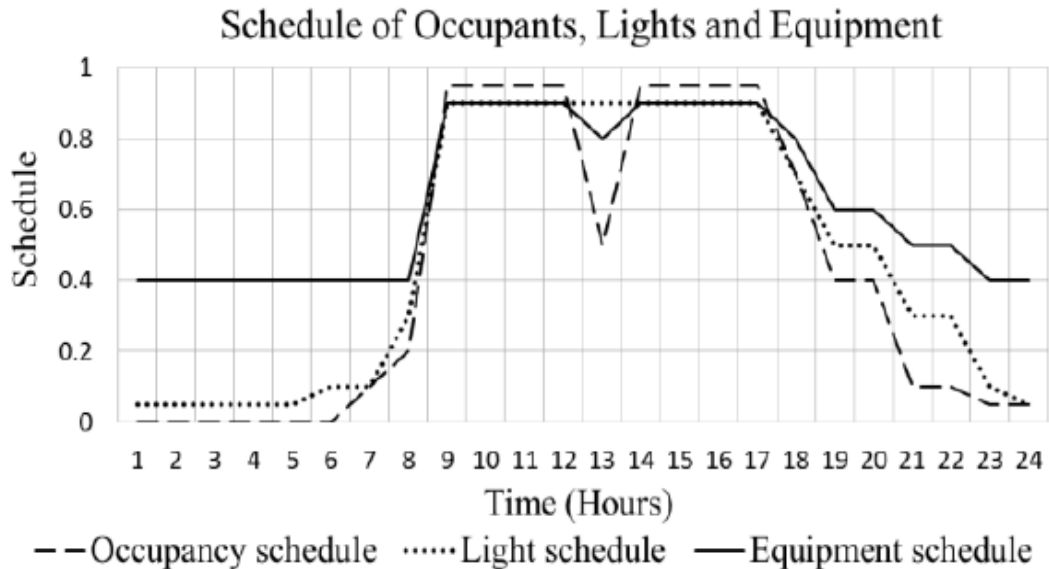


Fig. 7. Hourly schedule of occupants, lights, and equipment in the building

Occupancy details and schedules for lighting and equipment are provided as a number between 0 and 1. For example, a value of 0.5 means that during that hour, the power consumption of equipment is half of the maximum capacity. The maximum design occupancy in the building is 100 sq.ft. per person.

Information regarding the exterior climate of the building, *viz.* outdoor (dry bulb) temperature and relative humidity is obtained from Weather Underground [99], a third-party weather service provider.

Output of the eQUEST office building model is calibrated against measured smart meter data for a typical summer weekday. After these adjustments are made, any further patterns capturing day-to-day characteristics of building operations, are incorporated into the model. This reduced the error of the building model from 22.1 to 4.8% for the calibrated week. The calibrated building load profile for one-week

(June 12-16, 2017) is shown in [Fig. 8](#). This illustrates that simulated hourly load closely follows actual load with an average error of less than 5%.

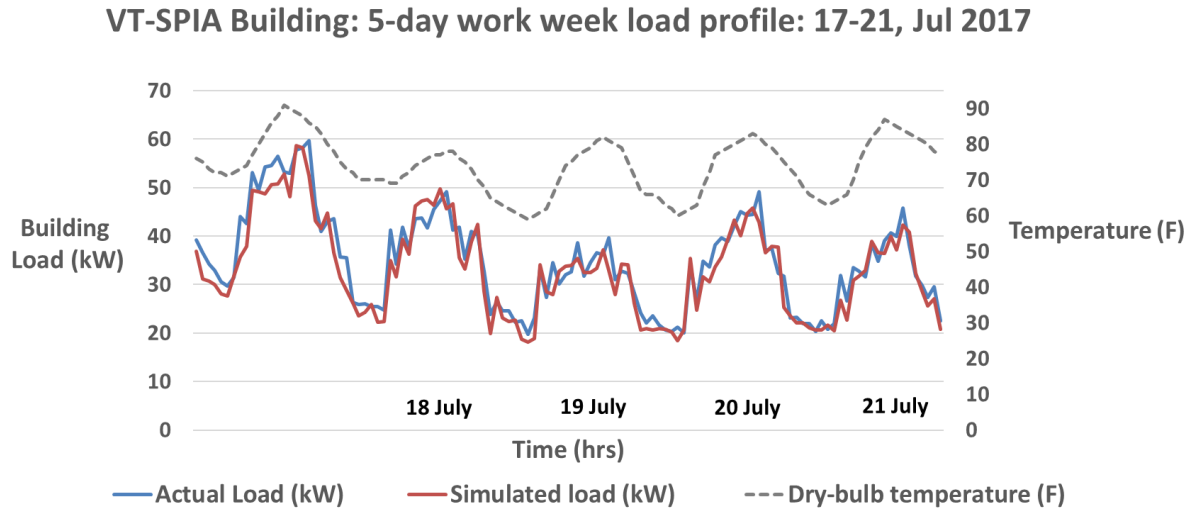


Fig. 8. Actual and simulated hourly building load (kW) for a week

The graph in blue shows the actual load and the graph in red shows simulated load in kW for five weekdays. This calibrated building model is further used to validate the eQUEST model for the rest of the summer season. A similar procedure is followed for winter and the calibrated model is thus used for validation as described in [section 3.5](#).

### 3.5 Model Validation

The calibrated VT SPIA building energy model is now validated using hourly averaged energy demand data obtained from the smart meter. A comparison between monthly electrical energy consumption of the simulated building and metered data for the summer months, is illustrated in [Fig. 9](#).

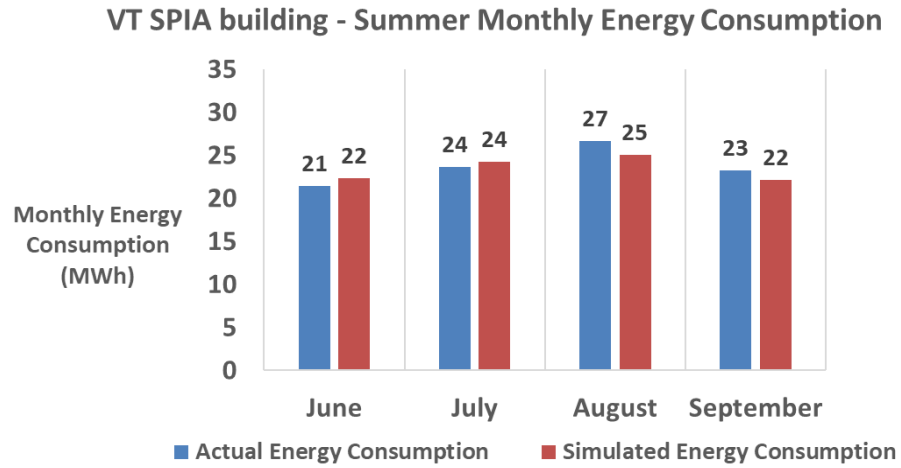


Fig. 9. Actual and simulated monthly building electricity consumption (MWh)

The blue bars in [Fig. 9](#) represent actual energy consumption and the red bars represent simulated energy consumption for twelve months. Y-axis represents the monthly energy consumption (in MWh) and x-axis represents months of the year. This justifies the VT-SPIA building energy model developed in eQUEST. The corresponding monthly energy consumption of the building is shown in [Table III](#).

TABLE III MONTHLY ENERGY CONSUMPTION OF THE BUILDING DURING SUMMER MONTHS

Month	Actual Energy Consumption (MWh)	Simulated Energy Consumption (MWh)	Error (%)
June	21.41	22.32	4.3
July	23.65	24.26	2.6
August	26.66	25.05	6.0
September	23.27	22.11	5.0

MAPE is used as a metric to evaluate the accuracy of building load models, and is calculated as given in equation (2)

$$MAPE \% = \frac{Actual\ load - Simulated\ load}{Actual\ load} * 100 \quad (2)$$

*Actual load* : Smart meter power data (kW)

*Simulated load* : Output of the eQUEST model (kW)

As shown, the simulated monthly electricity consumption closely fits the actual consumption with an average monthly error of 4.5%. [Fig. 10](#) depicts the detailed hourly validation during the 12-month period. It demonstrates that the hourly load pattern can be modeled satisfactorily, and the developed building load model is able to respond to seasonal variation in outdoor temperature.

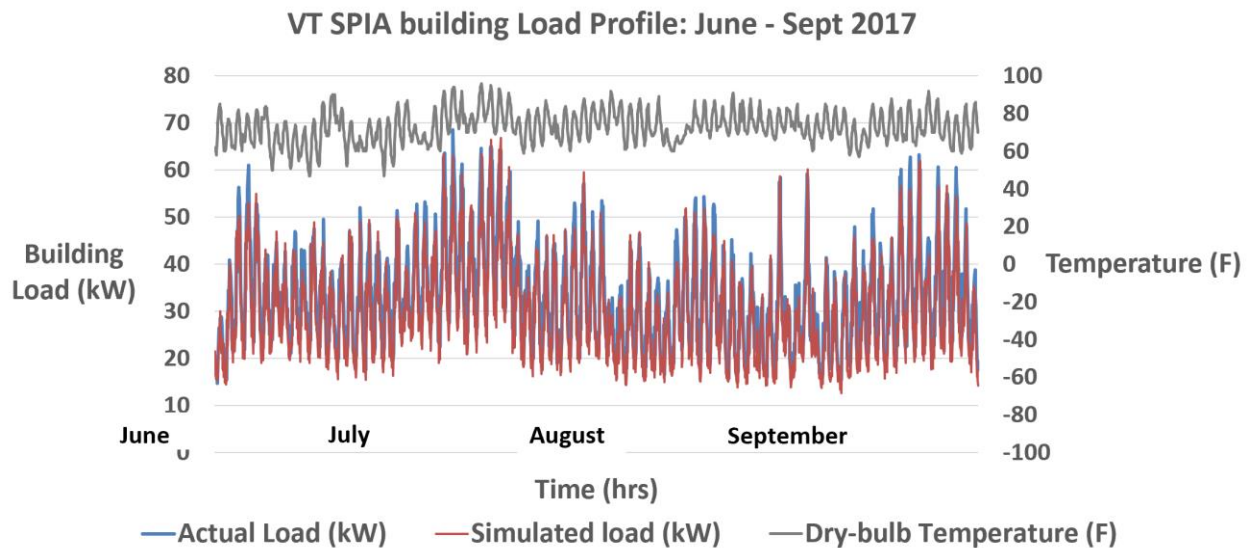


Fig. 10. Actual and simulated hourly building load (kW) from June 1, 2017 to September 30, 2017

The graph in blue represents actual load and the graph in red represents simulated load in kW. The y-axis represents the building load (in kW) and x-axis represents time (hrs). The analysis is performed over summer weekdays (June - September). There are 86 weekdays in total, accounting for approximately 17 weeks.

The close match between monthly, daily, and hourly consumption patterns between actual and simulated power consumption validates underlying assumptions and demonstrates that the eQUEST building model is reasonably accurate and reflects actual operating characteristics in the building effectively, thereby validating the model. The validation results indicate that average hourly error percentage

during summer is close to 7%. [TABLE IV](#) summarizes minimum, maximum, and mean values of error percentages for the VT SPIA building across 2064 hours of Summer (June – September).

TABLE IV MODELED BUILDING LOAD ERROR

Attribute	Value
Min error %	0.0
Max error %	37.9
MAPE %	6.7
Standard deviation ( $\sigma$ )	13.1
CV(RMSE) %	1.96

The values of standard deviation and CV(RMSE) shown in [TABLE IV](#), indicate a high precision in modeling which enable these high-fidelity building energy models to serve as digital twins of the actual commercial buildings. To test the robustness of the modeling procedure, a parametric analysis of HVAC thermostat setpoint is presented in [section 3.6](#).

### 3.6 Sensitivity Analysis – Thermostat Setpoint Temperature

For an initial HVAC thermostat setpoint temperature, a typical value of 70°F has been assumed. The MAPE% of eQUEST model with respect to different initial thermostat setpoint temperatures is summarized in [TABLE V](#).

TABLE V ACCURACY OF THE BUILDING LOAD MODEL W.R.T. INITIAL HVAC THERMOSTAT SETPOINT TEMPERATURE

HVAC Setpoint Temperature (°F)	68	69	70	71	72
MAPE %	6.2	5.1	6.7	6.6	6.8

There is an increasing trend in average error percentages corresponding to initial thermostat setpoint temperatures due to the difference in number of HVAC operational hours accounted by the simulated model vis-à-vis actual data. For example, when the thermostat setpoint temperature in the simulated building model is higher than that in the actual building, the HVAC system in the simulation model is inoperative, but in reality, it is operational.

[TABLE V](#) also suggests that a change in initial thermostat setpoint temperature assumption results in modest variation in accuracy of the building energy model. This establishes robustness of the developed model, hence validating the discussed methodology. While the devised modeling methodology produced robust and accurate building energy models, further investigation is required to identify which parameters have higher influence in making the building energy models accurate and robust without compromising integrity. This topic is further investigated in [section 3.7](#).

### 3.7 Reduced Order Building Energy Model - Minimal Dataset Model for Optimal Accuracy

The development of a high-fidelity building energy model requires several input parameters which might be difficult to procure in a day-to-day field environment. This necessity of several input parameters presents challenges in mass-scaling. Therefore, efforts have been made to identify a minimal set of accurately specified input data to develop reasonably accurate building energy models with a modest amount of effort [22].

Authors in [22] identified minimum input datasets for four buildings out of several parameters required to define the building envelope. Among the identified parameters, the U-value of walls and glass, window-to-wall ratio, solar heat gain coefficient, domestic hot water usage, cooling setpoint temperature, efficiency of the HVAC system, and air changes per hour proved to be the most influential. In this work, we focus on identifying further influential parameters that affect accurate modeling of the HVAC system. A simulation-based approach is taken, and the optimal solution is found through multiple iterations, given the set (and range) of valid assumptions.

eQUEST, has been used to develop the initial high fidelity commercial building energy models, given the rich set of input data. The level of input data detail given to the building model in eQUEST is now varied to identify the most influential parameters affecting the overall accuracy. Differential sensitivity analysis is chosen as the method of parametric analysis and a useful minimal input dataset is constructed using parameters that have the most influence on accuracy of the developed building energy models; [Table VI](#) presents details of the parametric analysis with respect to various HVAC and building input variables. The parameters are listed in the order of decreasing importance.

TABLE VI INFLUENTIAL HVAC AND BUILDING PARAMETERS

S. No.	Parameter	Unit	Type
1	HVAC thermostat setpoint	°F	HVAC
2	Air changes per hour (ACH)	CFM/person	HVAC
3	$U_{\text{glass}}, U_{\text{wall}}, U_{\text{roof}}$	W/ (ft <sup>2</sup> °F)	Building
4	Window-to-wall ratio	-	Building
5	Solar Heat Gain Factor	-	Building
6	Domestic hot water usage	lit/ft <sup>2</sup>	Building
7	Energy Efficiency Ratio (EER)	-	HVAC
8	Orientation	-	Building
9	Plug load density	W/ft <sup>2</sup>	Building
10	Roof – Absorptance/emissivity	-	Building

Results show that the monthly energy demand values match well and the hourly energy demand values over the summer period for the simplified energy model are 6% over the actual calibrated model.

Further, to study the impact of HVAC thermostat setpoint interventions, high fidelity commercial building energy models are developed by using the methodology presented in sections [3.2-3.5](#).

### 3.8 Commercial Building Portfolio - Description of eQUEST Building Energy Models

A portfolio of diverse commercial buildings is constructed from US-DOE's commercial buildings list [105] and are developed in conformity with ASHRAE 90.1 and ASHRAE 55 standards. The buildings are also LEED new construction compliant. This building portfolio is used in conducting case studies in Chapter 4 (to assess the impact of HVAC thermostat setpoint interventions) and Chapter 5 (to evaluate the proposed AHP-based demand curtailment tool).

These buildings are located in Blacksburg, VA (ASHRAE climate zone 4A: mild, humid). Typical meteorological year (TMY2) weather data file for Roanoke, VA is used for building model development. These high-fidelity commercial building energy models developed using the proposed modeling technique are accurate and hence can help reverse estimate the necessary set point intervention for a given amount of demand reduction.

The key attributes of the selected commercial buildings portfolio used in this chapter are given in [Table VII](#); the chosen buildings are of different sizes, orientation, nature of activity and fenestration, hence reflecting a scenario close to reality.

TABLE VII INPUT DATASET DESCRIPTION – OVERALL BUILDINGS PORTFOLIO

Building Type	Area (ft <sup>2</sup> )	No. of Floors	Timings	Peak Load (kW)	HVAC-to peak load ratio (%)
High-rise Office	250,000	8	8AM-5PM	1773.5	30.9
Mid-rise Office	125,000	4	8AM-5PM	921.0	30.4
Middle School	75,000	1	9AM-2PM	248.7	62.8
Strip Mall	15,000	1	8AM-9PM	92.7	64.4
Hospital	250,000	4	6AM-8PM	1595.1	24.5

As shown in [TABLE VII](#), the portfolio includes a wide array of buildings, such as a strip mall with an area of 15,000 ft<sup>2</sup> and a large office building with a total area of 250,000 ft<sup>2</sup>. Also, there is a significant gradation in peak demand of each building, ranging from 92.7-1773.5 kW. HVAC-to-peak load ratio is defined as ratio of total HVAC load to peak load of a building and is an indicator of thermal load capacity of a building. Smaller buildings like strip malls and middle schools use DX coils and larger buildings like mid-rise, high-rise and hospital buildings use CHW loops with variable air volume systems for cooling. The temporal variation of the ambient temperature is included in the simulation and is assumed that the prediction for the next day is available and accurate.

The eQUEST building energy models of the buildings described in [TABLE VII](#) are shown in [Fig. 11](#).

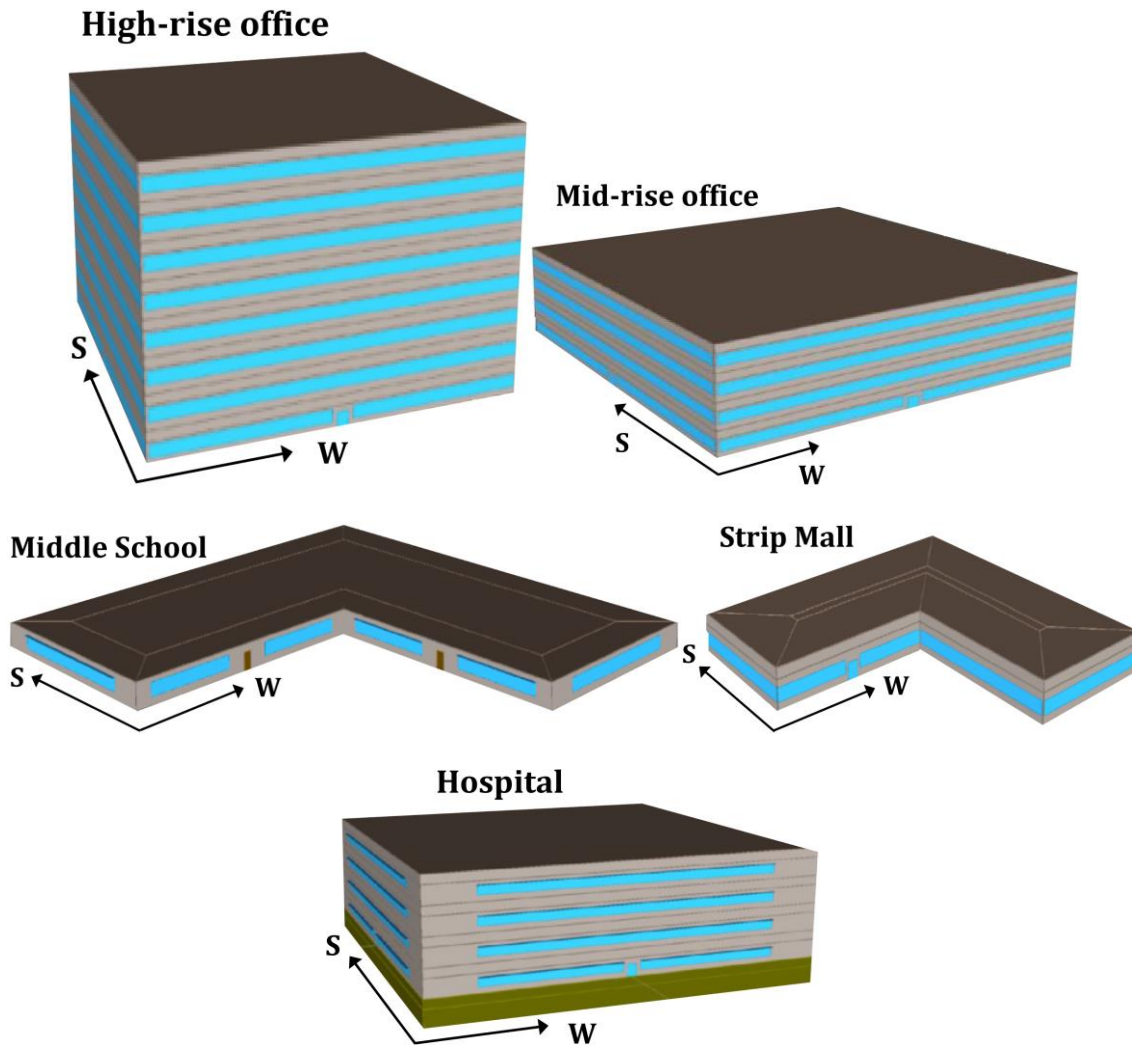


Fig. 11. eQUEST building energy models of the selected five commercial buildings

This commercial building portfolio is used for various studies that are conducted in Chapter 4 and Chapter 5. Specifically, Chapter 4 provides insights into the impact of HVAC thermostat setpoint interventions on peak demand curtailment and their corresponding energy savings across different buildings

# 4. PEAK DEMAND REDUCTION AND ENERGY SAVINGS USING HVAC THERMOSTAT SETPOINT INTERVENTION

## 4.1 Introduction

This chapter discusses information about the procedure for conducting HVAC thermostat setpoint interventions and their effect on peak demand reduction. Additionally, it also addresses the corresponding energy savings produced as a result of performing HVAC thermostat setpoint interventions in buildings listed in the commercial building portfolio presented in [section 3.8](#).

## 4.2 Peak Demand Reduction Potential Across Buildings due to HVAC Thermostat Setpoint Interventions

Once the developed eQUEST building models have been validated against smart meter data within an acceptable error range, they are then used to analyze the peak demand reduction potential, as shown in [Fig. 12](#).

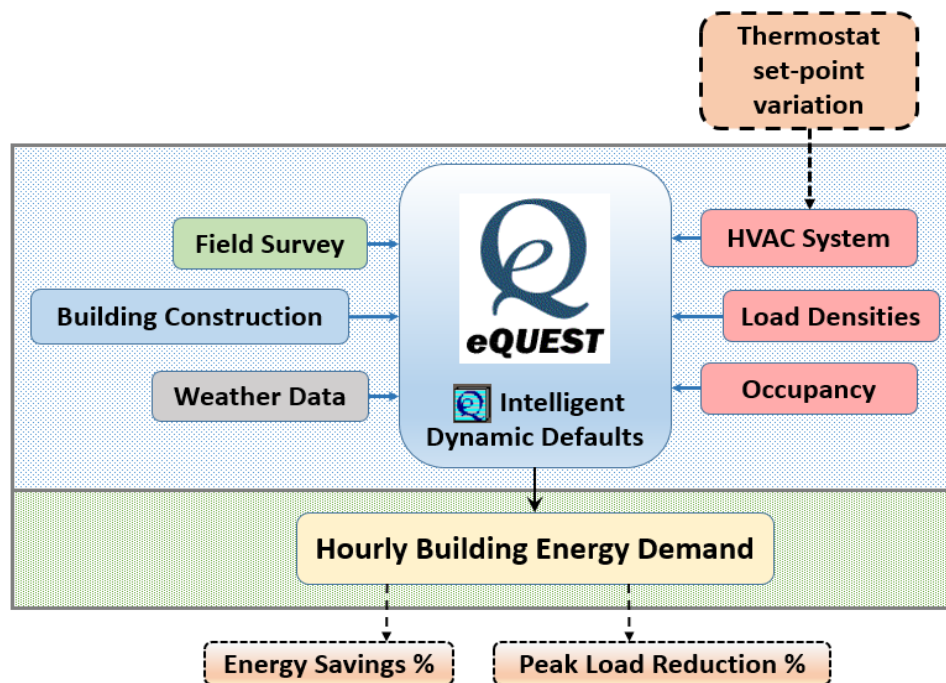


Fig. 12. Overall scheme for estimation of peak demand reduction and energy savings in commercial buildings using eQUEST software

In this figure, HVAC thermostat setpoint interventions are performed on the eQUEST building energy model during the DR period and the resulting energy savings% and peak load reduction potential% are calculated. This study focuses on restricting peak demand in the building via affecting HVAC thermostat setpoint intervention during a 4-hour window, encompassing the afternoon building peak. Since load begins to drop after the selected DR period, demand restrike peak (if any) after DR period is lower than the initial building peak. This results in overall peak demand reduction.

#### 4.2.1 Method for HVAC Thermostat Setpoint Interventions

An intervention is made in the HVAC thermostat cooling setpoint by raising the setpoint by +1, 2, 3, 4 and 5°F from the base-case setpoint (i.e., 70°F), during the DR period.

#### 4.2.2 Calculation of Peak Demand Reduction Potential

Upon performing the HVAC thermostat setpoint intervention, building power consumption during the DR period is reduced. To observe the peak demand reduction potential during DR period, a peak reduction index ( $\Delta PR_{DR}\%$ ) is defined, as shown in equation (3). This reflects the amount of peak demand reduction possible during the DR period.

$$\Delta PR_{DR}\% = \frac{\max (load_B)_{DR} - \max (load_{B+\delta t})_{DR}}{\max (load_B)_{DR}} \cdot 100 \quad (3)$$

Where,

$\Delta PR_{DR}\%$  : Peak demand reduction % during DR period

$\max (load_B)_{DR}$  : Maximum power consumption with base case thermostat setpoint of 70°F, during DR period (kW)

$max (load_{B+\delta t})_T$  : Maximum power consumption with setpoint intervention, during DR period (kW)

These  $\Delta PR\%$ s are calculated by comparing base case peak demand (i.e., when the thermostat setpoint is 70°F) with peak demand after thermostat setpoint intervention (i.e., when thermostat setpoint is increased by  $\delta t$  °F from the base case thermostat setpoint).

#### 4.2.3 Analysis of Peak Demand Reduction Potentials

The effect of HVAC thermostat setpoint interventions is studied to quantify peak demand reduction potential across the selected commercial buildings portfolio. To estimate the average daily peak demand reduction, a thermostat setpoint intervention is made as described in [section 4.2.1](#) and ( $\Delta PR_{DR}\%$ ) is calculated using (3).

The average annual peak demand reduction % during the DR period resulting from 1-5°F interventions in thermostat setpoint temperatures across all buildings is summarized in [TABLE VIII](#).

The information about building sizes in sq.ft. and the ratio of HVAC load to the total building peak load is also presented. The HVAC-to-building peak load ratio is defined as per equation (4).

$$\begin{aligned} & HVAC - to - Building Peak Load Ratio (\%) \\ & = \frac{HVAC\ peak\ load}{Building\ peak\ load} \cdot 100 \end{aligned} \tag{4}$$

The correlation between peak demand reduction, outdoor temperature, and HVAC-to-building peak load ratio is discussed below.

#### 4.2.4 Correlation Between Peak Demand Reduction and Outdoor Temperature across Buildings

Peak demand reduction potential ( $\Delta PR$  %) due to thermostat setpoint intervention during the DR period is calculated according to equation (3). Note that peak demand for each building occurs during different times, based on operational schedule and load usage pattern of each building. Thermostat setpoint intervention during a specified time window is distinctively used as a tool for reducing peak power consumption of the building. The relationship between peak demand reduction potential at different thermostat setpoint interventions and average outdoor temperature ( $^{\circ}\text{F}$ ) during DR period ( $\Delta PR_{DR}$  %) is illustrated in Fig. 13.

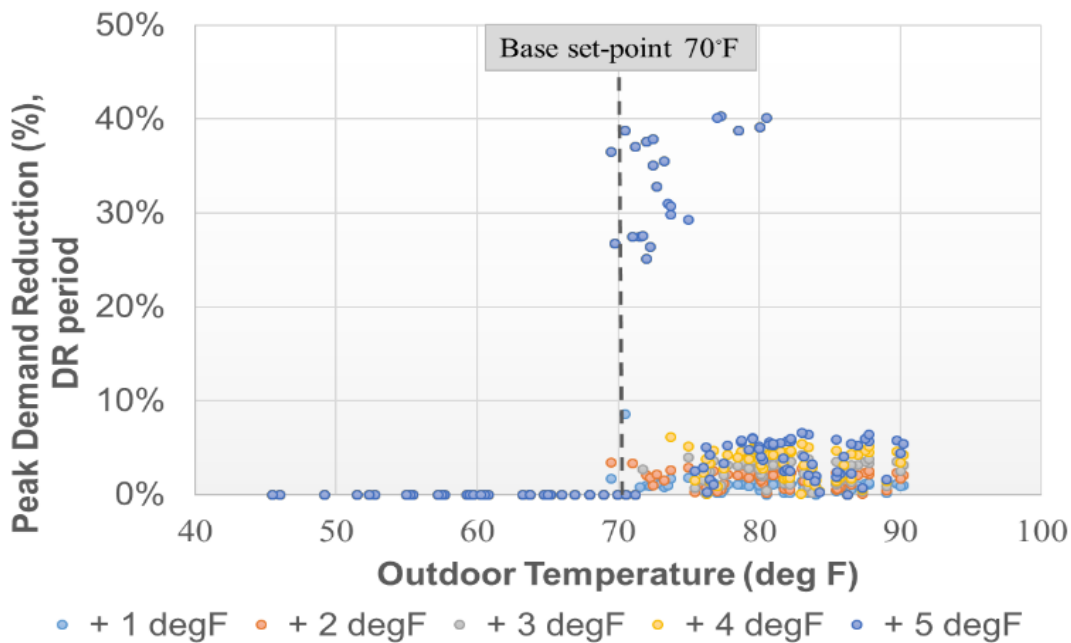


Fig. 13. Peak demand reduction ( $\Delta PR_{DR}$  %) vs. average outdoor temperature ( $^{\circ}\text{F}$ ) during DR period

Light blue dots represent peak demand reduction % during DR period for a 1 $^{\circ}\text{F}$  setpoint intervention, orange for 2 $^{\circ}\text{F}$ , gray for 3 $^{\circ}\text{F}$ , yellow for a 4 $^{\circ}\text{F}$  and blue for 5 $^{\circ}\text{F}$  thermostat setpoint interventions respectively. The y-axis represents peak demand reduction ( $\Delta PR$  %) across the DR period and the x-axis represents outdoor temperature ( $^{\circ}\text{F}$ ). The following specific observations are made, which are valid for all buildings under study:

- When average outdoor temperature during a DR event is below the base case thermostat setpoint, a thermostat setpoint intervention results in null value for peak demand reduction percentage. This is intuitive because on these cool days there is no HVAC operation. Hence, no savings can be achieved due to thermostat setpoint interventions.
- When average outdoor temperature is higher than the thermostat setpoint, but within a certain threshold (e.g.,  $70^{\circ}\text{F} < T < 80^{\circ}\text{F}$ ), peak demand reduction % during DR period varies greatly. This is because, in this temperature range, the HVAC unit may be either running or not running depending on indoor and outdoor temperature conditions. If the HVAC unit is running, a thermostat setpoint intervention could potentially lead to completely turning OFF the HVAC system, resulting in high savings. However, if the HVAC unit is not running, a thermostat setpoint intervention will not change the HVAC status, resulting in zero peak demand reduction. This explains why the peak demand reduction ( $\Delta PR_{DR}\%$ ) in this temperature band varies greatly.
- During hot days, when the average outdoor temperature is higher than  $80^{\circ}\text{F}$ , it is observed that raising the thermostat setpoint temperature results in a relatively predictable peak demand reduction % during the DR period.

#### 4.2.5 Correlation between Peak Demand Reduction and HVAC-to-Building Peak Load Ratio

TABLE VIII summarizes peak demand reduction potential across the five commercial buildings for different HVAC thermostat setpoint interventions.

TABLE VIII AVERAGE PEAK DEMAND REDUCTION ( $\Delta PR_{DR}\%$ ) ACROSS BUILDINGS AS A RESULT OF THERMOSTAT SETPOINT INTERVENTION

Building	Area (sq.ft.)	HVAC (%)	+1 degF (%)	+2 degF (%)	+3 degF (%)	+4 degF (%)	+ 5 degF (%)
High-rise Office	250,000	30.9	1.9	4.9	9.3	12.4	14.5
Mid-rise Office	125,000	30.4	1.0	2.2	4.5	7.2	8.9
Middle School	75,000	62.8	4.3	8.1	10.6	12.6	16.3
Strip Mall	15,000	64.4	3.8	7.7	11.8	16.1	20.1
Hospital	250,000	24.5	2.3	4.0	5.8	6.5	8.1

As shown, peak demand reduction potential during DR period ( $\Delta PR_{DR}\%$ ) ranges between 8.1% and 20.1% across the building portfolio, for a 5°F increase in setpoint temperature.

[TABLE VIII](#) also indicates that the hospital building offers least peak demand reduction% (8.1% at 5°F setpoint raise), while the strip mall building has highest peak demand reduction potential (20.1% at 5°F setpoint raise). This can be attributed to the HVAC-to-building peak load ratio. Buildings with higher HVAC-to-building peak load ratio have a higher peak demand reduction potential.

A plot between peak demand reduction potential during DR ( $\Delta PR_{DR}\%$ ) and HVAC-to-building peak load ratio is presented in [Fig. 14](#) for 5°F setpoint increase.

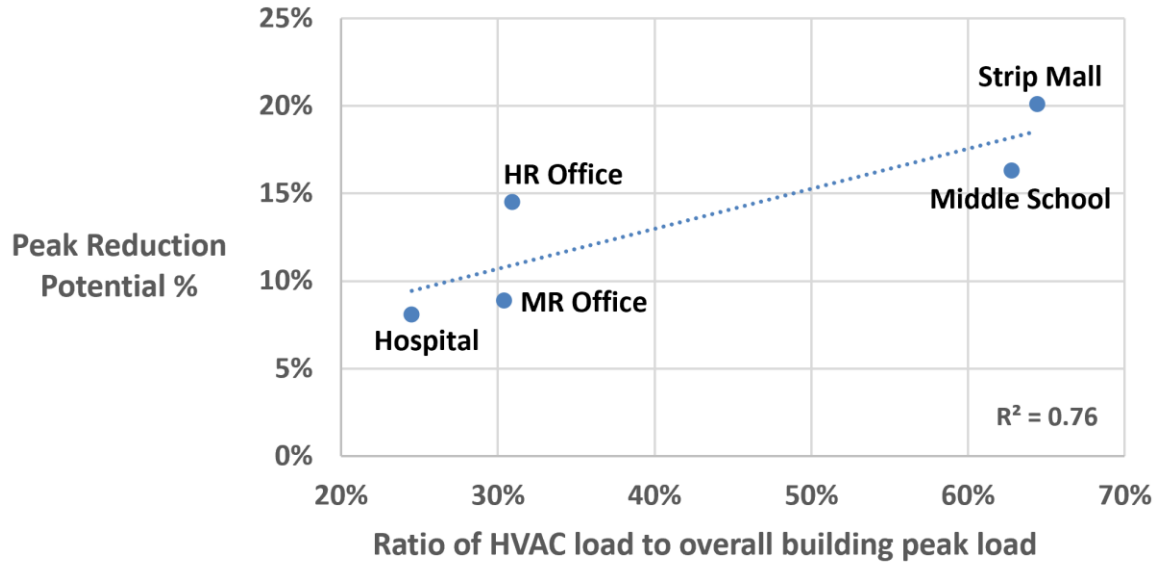
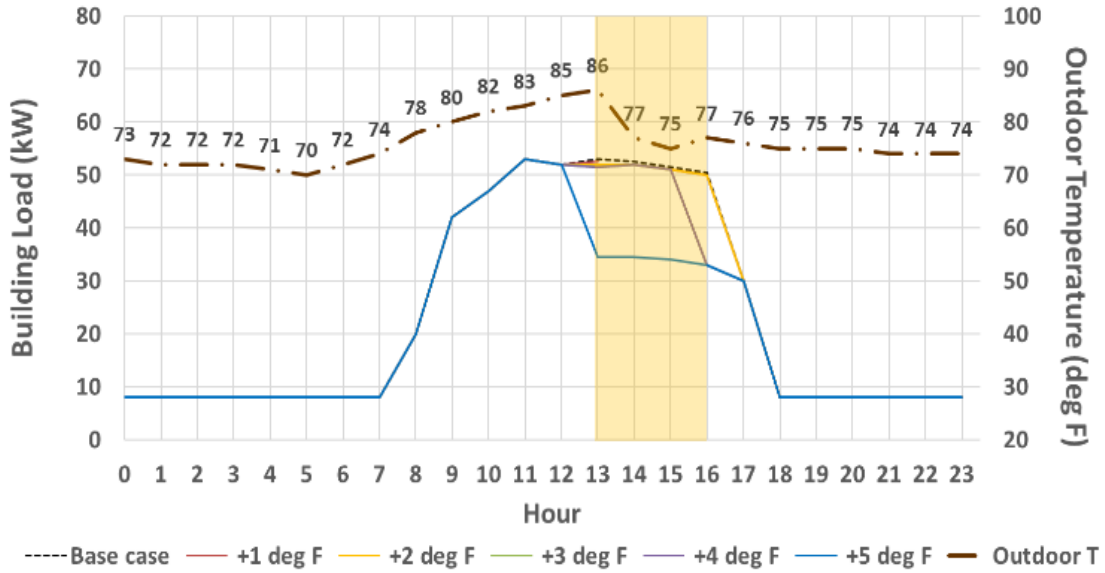
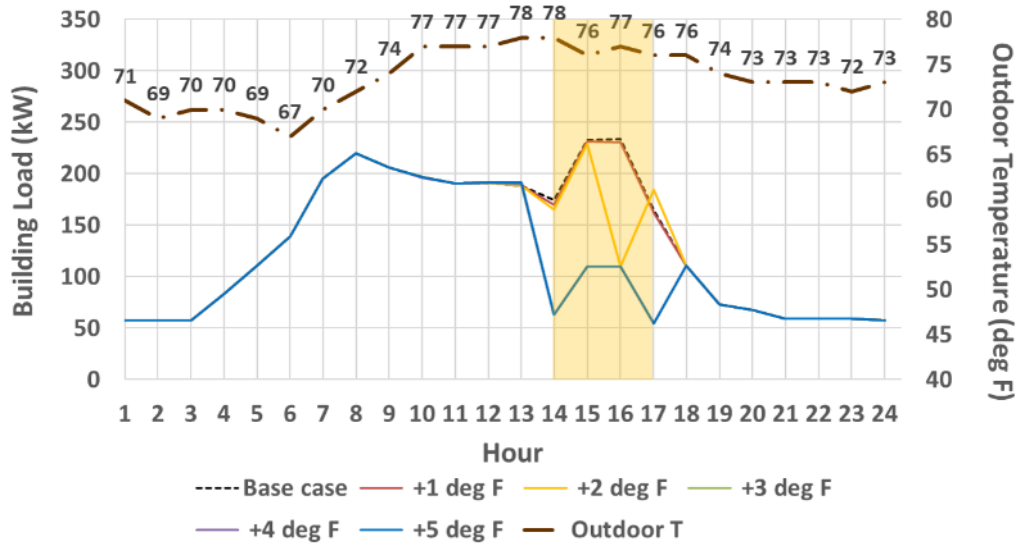


Fig. 14. Peak demand reduction ( $\Delta PR_{DR}$  %) vs. HVAC-to-building peak load ratio across all buildings for 5°F setpoint intervention

In [Fig. 14](#), blue dots represent the five commercial buildings; the y-axis represents peak demand reduction potential, and the x-axis represents the ratio of HVAC-to-total building peak load. (Same Fig. scheme conventions are extended to [Fig. 17](#) and [Fig. 19](#)). [Fig. 14](#) illustrates a linear correspondence between peak demand reduction % and HVAC-to-building peak load ratio across all buildings. As an example, [Fig. 15](#) shows the peak demand reduction potential of the strip mall and mid-rise office for different thermostat setpoint increments on corresponding days when maximum peak demand reduction occurs.



(a). Load profile of strip mall on 29th August 2016



(b). Load profile of mid-rise office on 15th August 2016

Fig. 15. Daily load profiles of two buildings with different HVAC-to-building peak load ratios on maximum peak reduction days

In Fig. 15, the black dotted line indicates actual building load, red for 1°F, yellow for 2°F, green for 3°F, purple for 4°F and blue for 5°F thermostat setpoint interventions, respectively. The dashed brown line indicates the hourly outdoor temperature in °F. The y-axis represents the building load (kW), and the x-axis represents time (hrs). The same naming convention and color scheme is extended to

([Fig. 18](#) and [Fig. 20](#)) as well. As shown, the HVAC-to-building peak load ratio has a significant influence on peak demand reduction potential of a building. Intuitively, this can be understood as a parameter representing load sensitivity of the building to thermostat setpoint temperature variation. Additionally, the peak demand reduction with each incremental degree has a somewhat linear trend. However, it is not strictly linear since peak demand reduction % due to thermostat setpoint change depends on initial setpoint temperature and variation in outdoor temperature with respect to it. This is because the HVAC system turns off upon performing a setpoint intervention, when the setpoint temperature is close to outdoor temperature.

### 4.3 Energy Savings across Buildings due to Thermostat Setpoint Interventions

This section describes the calculation of energy savings in different commercial buildings for each case of HVAC thermostat setpoint intervention. Correlation analyses of energy savings with respect to outdoor dry-bulb temperature and HVAC-to-building peak load ratio are also presented.

#### 4.3.1 Method for Thermostat Setpoint Interventions

The same method of thermostat setpoint interventions as discussed in [Section 4.2.1](#) is used.

#### 4.3.2 Calculation of Energy Savings Potential

Energy savings percentage (ES%), due to thermostat setpoint intervention, is calculated by comparing energy consumptions of the setpoint raise case (1-5°F increment) to base case (i.e., when the thermostat setpoint is 70°F) using equation (5).

$$\Delta ES\% = \frac{Energy_B - Energy_{B+\delta t}}{Energy_B} * 100 \quad (5)$$

$Energy_B$  : Energy consumption with base case thermostat setpoint of 70°F (kWh)

$Energy_{B+\delta t}$  : Energy consumption with thermostat setpoint interventions, i.e., when the setpoint temperature is increased by  $\delta t$  °F (kWh)

### 4.3.3 Analysis of Energy Savings Potential

The effect of thermostat setpoint intervention is studied to quantify corresponding energy savings potential across the selected five commercial buildings.

Observations regarding correlation between energy savings and outdoor temperatures, as well as correlation between energy savings and HVAC-to-building peak load ratio, are discussed below.

### 4.3.4 Correlation between Energy Savings and Outdoor Temperature across Buildings

To study the relationship between energy savings and outdoor temperature, a thermostat setpoint intervention is made, as described in [Section 4.2.1](#). Using (5), energy savings % due to thermostat setpoint intervention during the DR period, for each day is calculated for the indicated duration of summer. It is observed that energy savings percentage ( $\Delta ES\%$ ) at different setpoint interventions correlates with average outdoor temperature (°F), as depicted in [Fig. 16](#) (using middle school as example).

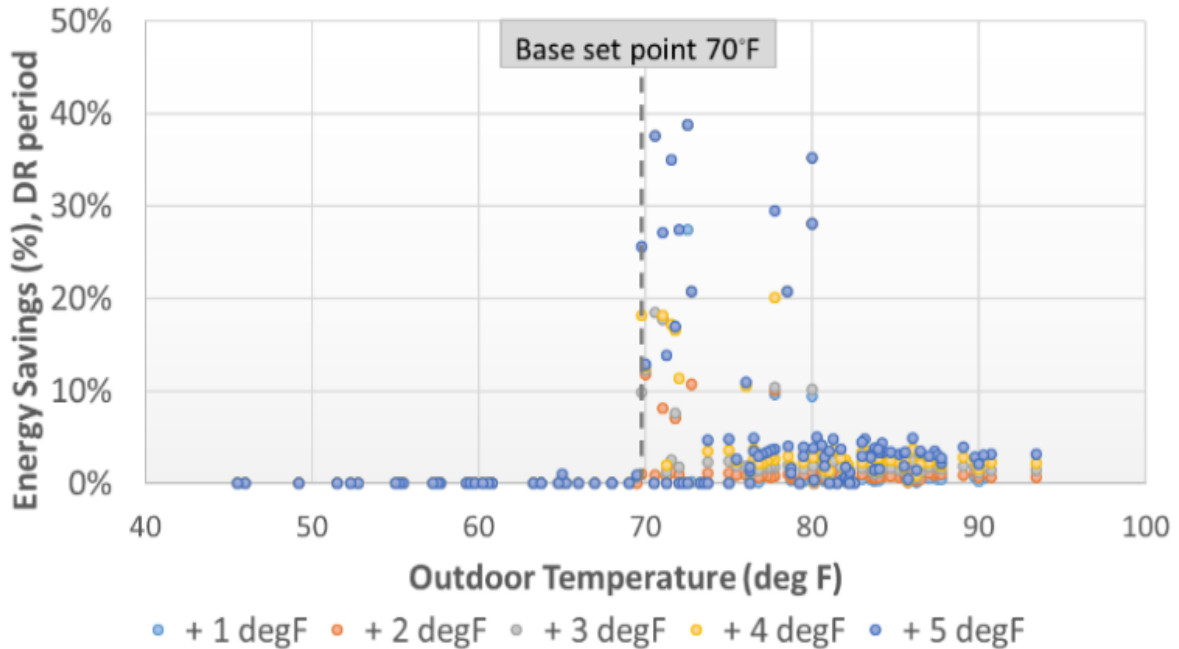


Fig. 16. Energy savings % due to HVAC interventions vs average daily outdoor temperature during DR period

The light blue dots represent energy savings % during the DR period for a 1°F setpoint intervention, orange for 2°F, gray for 3°F, yellow for 4°F and blue for 5°F thermostat setpoint interventions, respectively. The y-axis represents peak demand reduction ( $\Delta PR\%$ ) across the DR period, and the x-axis represents outdoor temperature (°F). As shown in [Fig. 16](#), the following patterns are observed, which are valid for all buildings under study:

- When the average outdoor temperature during a DR event is less than the base case thermostat setpoint, an increase in thermostat setpoint temperature will not contribute to energy savings. This is because AC does not operate on these days, and hence no energy savings can be achieved. This observation is similar to that of peak demand reduction cases.
- When the average outdoor temperature is higher than the thermostat setpoint temperature, but within a certain threshold (e.g.,  $70^{\circ}\text{F} < T < 80^{\circ}\text{F}$ ), setpoint interventions result in high variation in energy savings. The reason is the same as that of peak demand reduction cases.

- When average outdoor temperature is higher than the thermostat setpoint, but outside the threshold (i.e., for  $T > 80^{\circ}\text{F}$ ), a somewhat predictable energy savings % is observed with thermostat setpoint interventions. This is because raising the setpoint temperature will result in relatively lesser cooling needs of indoor space and hence proportionally lesser operational time of the units. This correlation is observed across all buildings, but with variations in energy savings percentage, which is further examined below.

#### 4.3.5 Correlation between Average Energy Savings and HVAC-to-Building Peak Load Ratio

[TABLE IX](#) summarizes average energy savings resulting from thermostat setpoint intervention across buildings when outdoor temperature is above the thermostat setpoint temperature.

TABLE IX AVERAGE ENERGY SAVINGS AS A RESULT OF THERMOSTAT SETPOINT INTERVENTIONS ACROSS ALL BUILDINGS

Building	Area (sq.ft.)	HVAC (%)	+1 degF (%)	+ 2 degF (%)	+ 3 degF (%)	+ 4 degF (%)	+ 5 degF (%)
High-rise Office	250,000	30.9	2.2	5.0	9.0	11.8	13.9
Mid-rise Office	125,000	30.4	4.6	5.9	8.1	10.1	11.7
Middle School	75,000	62.8	10.1	13.4	15.6	17.7	20.5
Strip Mall	15,000	64.4	3.6	7.5	11.4	15.4	19.1
Hospital	250,000	24.5	1.7	3.3	4.8	6.3	7.6

Energy savings potential across the buildings varies based on several attributes. As seen from [TABLE IX](#), similar to peak demand reduction case, the hospital building with lowest HVAC-to-building peak load ratio of 24.5%, offers least energy savings (7.6% at 5°F setpoint raise), while the strip mall with highest HVAC-to-building peak load ratio of 64.4%, offers high energy savings (19.1% at 5°F setpoint raise). Note that the middle school operates only for two hours during the DR window and hence the obtained energy savings are averaged across those two hours to keep the

% representation accurate. Hence, there exists a relationship between average annual energy savings and HVAC-to-building peak load ratio. A plot between these two parameters is presented in [Fig. 17](#), for a 5°F setpoint increase.

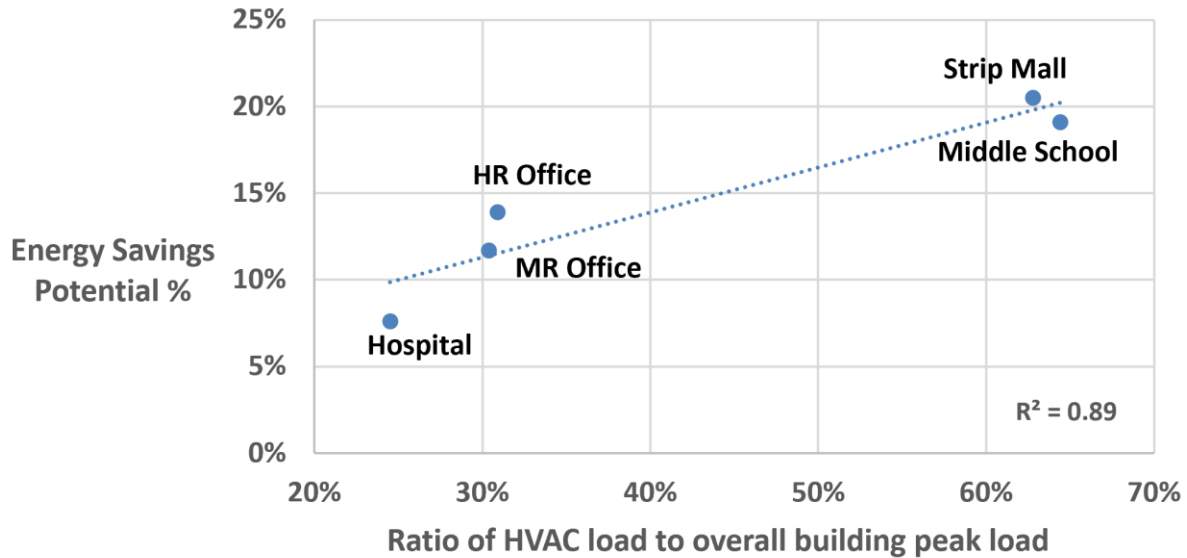
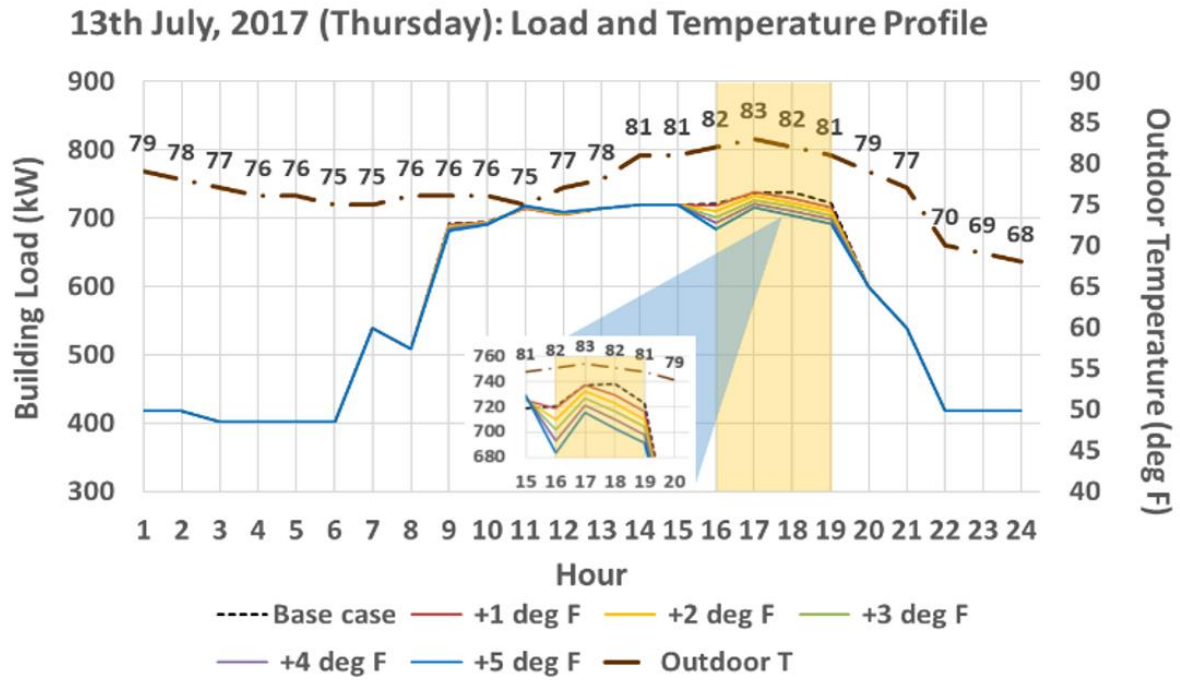


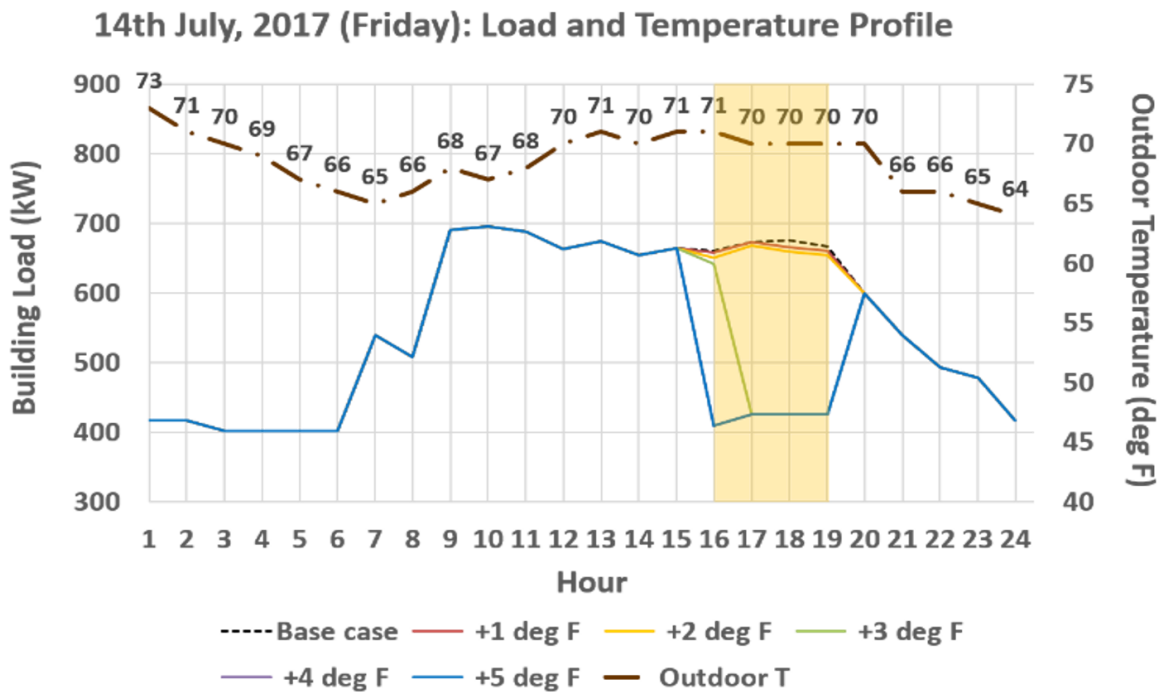
Fig. 17. Average annual energy savings % vs HVAC-to-building peak load ratio across all buildings for 5°F setpoint intervention

Note that the  $|R|$  value (Pearson’s correlation coefficient) for this plot is 0.94 indicating a strong linear correspondence between average energy savings and HVAC-to-building peak load ratio. That is, a building with higher HVAC-to-building peak load ratio provides larger overall energy savings. This can be reasoned as follows: any change in thermostat setpoint temperature has a direct impact on the operating cycle of the HVAC system. An increase in thermostat cooling setpoint temperature will decrease the HVAC operational time (i.e., AC compressor will be off until indoor temperature reaches the new setpoint temperature), therefore proportionally reducing HVAC energy consumption. Hence, intuitively it can be understood that higher HVAC load contribution in a building will result in higher energy.

Also, the nonlinear nature of energy savings for every incremental degree rise can be understood from [Fig. 18](#), which compares the operation of mid-rise office building on two consecutive summer days (13th July 2017 and 14th July 2017), with different outdoor temperature conditions.



(a). Load profile of mid-rise office building on 13th July 2017



(b). Load profile of mid-rise office building on 14th July 2017

Fig. 18. Load profile of the mid-rise office building with thermostat setpoint increments on two days with different outdoor temperature conditions

In [Fig. 18](#), on 13th July 2017, the outdoor temperature ranged between 81-83°F during the DR period and reached a peak value of 83°F between 3-4 PM. On this day, the HVAC system was continuously *on* throughout the building’s operation and hence, we see a relatively small energy savings ranging between 1 – 3.7% for a 1-5°F setpoint increment, throughout the day. Whereas, on 14th July 2017, a setpoint raise of 5°F turned off the HVAC system as the outdoor temperature dropped, resulting in much higher energy savings. A comparison of load and outdoor temperature profiles on 13th and 14th July 2017, shows that energy savings due to thermostat setpoint change depends on initial setpoint temperature and variation in outdoor temperature with respect to it.

#### 4.3.6 Correlation between Maximum Energy Savings and HVAC-to-Building Peak Load Ratio

The maximum energy savings in buildings also has a linear correlation with respect to HVAC-to-building peak load ratio, as depicted in [Fig. 19](#).

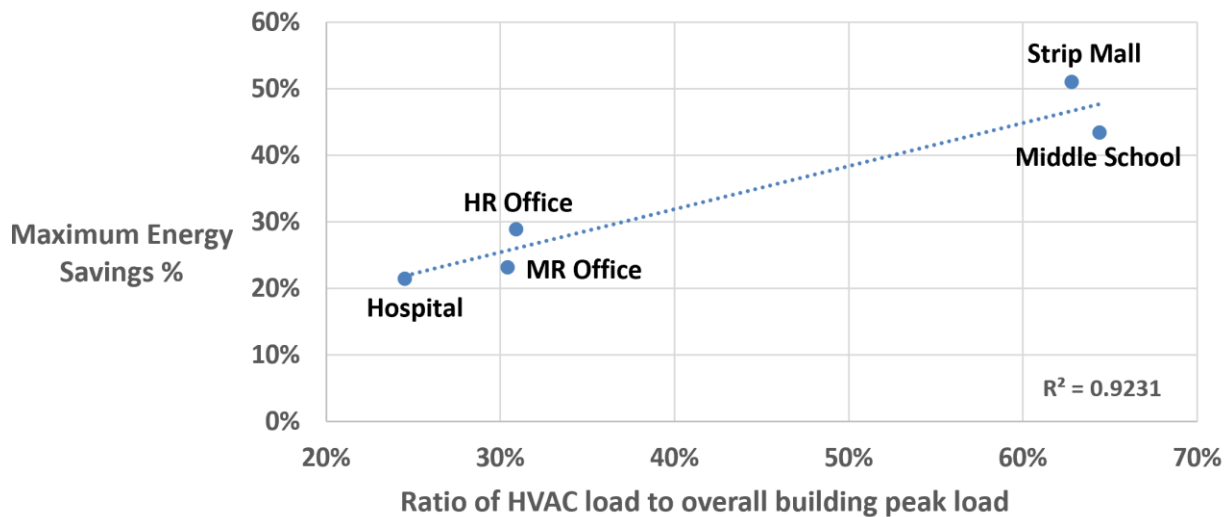
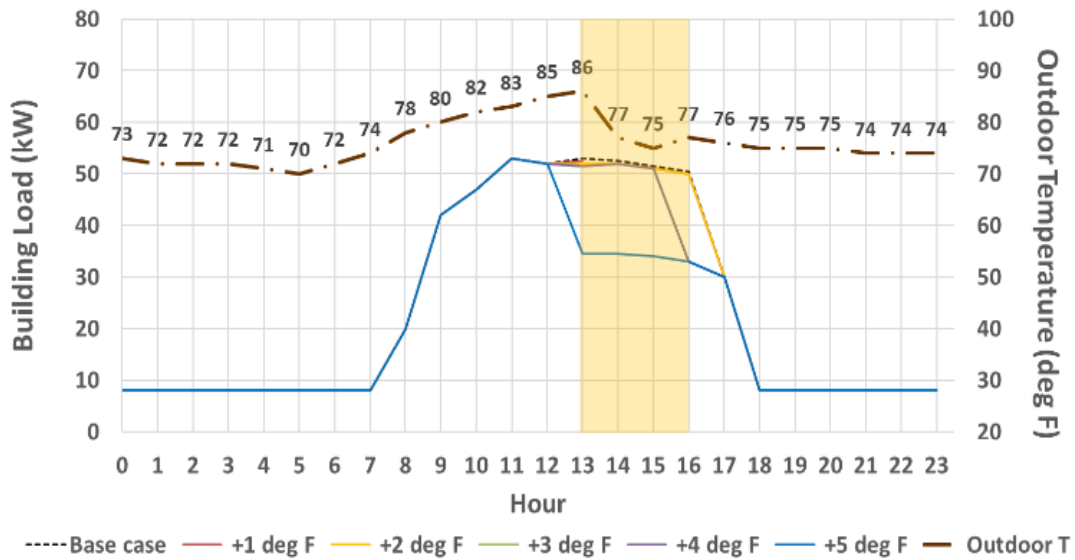


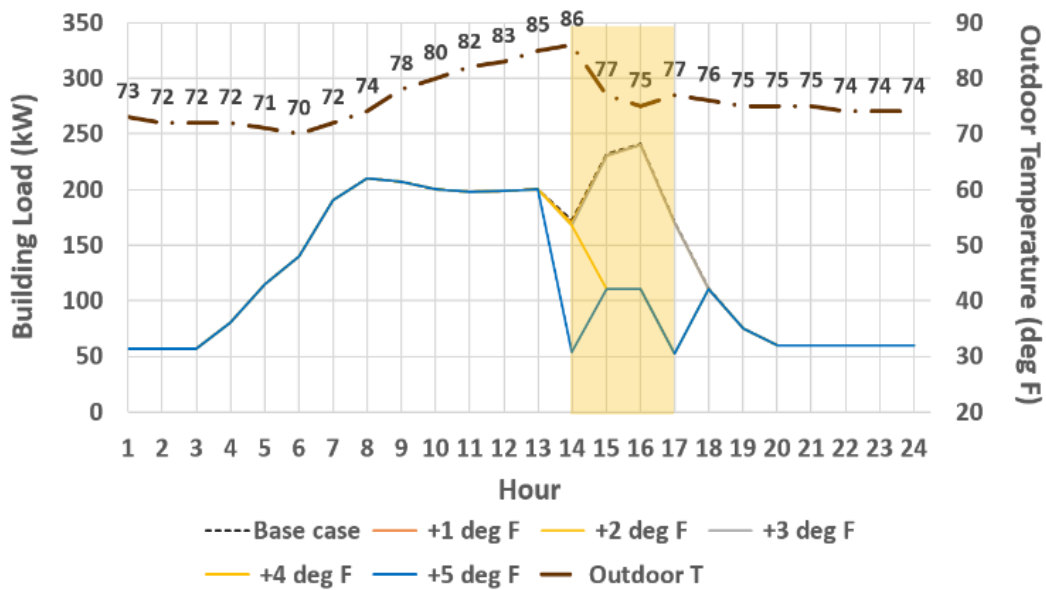
Fig. 19. Maximum energy savings % vs HVAC-to-building peak load ratio across all buildings for 5°F setpoint interventions

A strong linear relationship is observed between maximum energy savings obtained in a building and its HVAC-to-building peak load ratio. As depicted in [Fig. 19](#), hospital building with lowest HVAC-to-building peak load ratio has the least energy savings % and strip mall with the highest HVAC-to-building peak load ratio has the highest energy savings percentage.

Fig. 20 compares load profiles of buildings with different HVAC-to-building peak load ratios, on the maximum energy savings day.



(a). Load profile of the strip mall on 29th August 2016



(b). Load profile of the mid-rise office building on 29th August 2016

Fig. 20. Daily load profiles of two buildings (strip mall and mid-rise office) with different HVAC-to-building peak load ratios during respective maximum energy saving days

As seen from Fig. 20, HVAC-to-building peak load ratio has a strong bearing on maximum energy savings percentage, since maximum energy savings due to

thermostat setpoint intervention during DR period is primarily contributed by HVAC load in the building.

Based on the insights gained by studying the impact of HVAC thermostat setpoint interventions on peak demand reduction in commercial buildings, an AHP-based demand curtailment tool is developed. This tool operates in a day-ahead electricity market and addresses the co-incidental peak demand (see [section 2.1.1.1](#)) occurring in the electrical distribution grid. Further details regarding the construction, operation and performance of the proposed demand curtailment tool are presented in Chapter 5.

# **5. AHP-BASED PEAK DEMAND CURTAILMENT ALLOCATION USING HVAC THERMOSTAT SETPOINT INTERVENTIONS**

## **5.1 Introduction**

The objective of this research is to develop a peak demand curtailment tool to obtain the distribution of demand curtailment allocation among a group of commercial buildings. The affected demand curtailment in these commercial buildings is subject to occupant indoor thermal comfort and other logistical constraints.

During peak summer months, electric utility companies often try to curtail load to alleviate grid stress conditions by incentivizing larger organizations, comprising multiple commercial buildings, for demand reduction. Therefore, contracts are signed with the parent organization for ensuring a specified amount of demand curtailment on any given day. To ensure that this requirement is met, appropriate demand curtailment allocation must be made amongst the group of participating commercial buildings. Each building is unique and thus expert opinion is required to assess the limits of building demand reduction capacity.

To fulfill this objective, an AHP-based framework is developed for demand curtailment allocation between different commercial buildings. This is affected solely through demand management strategies; specifically, using HVAC thermostat setpoint interventions and lighting control.

## **5.2 Literature Review: Uniqueness of the Proposed AHP-based Approach**

The grid peak demand curtailment problem is a critical one to solve in order to extend the service life of grid assets like transformers, relays, lines, etc., Addressing this challenge using a building-to-grid integrating framework is both complex and difficult. However, a well-engineered solution accounting for interactions between different stakeholders in the system provides an excellent solution by very effectively managing the peak demand at the electric utility grid level. The buildings are complex dynamic systems with multiple thermo-mechanical elements to

coordinate and cannot respond to real-time control quickly enough. While this is so, the electric grid is a real-time power processing dynamic system wherein the energy balance equation must be always satisfied, allowing for no internal storage. Hence, latency is an inevitable part of grid-to-building command execution. Therefore, this solution works in the day-ahead electricity market, hence facilitating the coordination between electric grid and buildings. In addition, we have to coordinate with a number of stakeholders like the weather monitoring station and the participating commercial buildings. This involves integrating heterogeneous data into one place to arrive at a convergent solution. Additionally, this solution has to be executed every day, as the energy usage in the buildings varies on a day-to-day basis. So far, the traditional approaches to grid peak shaving only include solutions using solar PV and battery storage systems to effectively utilize alternate forms of energy during peak demand times.

For example, in [106], the authors present a design of grid-connected rooftop solar PV system for electrical peak demand shaving. Design details of the corresponding grid-connected PV system at Andalas University, Indonesia are included. In [107], authors discuss peak demand shaving in a community energy service center (with 3000 households) using an ESS. They also discuss variation in peak shaving with an increase in capacity of ESSs used in the community grid. The authors in [108] developed an adaptive method for load-based mechanism supporting peak shaving with ESS, using load curve of a power substation. In [109], a microcontroller-based solution for battery ESS, integrated with the solar PV system, was designed and developed. Here, the authors have used a solar PV system to charge a lead acid battery and microcontroller to appropriately discharge it during peak demand times, along with keeping battery life in purview. Further, the authors in [110] present a case for improved peak shaving in grid-connected domestic power systems combining PV generation, battery storage and vehicle-to-grid-capable EV. Results indicate that by effectively utilizing these technologies, a grid peak shaving of 37% was achieved.

While the proposed methods have been able to successfully address peak shaving, additional infrastructure and significant design modifications to the status quo are essential. In this paper, we propose to influence grid peak shaving by solely using

demand management strategies. This is done by utilizing the building-to-grid integration framework to perform coordinated HVAC thermostat setpoint interventions in participating commercial buildings. This paper details the development of a peak-shaving tool which is robust, agile and can be scaled easily. The solution's architecture is composed of three aspects: building information modeling (BIM), an AHP-based framework, and smart thermostats [111].

As a first step, hourly building energy models of participating commercial buildings are created using a BIM framework. In this study, we are using eQUEST 3.65 to construct building energy models. A four-level AHP framework is constructed to effectively allocate demand curtailment between participating commercial buildings. The developed building models are now utilized to translate this demand curtailment into required HVAC thermostat setpoint interventions.

Due to increasing adoption of smart thermostats, recent studies have shown a growing interest in DSM of air-conditioning loads. It is evidenced that performing an HVAC thermostat setpoint intervention is an effective way of demand control. In [112], DSM of air conditioning cooling loads for intra-hour load balancing is studied. In [113], authors propose an interruptible load scheme for DR management in buildings. In this study, the EV charging station, HVAC system, corridor lighting, car parking ventilation fan and storage tank water pump are considered as interruptible loads. Occupant-based HVAC setpoint interventions for energy savings in buildings has been studied in [114]. Impact of HVAC setpoint adjustment on energy savings and peak demand reductions in buildings has been studied in [20]. Further, the impact of Solar PV, battery storage and HVAC setpoint adjustments on energy savings and peak demand reduction potentials in buildings have been examined in [115]. Modeling and control of central air conditioning loads for peak shaving has been researched in [116].

These solutions are one-sided and require additional infrastructure to address this problem. In order to engineer a thorough building-to-grid integration framework, we need to approach the grid peak demand curtailment problem more holistically. We must consider the buildings as a part of the system and account for the interactions between different stakeholders in the system. The focus of this paper is to present an AHP-based scheme for grid peak shaving using HVAC thermostat setpoint

interventions in commercial buildings. While these methods deliver insights at an individual building level, they are of little utility when it comes to a global scheme of operation where several buildings must be coordinated synergistically, especially with reduced modes of operations. AHP is an excellent multi-criteria decision-making tool with a wide variety of applications. This is especially useful in situations where quick approximate solutions are sought with imprecise input details. Relevant studies using AHP-based solutions include demand curtailment allocation among different distribution substations [97] and for demand limit allocation between different customer groups and corresponding appliance schedule modifications (clothes dryer, HVAC, and water heater) in residential buildings [98]. Due to this versatile nature, utilizing the AHP based framework appears to be the appropriate avenue towards designing the solution. Hence, we have devised a grid peak mitigation scheme grounded on AHP to address this research gap.

The strength of this work is further demonstrated by evaluating the proposed scheme via case studies for varying amounts of electric grid peak demand curtailment on a very hot day (1<sup>st</sup> July 2019) in Blacksburg, VA. The key research gap addressed here is the development of an aggregated DR-scheme among a portfolio of diverse commercial buildings under the control of a DR aggregator. The unique contribution of this paper is in developing an expert opinion-based distribution of demand curtailment among a portfolio of buildings based on various parameters pertaining to individual buildings and corresponding translation of the appropriate demand curtailment into HVAC thermostat setpoint interventions using building energy models. The overall idea of this study is depicted in [Fig. 21](#). This chapter is organized as follows: [Section 5.3](#) gives an overview of the tool's operation in a day-ahead electricity market; [section 5.4](#) describes the methodology and model development of the proposed AHP framework; [section 5.5](#) details the operation of the overall system using case studies conducted on a hot summer day in Blacksburg, VA; corresponding results are presented in [section 5.6](#); and [section 5.7](#) concludes the chapter by summarizing findings and discussing the scope of future work.

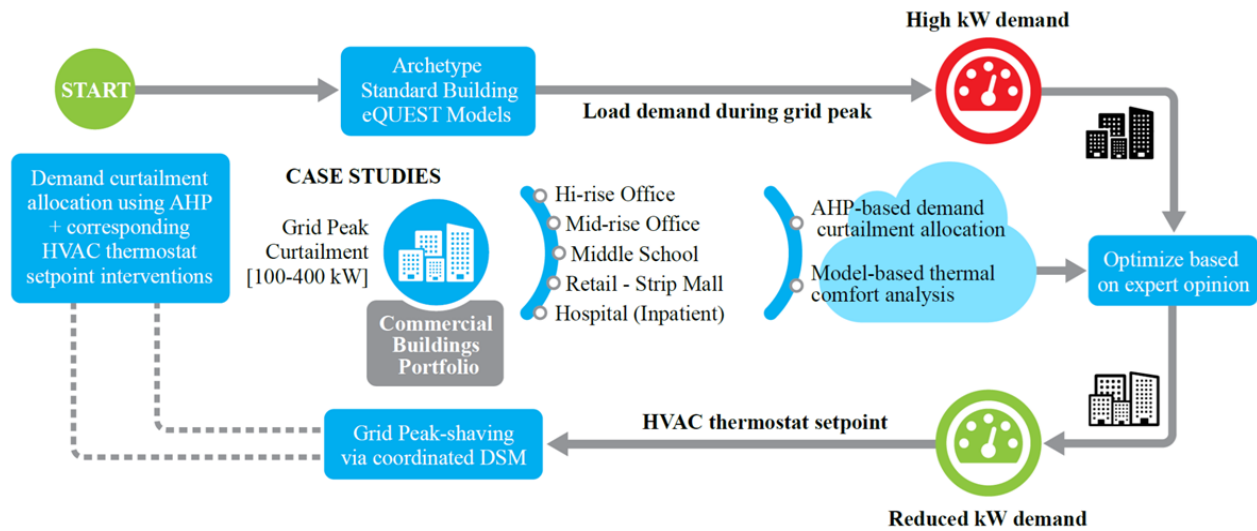


Fig. 21. Overall operation of the AHP-based HVAC setpoint intervention scheme

### 5.3 Scheme of Operation in a Day-ahead Electricity Market

The proposed AHP-based demand curtailment tool is envisioned to operate in a day-ahead electricity market. The flow of information between electric grid operator, third party service provider (building aggregator) and building operator is represented in Fig 22. The communication between these participating entities can be classified into three stages: pre-transaction, during transaction and post-transaction. Since the tool is positioned to operate in the day-ahead electricity market, the end-to-end execution of the DR event spans two days: day-prior to DR event and day-of DR event. The pre-transaction phase occurs on the prior day while the transaction and post-transaction phase happens on the DR event day. Note that in this scheme of operation, whenever a signal is sent between two entities, the receiving entity will always return a confirmation message of communication, ensuring the integrity of the transaction.

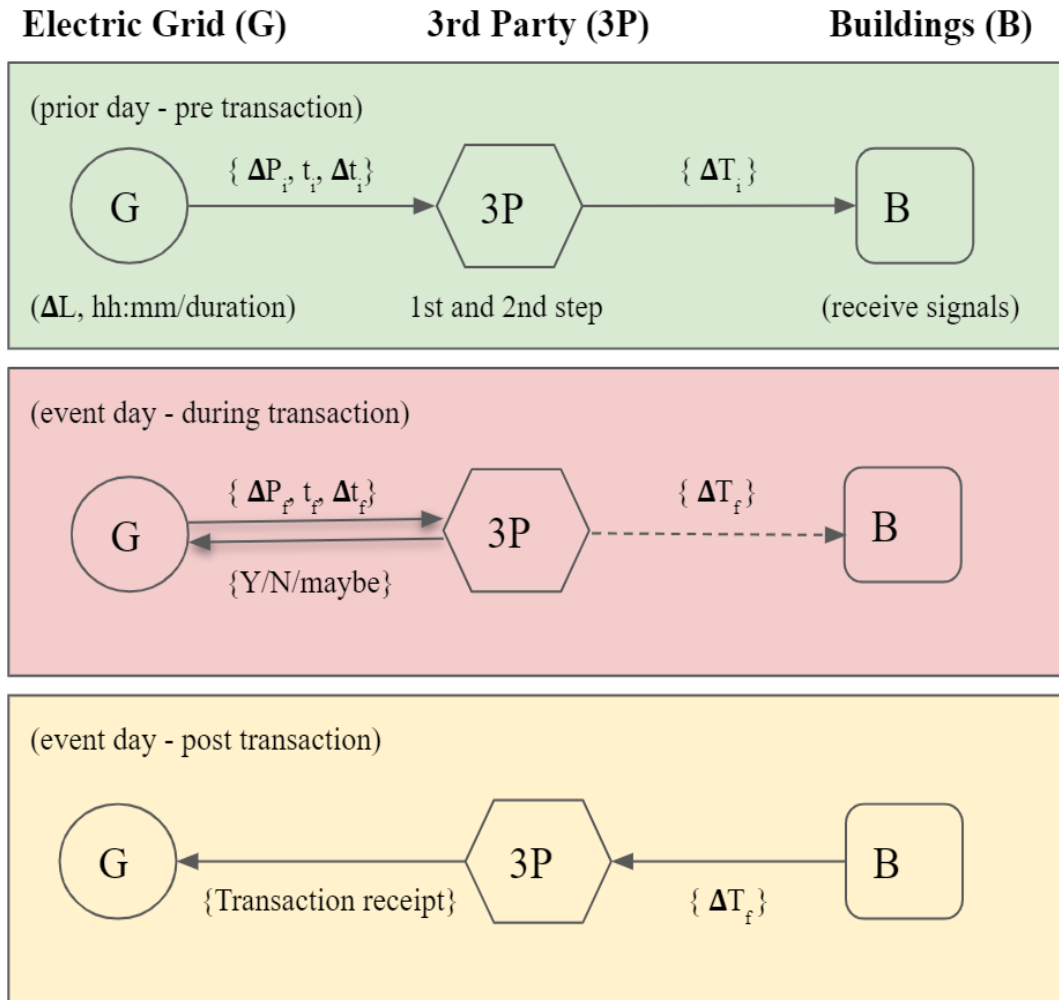


Fig. 22. Communication scheme for the AHP-based demand curtailment tool in a day-ahead electricity market

In the pre-transaction phase, the electric grid operator (G) sends information regarding the requested load curtailment ( $\Delta P_i$ ), start time of the DR event on the next day ( $t_i$ ) and duration of the DR event ( $\Delta t_i$ ), to the third-party service provider (3P). The third-party service provider now executes the two-step AHP algorithm (see [Fig. 23](#)) and gives the appropriate HVAC thermostat setpoint interventions  $\{\Delta T_i\}$  as output. Note that the proposed demand curtailment scheme is designed to incorporate an overwrite on the pre-transaction phase information until two hours prior to the start of the DR event. The dashed arrow during the transaction indicates a conditional possibility of a data overwrite. This feature is incorporated to provide flexibility in execution in case of changes in requested demand curtailment or DR event start time or duration. When there is an event data overwrite, steps in the pre-

transaction phase are repeated with a new dataset  $\{\Delta P_f, t_f, \Delta t_f\}$  resulting in the corresponding HVAC thermostat setpoint intervention dataset  $\{\Delta T_f\}$ . Supposing there are no changes on the DR event day,  $\Delta T_i = \Delta T_f$ . On the DR event day, after the DR event takes place, the final values of HVAC thermostat setpoint interventions are communicated back to the third-party service provider. The third-party service provider now generates a transaction report encompassing all the details of the DR event. In this way, a two-day spanning end-to-end transaction is executed to perform the necessary DR event. The detailed steps in operation of electric grid peak demand curtailment algorithm described in [Fig 20](#) are listed below:

**Algorithm: Procedure for grid peak demand curtailment**

1. 3P gathers input information:
  - a. Grid peak curtailment information ( $\Delta P_i, t_i, \Delta t_i$ )
  - b. Weather data [48hrs] ( $T_{\text{dry-bulb}}, \text{Rh}\%$ )
  - c. Expert opinions
  - d. Physical attributes of buildings
  - e. Initial setpoint temp and indoor temp ( $T_o, T_{\text{ind}}$ )
2. Run the AHP module - output ( $\Delta p_i$ )
3. Translating ( $\Delta p_i$ ) into ( $\Delta T_i$ )
4. Indoor Temperature check - ASHRAE Standard 55 - identify the building reaching its thermal limit
5. **while** indoor temperature of all buildings  $> T_{\text{max}}$ 
  - a.  $\Delta T_i$  is modified into  $\Delta T_i^*$  in this building (capping)
  - b. Calculate deficit reduction to be redistributed
  - c. Run the AHP module - redistribute load
  - d. Translating ( $\Delta p_i$ ) into ( $\Delta T_i$ )
  - e. Indoor Temperature check - ASHRAE Standard 55 - identify the building reaching its thermal limit

6. **end while**
7. Outputs ( $\Delta p_f$ ) and ( $\Delta T_f$ )

Where,

- 3P : third party service provider
- $\Delta P_i$  : demand curtailment request (kW)
- $t_i$  : timestamp of start of DR event (hh:mm)
- $\Delta t_i$  : duration of the DR event (min)
- $T_{\text{dry-bulb}}$  : outdoor dry-bulb temperature ( $^{\circ}\text{F}$ )
- Rh : relative humidity (%)
- $T_o$  : initial HVAC thermostat setpoint temperature ( $^{\circ}\text{F}$ )
- $T_{\text{ind}}$  : zonal indoor temperature of the building ( $^{\circ}\text{F}$ )
- $T_{\text{max}}$  : maximum value of indoor temperature per ASHRAE 55 standard ( $^{\circ}\text{F}$ )
- $\Delta p_i$  : initial building demand curtailment calculated by AHP model (kW)
- $\Delta p_f$  : final (adjusted) building demand curtailment (kW)
- $\Delta T_i$  : initial HVAC thermostat setpoint intervention ( $^{\circ}\text{F}$ )
- $\Delta T_i^*$  : modified HVAC thermostat setpoint intervention due to capping ( $^{\circ}\text{F}$ )
- $\Delta T_f$  : final (adjusted) HVAC thermostat setpoint intervention ( $^{\circ}\text{F}$ )

Overall flow chart of the algorithm is depicted in [Fig. 23](#)

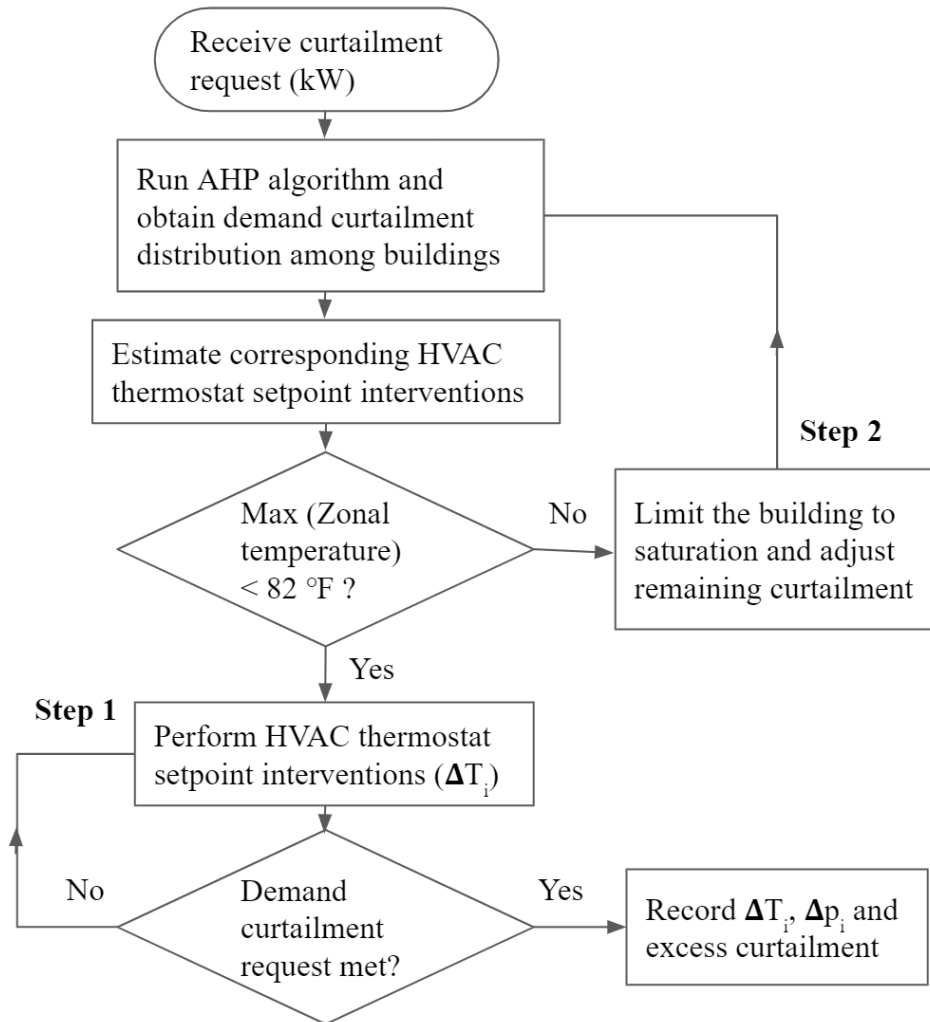


Fig. 23. Flowchart illustrating the two step AHP-based demand curtailment algorithm

As listed in the algorithm procedure and [Fig. 23](#), once the relevant details are gathered and the demand curtailment request is received, the AHP algorithm is run to obtain the required demand curtailment allocated to each participating building. This is now translated into corresponding HVAC thermostat setpoint intervention using the high-fidelity building energy models described in [Chapter 3](#). The indoor temperature of all the zones in the building are monitored to ensure that the indoor temperature lies within the limits specified by ASHRAE standard 55 (Thermal Environmental Conditions for Human Occupancy). If this condition is respected, the corresponding setpoint interventions are deemed valid. In case of a violation, the second step is taken to cap the intervention on the building that reaches limiting conditions and the deficit curtailment is redistributed among the remaining

participating commercial buildings. This ensures that the requested electric grid peak demand curtailment is successfully honored without violating the thermal comfort constraints within any zone of the participating commercial buildings. A detailed methodology and model description of the proposed AHP-based peak demand curtailment scheme is described further in [section 5.4](#).

## 5.4 Methodology and Model Description

This section describes the AHP model constructed as a part of the overall solution and gives specific details about its working.

### 5.4.1 Overall Methodology:

The overall methodology followed in this study is depicted in [Fig. 24](#). The first step entails development of building energy models based on attributes like layout, area, orientation, fenestration information, ASHRAE standards and LEED new construction certification requirements. A four-level AHP structure is developed by taking input from relevant experts – a building engineer and electric utility operator/independent system operator (ISO) (see [Fig. 25](#) for more details). Along with these experts' opinions, information regarding the building's physical attributes is given as input to the AHP framework, as illustrated in level 3 of [Fig. 25](#). These details are used to make pairwise comparisons between different criteria. Optimal demand curtailment required in each building is then calculated based on these pairwise comparisons. This research primarily focuses on affecting demand curtailment via HVAC thermostat setpoint interventions as the magnitude of the HVAC load is the highest in commercial buildings. Following the procedure shown in [Fig. 24](#), case studies are conducted for varying levels of load curtailment requests to understand the tool's performance in extreme conditions. The outcome of these experiments is summarized in the results, discussion, and conclusion sections, respectively.

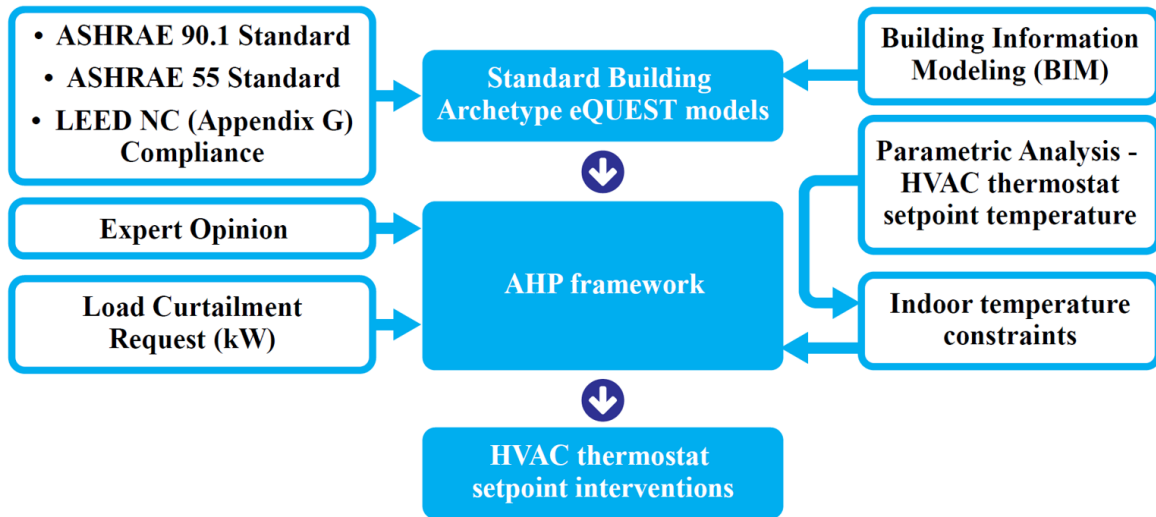


Fig. 24. Block diagram of AHP-based demand curtailment procedure among commercial buildings

#### A. AHP-based framework

The AHP based framework used here, as discussed in [section 5.4.2.1](#), allocates the appropriate amount of demand curtailment to different commercial buildings.

#### B. Commercial building energy models

The commercial building energy models used in this chapter have been developed using the portfolio of commercial buildings showcased in [section 3.8](#). Since all the buildings used in this study are located in Blacksburg, the spatial variance of outdoor temperature has been ignored.

#### C. HVAC thermostat setpoint interventions

Now, an intervention is made in the HVAC thermostat cooling setpoint during the DR period by raising the base case setpoint appropriately. 70°F is chosen as the base case setpoint for all the buildings.

After the AHP algorithm yields the necessary vector of weights for demand curtailment allocation, the developed building energy models are employed to translate corresponding demand curtailment into appropriate HVAC thermostat setpoint interventions. The bracket of HVAC thermostat setpoint interventions used in this study, ranges from 1-5°F. For the sake of simplicity, only integral values of HVAC thermostat setpoint interventions are considered in this study.

### 5.4.2 Methodology of AHP:

This section describes the AHP model and details the inputs and outputs of the model. Further, the overall working of the model is presented with clearly illustrated computations at each level.

#### 5.4.2.1 Description of AHP Model

A four-level AHP structure (shown in Fig. 25) is used for allocating demand curtailment among different commercial buildings. The expert opinion at level 1 and building attributes at level 3 serve as inputs to the AHP model. The expected output of the AHP model is distribution of demand curtailment among various participating buildings shown in level 4. The working principle behind AHP framework is performing pairwise comparisons between attributes at the  $n^{\text{th}}$  level to arrive at an eigenvector of weights/priorities for criteria at  $(n-1)^{\text{th}}$  level.

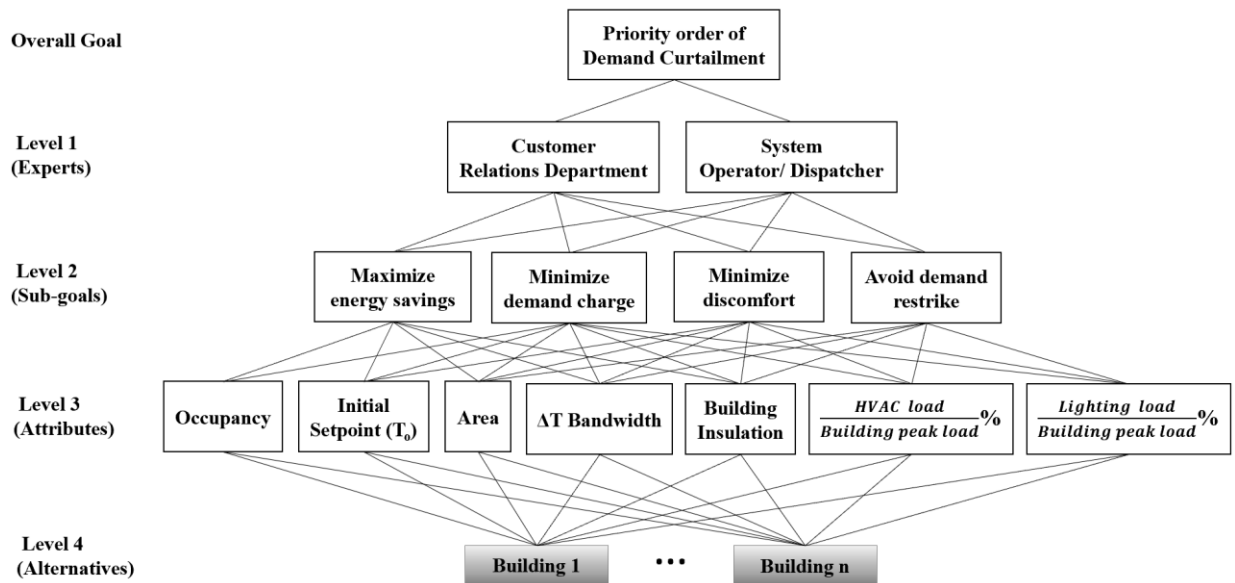


Fig. 25. Four-level hierarchical AHP structure for grid peak demand curtailment

#### 5.4.2.2 AHP Model: Inputs and Outputs

This section describes the overall inputs and outputs of the proposed AHP model. It also presents the inputs and outputs at each level of the four-level hierarchical structure.

#### 5.4.2.2.1 Inputs

In addition to building attributes, inputs to the AHP model at different levels include grid peak curtailment request, weather data from the weather monitoring station, and expert opinions from the commercial building operator and electric utility operator.

#### 5.4.2.2.2 Outputs

Using expert opinions and the attributes shown in level 3 of [Fig. 25](#), the AHP model is expected to deliver a building load curtailment vector as the output. To calculate demand side curtailment factor ( $W$ ), a table with actual data of seven attributes across selected buildings must be obtained. For each attribute, a pairwise comparison matrix is created. The eigenvectors are calculated, and resulting normalized eigenvectors associated with the maximum eigenvalue are taken as weighting factors for that criterion. By repeating the aforementioned steps, a priority vector for each attribute is obtained. By combining priority vectors for the seven attributes, the overall building load curtailment priority vector (of size  $5 \times 7$ ) is obtained.

#### 5.4.2.2.3 AHP Process Flow: Pairwise Comparisons and Priority Vector Computations

To obtain the overall curtailment priority order, pairwise comparison matrices need to be constructed at every level of the hierarchy using the scale of relative preference given in [TABLE X](#) [117].

TABLE X AHP SCALE OF PREFERENCE BETWEEN TWO ELEMENTS

Scale of Importance	Interpretation
1	Equal importance
3	Moderate importance
5	Strong importance
7	Very strong importance
9	Absolute importance
2, 4, 6, 8	Intermediate values between adjacent scale values

#### 5.4.2.3 Pairwise Comparison Matrices at each level of the AHP Structure in [Fig. 25](#)

The corresponding pairwise comparison matrices at each level of the AHP structure are listed in [section 5.4.2.3.1](#) - [section 5.4.2.3.4](#).

##### 5.4.2.3.1 Level 1 - Pairwise Comparison Matrix of Expert Opinions with Respect to Demand Curtailment Allocation (Overall Goal)

[TABLE XI](#) represents a pairwise comparison matrix showing the importance of the customer relations department (building manager) and electric utility operator.

TABLE XI PAIRWISE COMPARISON MATRIX OF EXPERT OPINIONS

Experts	Customer Relations	System Operator
Customer Relations	1	1/3
System Operator	3	1

#### 5.4.2.3.2 Level 2 - Pairwise Comparison Matrix of the Sub-goals with respect to Experts

Pairwise comparison matrices of sub-goals with respect to the customer relations department and system operator are shown in [TABLE XII](#) and [TABLE XIII](#), respectively.

TABLE XII PAIRWISE COMPARISON MATRIX OF THE SUB-GOALS WITH RESPECT TO CUSTOMER RELATIONS DEPARTMENT

<b>Sub-goal description</b>	Maximize energy savings	Minimize demand charge	Minimize discomfort	Avoid demand restrike
Maximize energy savings	1	1	4	4
Minimize demand charge	1	1	3	2
Minimize discomfort	1/4	1/3	1	2
Avoid demand restrike	1/4	1/2	1/2	1

TABLE XIII PAIRWISE COMPARISON MATRIX OF THE SUB-GOALS WITH RESPECT TO SYSTEM OPERATOR

<b>Sub-goal description</b>	Maximize energy savings	Minimize demand charge	Minimize discomfort	Avoid demand restrike
Maximize energy savings	1	1/2	3	1/5
Minimize demand charge	2	1	3	1/5
Minimize discomfort	1/3	1/3	1	1/6
Avoid demand restrike	5	5	6	1

5.4.2.3.3 Level 3 - Pairwise Comparison Matrix of the Attributes with respect to each Sub-goal:

Similar pairwise comparisons are made between different attributes with respect to each sub-goal. The corresponding pairwise comparison matrices are shown in [TABLES XIV-XVII](#). Equivalent to defining HVAC-to-building peak load ratio in Chapter 4, the lighting-to-building peak load ratio is defined as per equation (6).

$$\begin{aligned} & \text{Lighting – to – Building Peak Load Ratio (\%)} \\ & = \frac{\text{Lighting load}}{\text{Building peak load}} \cdot 100 \end{aligned} \quad (6)$$

TABLE XIV MAXIMIZING ENERGY SAVINGS – PAIRWISE COMPARISON OF ATTRIBUTES

Attributes	Occupancy	Initial setpoint (T <sub>o</sub> )	Area	ΔT bandwidth	Building Insulation	$\frac{\text{HVAC load}}{\text{Building peak load}} \%$	$\frac{\text{Lighting load}}{\text{Building peak load}} \%$
Occupancy	1	1/5	1/7	1/3	1/5	1/5	1/3
Initial setpoint (T <sub>o</sub> )	5	1	1/2	1/2	1/3	1/2	3
Area	7	2	1	1/3	1/2	1/3	3
ΔT bandwidth	3	2	3	1	1/2	1/3	3
Building Insulation	5	3	2	2	1	1/3	2
$\frac{\text{HVAC load}}{\text{Building peak load}} \%$	5	2	3	3	3	1	2
$\frac{\text{Lighting load}}{\text{Building peak load}} \%$	3	1/3	1/3	1/3	1/2	1/2	1

TABLE XV MINIMIZING DEMAND CHARGE – PAIRWISE COMPARISON OF ATTRIBUTES

<b>Attributes</b>	Occupancy	Initial setpoint ( $T_o$ )	Area	$\Delta T$ bandwidth	Building Insulation	$\frac{HVAC \text{ load}}{\text{Building peak load}} \%$	$\frac{Lighting \text{ load}}{\text{Building peak load}} \%$
Occupancy	1	1	1/2	1/5	1/3	1/7	1/7
Initial setpoint ( $T_o$ )	1	1	1	1/3	1	1/3	1/4
Area	2	1	1	1/5	1/3	1/4	1/3
$\Delta T$ bandwidth	5	3	5	1	2	1	1/2
Building Insulation	3	1	3	1/2	1	1/4	1/5
$\frac{HVAC \text{ load}}{\text{Building peak load}} \%$	7	3	4	1	4	1	2
$\frac{Lighting \text{ load}}{\text{Building peak load}} \%$	7	4	3	2	5	1/2	1

TABLE XVI MINIMIZING DISCOMFORT – PAIRWISE COMPARISON OF ATTRIBUTES

<b>Attributes</b>	Occupancy	Initial setpoint ( $T_o$ )	Area	$\Delta T$ bandwidth	Building Insulation	$\frac{HVAC\ load}{Building\ peak\ load}$ %	$\frac{Lighting\ load}{Building\ peak\ load}$ %
Occupancy	1	2	3	1/2	2	3	7
Initial setpoint ( $T_o$ )	1/2	1	1	3	1	4	5
Area	1/3	1	1	2	1	2	3
$\Delta T$ bandwidth	2	1/3	1/2	1	1	3	4
Building Insulation	1/2	1	1	1	1	5	6
$\frac{HVAC\ load}{Building\ peak\ load}$ %	1/3	1/4	1/2	1/3	1/5	1	4
$\frac{Lighting\ load}{Building\ peak\ load}$ %	1/7	1/5	1/3	1/4	1/6	1/4	1

**TABLE XVII AVOID DEMAND RESTRIKE – PAIRWISE COMPARISON OF ATTRIBUTES**

<b>Attributes</b>	Occupancy	Initial setpoint ( $T_o$ )	Area	$\Delta T$ bandwidth	Building Insulation	$\frac{HVAC\ load}{Building\ peak\ load}$ %	$\frac{Lighting\ load}{Building\ peak\ load}$ %
Occupancy	1	1/3	1/3	1/5	1/3	1/5	1/4
Initial setpoint ( $T_o$ )	3	1	1	1/3	1/2	1/4	1/3
Area	3	1	1	1/3	1/2	1/3	1/4
$\Delta T$ bandwidth	5	3	3	1	3	1/2	1
Building Insulation	3	2	2	1/3	1	2	3
$\frac{HVAC\ load}{Building\ peak\ load}$ %	5	4	3	2	1/2	1	1
$\frac{Lighting\ load}{Building\ peak\ load}$ %	4	3	4	1	1/3	1	1

**5.4.2.3.4 Level 4 - Pairwise Comparison Matrix of the Alternatives with respect to each Attribute:**

Pairwise comparison matrices between the five commercial buildings with respect to different attributes are shown in [TABLE XVIII](#) - [TABLE XXIV](#)

TABLE XVIII PAIRWISE COMPARISON MATRIX OF BUILDINGS WITH RESPECT TO OCCUPANCY

Occupancy	High-rise Office	Mid-rise Office	Middle School	Strip Mall	Hospital
High-rise Office	1	1/3	3	1/5	3
Mid-rise Office	3	1	3	1/3	3
Middle School	1/3	1/3	1	1/7	2
Strip Mall	5	3	7	1	5
Hospital	1/3	1/3	1/2	1/5	1

TABLE XIX PAIRWISE COMPARISON MATRIX OF BUILDINGS WITH RESPECT TO INITIAL THERMOSTAT SETPOINT TEMPERATURE ( $T_o$ )

Initial setpoint ( $T_o$ )	High-rise Office	Mid-rise Office	Middle School	Strip Mall	Hospital
High-rise Office	1	3	6	5	6
Mid-rise Office	1/3	1	7	4	7
Middle School	1/6	1/7	1	1/2	1
Strip Mall	1/5	1/4	2	1	1/2
Hospital	1/6	1/7	1	2	1

TABLE XX PAIRWISE COMPARISON MATRIX OF BUILDINGS WITH RESPECT TO AREA

Area	High-rise Office	Mid-rise Office	Middle School	Strip Mall	Hospital
High-rise Office	1	2	5	9	1
Mid-rise Office	1/2	1	2	8	1/2
Middle School	1/5	1/2	1	5	1/3
Strip Mall	1/9	1/8	1/5	1	1/9
Hospital	1	2	3	9	1

TABLE XXI PAIRWISE COMPARISON MATRIX OF BUILDINGS WITH RESPECT TO CHANGE IN THERMOSTAT SETPOINT TEMPERATURE

$\Delta T$ change	High-rise Office	Mid-rise Office	Middle School	Strip Mall	Hospital
High-rise Office	1	7	3	2	1
Mid-rise Office	1/7	1	1/5	1/7	1/9
Middle School	1/3	5	1	1	1/3
Strip Mall	1/2	7	1	1	1/3
Hospital	1	9	3	3	1

TABLE XXII PAIRWISE COMPARISON MATRIX OF BUILDINGS WITH RESPECT TO BUILDING ENVELOPE INSULATION

<b>Building Insulation</b>	High-rise Office	Mid-rise Office	Middle School	Strip Mall	Hospital
High-rise Office	1	1	5	3	3
Mid-rise Office	1	1	3	2	3
Middle School	1/5	1/3	1	1/3	1/5
Strip Mall	1/3	1/2	3	1	1
Hospital	1/3	1/3	5	1	1

TABLE XXIII PAIRWISE COMPARISON MATRIX OF BUILDINGS WITH RESPECT TO HVAC-TO-BUILDING-PEAK LOAD RATIO

$\frac{\text{HVAC load}}{\text{Building peak load}}\%$	High-rise Office	Mid-rise Office	Middle School	Strip Mall	Hospital
High-rise Office	1	1	1/5	1/5	3
Mid-rise Office	1	1	1/5	1/5	3
Middle School	5	5	1	1	3
Strip Mall	5	5	1/3	1	3
Hospital	1/3	1/3	1/3	1/3	1

TABLE XXIV PAIRWISE COMPARISON MATRIX OF BUILDINGS WITH RESPECT TO LIGHTING-TO-BUILDING-PEAK LOAD RATIO

$\frac{\text{Lighting load}}{\text{Building peak load}} \%$	High-rise Office	Mid-rise Office	Middle School	Strip Mall	Hospital
High-rise Office	1	2	1/5	1/6	1/3
Mid-rise Office	1/2	1	1/5	1/6	1/3
Middle School	5	5	1	1/2	4
Strip Mall	6	6	2	1	3
Hospital	3	3	1/4	1/3	1

#### 5.4.2.4 Normalized Eigenvectors at each level of the AHP Structure in [Fig. 25](#)

This section presents the resulting values of principal eigenvalue, consistency ratio (CR), normalized priorities (NP) and ranks of different alternatives at each level of the AHP structure (using AHP calculator [118]).

##### 5.4.2.4.1 Level 1 - Normalized Eigenvectors showing Weightage of Expert Opinions:

The normalized priority vector and order of ranking between the customer relations department and system operator is shown in [TABLE XXV](#).

TABLE XXV NORMALIZED WEIGHTS AND RANKS SHOWING WEIGHTAGE OF EXPERT OPINIONS

	$\lambda_{max} : 2$	CR: 0%
Experts	NP	Rank
Customer Relations	0.25	2
System Operator	0.75	1

5.4.2.4.2 Level 2 - Normalized Eigenvectors showing Weightage of each Sub-goal with respect to Expert Opinions:

The resulting principal eigenvalue, consistency ratio, normalized priorities and ranks of the sub-goals, with respect to each of the experts, is shown in [TABLE XXVI](#).

TABLE XXVI RESULTING WEIGHTS AND RANKS FOR SUB-GOALS BASED ON EXPERT OPINION

	Customer relations department		System operator	
	$\lambda_{max} : 4.143$	CR: 5.2%	$\lambda_{max} : 4.167$	CR: 6.1%
Sub-goal description	NP	Rank	NP	Rank
Maximize energy savings	0.420	1	0.130	3
Minimize demand charge	0.334	2	0.184	2
Minimize discomfort	0.138	3	0.066	4
Avoid demand restrike	0.108	4	0.620	1

#### 5.4.2.4.3 Level 3 - Normalized Eigenvectors showing Weightage of each Attribute with respect to Different Sub-goals:

The resulting principal eigenvalue and consistency ratio for pairwise comparison matrices of different building attributes with respect to the specified sub-goals is shown in [TABLE XXVII](#).

TABLE XXVII RESULTING WEIGHTS AND RANKS FOR VARIOUS ATTRIBUTES BASED ON SUB-GOALS

	Maximize energy savings		Minimize demand charge		Minimizing discomfort		Avoid demand restrike	
	$\lambda_{max}$ : 7.775	CR: 9.6 %	$\lambda_{max}$ : 7.366	CR: 4.6 %	$\lambda_{max}$ : 7.738	CR: 9.2 %	$\lambda_{max}$ : 7.695	CR: 8.6 %
Attributes	NP	Rank	NP	Rank	NP	Rank	NP	Rank
Occupancy	0.032	7	0.038	7	0.242	1	0.037	7
Initial setpoint ( $T_o$ )	0.108	5	0.065	5	0.195	2	0.071	6
Area	0.133	4	0.058	6	0.145	5	0.071	5
$\Delta T$ bandwidth	0.165	3	0.200	3	0.162	4	0.227	1
Building Insulation	0.195	2	0.091	4	0.165	3	0.212	3
$\frac{\text{HVAC load}}{\text{Building peak load}}\%$	0.295	1	0.281	1	0.061	6	0.212	2
$\frac{\text{Lighting load}}{\text{Building peak load}}\%$	0.070	6	0.266	2	0.030	7	0.172	4

#### 5.4.2.4.4 Level 4 - Normalized Eigenvectors showing Weightage of each Alternative with respect to Different Buildings:

The corresponding results of principal eigenvalue, consistency ratio, normalized priorities and ranks for pairwise comparison matrices between different commercial buildings with respect to aforementioned building attributes is shown in [TABLE XXVIII](#).

TABLE XXVIII RESULTING WEIGHTS AND RANKS FOR VARIOUS ALTERNATIVES  
BASED ON DIFFERENT ATTRIBUTES

Building	Occupancy		Initial setpoint ( $T_o$ )		Area		$\Delta T$ bandwidth		Building Insulation		$\frac{HVAC \text{ load}}{Building \text{ peak load}}$ (%)		$\frac{Lighting \text{ load}}{Building \text{ peak load}}$ (%)	
	$\lambda_{max}$ : 5.285	CR: 6.3%	$\lambda_{max}$ : 5.180	CR: 4%	$\lambda_{max}$ : 5.098	CR: 2.2%	$\lambda_{max}$ : 5.103	CR: 2.3%	$\lambda_{max}$ : 5.228	CR: 5.1%	$\lambda_{max}$ : 5.434	CR: 9.6%	$\lambda_{max}$ : 5.195	CR: 4.3%
	NP	Rank	NP	Rank	NP	Rank	NP	Rank	NP	Rank	NP	Rank	NP	Rank
High rise office	0.135	3	0.482	1	0.359	1	0.317	2	0.348	1	0.103	3	0.067	4
Midrise office	0.227	2	0.314	2	0.190	3	0.033	5	0.299	2	0.103	3	0.051	5
Middle School	0.073	4	0.055	5	0.102	4	0.133	4	0.058	5	0.362	1	0.323	2
Strip Mall	0.505	1	0.074	4	0.029	5	0.156	3	0.141	4	0.362	1	0.422	1
Hospital	0.060	5	0.075	3	0.319	2	0.361	1	0.153	3	0.070	5	0.137	3

In order to obtain the priority order of demand curtailment between the five participating commercial buildings, the normalized priority vectors at each level (shown in [sections 5.4.2.4.1 - 5.4.2.4.4](#)) must be multiplied. The overall demand curtailment allocation priority vector is obtained as shown in **equation set D**:

**Equation set D:**

$$L1 = \begin{bmatrix} 0.25 \\ 0.75 \end{bmatrix}$$

$$L2 = \begin{bmatrix} 0.420 & 0.130 \\ 0.334 & 0.184 \\ 0.138 & 0.066 \\ 0.108 & 0.620 \end{bmatrix}$$

$$L3 = \begin{bmatrix} 0.032 & 0.038 & 0.242 & 0.037 \\ 0.108 & 0.065 & 0.195 & 0.071 \\ 0.133 & 0.058 & 0.145 & 0.071 \\ 0.165 & 0.200 & 0.162 & 0.227 \\ 0.195 & 0.091 & 0.165 & 0.212 \\ 0.295 & 0.281 & 0.061 & 0.212 \\ 0.070 & 0.266 & 0.030 & 0.712 \end{bmatrix}$$

$$L4 = \begin{bmatrix} 0.135 & 0.482 & 0.359 & 0.317 & 0.348 & 0.067 \\ 0.227 & 0.314 & 0.190 & 0.033 & 0.229 & 0.051 \\ 0.073 & 0.055 & 0.102 & 0.133 & 0.058 & 0.323 \\ 0.505 & 0.074 & 0.029 & 0.156 & 0.141 & 0.422 \\ 0.060 & 0.075 & 0.319 & 0.361 & 0.153 & 0.137 \end{bmatrix}$$

$$\text{DS curtailment priority factor} = L4 * L3 * L2 * L1$$

The overall demand curtailment priority vector (W) calculated using **equation set D** is shown in [TABLE XXIX](#).

TABLE XXIX OVERALL BUILDING DEMAND CURTAILMENT WEIGHTS

	High-rise Office	Mid-rise Office	Middle School	Strip Mall	Hospital
Weight	0.2414	0.1480	0.1904	0.2441	0.1761

Note that this is the overall priority vector for distribution of demand curtailment among the five participating buildings. This is obtained considering sensitivities and judgements of different experts (see level 1 in [Fig. 25](#)) with respect to different objectives such as maximizing energy savings, minimizing discomfort etc., (see level 2 in [Fig. 25](#)) and various building attributes (see level 3 in [Fig. 25](#)).

Case studies are now performed by increasing the magnitude of load curtailment from 100-400 kW with increments of 50 kW. In the case of a building being unable

to honor a demand curtailment request allotted to it, the excess load is redistributed among remaining buildings keeping their relative ratio of contribution intact.

## 5.5 Case Studies

Typically, a DR event on a summer weekday can occur anytime between 1-7 PM [119]. In this chapter, a 4-hour period (1-5 PM) encapsulating the electrical grid peak is considered to execute HVAC thermostat setpoint interventions in commercial buildings. Case studies are performed on the hottest day of the year - July 1st, 2019 when dry-bulb temperature reached a peak of 96°F. Seven case studies are performed by varying the requested demand curtailment from 100kW to 400 kW in increments of 50kW. This demonstrates that the tool works under extreme conditions, thus validating its applicability in milder conditions. In this study, peak demand curtailment corresponds to a difference in hourly peak demand before and after the HVAC thermostat setpoint intervention. As an example, the operation of the tool for a 100kW curtailment is detailed below:

### **Demonstration of a 100-kW grid peak demand curtailment**

A demand curtailment (DC) request of 100 kW will be split among the participating five commercial buildings according to the split listed in [TABLE XXXI](#). Hence, the required demand curtailment contribution by each building should be as listed in [TABLE XXX](#).

TABLE XXX EACH BUILDING’S CONTRIBUTION FOR A 100 kW DEMAND CURTAILMENT REQUEST

	High-rise Office	Mid-rise Office	Middle School	Strip Mall	Hospital
Demand Curtailment (kW)	24.14	14.80	19.04	24.41	17.61

By doing a parametric analysis of the five building energy models with respect to HVAC thermostat setpoint interventions (see [section 4.2.1](#) for thermostat setpoint intervention method) during the control period, we obtain [TABLE XXXI](#).

TABLE XXXI DEMAND REDUCTION IN BUILDINGS DUE TO HVAC THERMOSTAT SETPOINT INTERVENTIONS

Building Type	+1°F	+2°F	+3°F	+4°F	+5°F	Req DC	Rank	DC excess
High-rise Office	12.7	32.5	108.5	191.0	218.3	<b>24.1</b>	2	8.4
Mid-rise Office	2.6	13.6	20.8	29.7	80.6	<b>14.8</b>	5	6.0
Middle School	6.1	12.3	18.6	24.9	31.2	<b>19.0</b>	3	5.9
Strip Mall	0.1	1.4	5.0	9.5	14.2	<b>24.4</b>	1	-10.2
Hospital	10.6	21.0	31.5	41.9	52.4	<b>17.6</b>	4	3.4

Note that the strip mall ranks first according to the AHP algorithm and is required to contribute 24.4 kW. But, as can be seen from [TABLE XXXI](#), the highest amount of demand curtailment provided by the strip mall is 14.2 kW, for a +5°F increment in setpoint temperature. This leaves a deficit of 10.2 kW, which needs to be redistributed among the remaining buildings. Considering this limiting condition, HVAC thermostat setpoint interventions have been performed optimistically, i.e., in a way that demand curtailment met is always higher than demand curtailment requested. This leads to a net excess demand curtailment of 23.7 kW. After considering the 10.2 kW demand curtailment deficit created by strip mall, in this case study, a total demand curtailment of 113.5 kW has been produced by all the participating commercial buildings, thus ensuring that the grid peak demand curtailment request (of 100 kW) has been met. As the magnitude of demand curtailment request increases, this iterative process is continued until a convergent mapping between sets of  $\{\Delta p\}$  and  $\{\Delta T\}$  is obtained.

## 5.6 Results and Discussion

Results indicate that the contribution of each building towards demand curtailment is heavily influenced by the change in thermostat setpoint temperature,

followed by occupancy. The HVAC-to-building peak load ratio and initial thermostat setpoint temperature have similar weightage. The tonnage of HVAC system is sized based on the floor area it serves and the indoor temperature is in the range of 67 – 82°F. The thermal insulation level of the envelope and operational timings of the building have the least influence among the selected attributes of the building. Ranking of demand curtailment amongst buildings with respect to each sub-goal is shown in [TABLE XXXII](#).

TABLE XXXII DEMAND CURTAILMENT PRIORITY FACTOR AND RANKS FOR VARIOUS BUILDINGS BASED ON DIFFERENT SUB-GOALS

Bldg #	Minimizing discomfort		Maximize energy savings		Minimize demand charge		Avoid demand restrike		Overall	
	NP	Rank	NP	Rank	NP	Rank	NP	Rank	NP	Rank
1	0.4285	1	0.4616	1	0.4413	1	0.4448	1	0.4378	1
2	0.2064	2	0.1954	2	0.2028	2	0.2024	2	0.2035	2
3	0.1092	5	0.1076	5	0.1126	5	0.1107	5	0.1097	5
4	0.1291	4	0.1299	4	0.1411	4	0.1304	4	0.1316	4
5	0.1518	3	0.1400	3	0.1416	3	0.1404	3	0.1471	3

In this case, the ranking order of buildings with respect to each of the sub-goals is consistent in revealing that the change in thermostat temperature is heavily influencing the ranking order of demand curtailment amongst buildings.

As shown in [section 5.4.2.3.1](#), [TABLE XI](#) represents a pairwise comparison matrix showing the importance of the customer relations department (building manager) and electric utility operator. Since the initial thermostat setpoint (70°F) is well within thermal comfort limits, the system operator’s opinion is given a higher weightage (marked as 3) reinforcing a strong top-down control. The priority vector corresponding to maximum eigenvalue at this level is [0.25; 0.75]. Similar

comparison matrices at each level result in corresponding priority vectors, as indicated in [section 5.4.2.3](#). The corresponding normalized eigenvectors at each level are presented in [section 5.4.2.4](#). By multiplying the eigenvectors at each level as per equation (1), overall building demand curtailment weights shown in [TABLE XXIX](#) are obtained.

[TABLE XXXIII](#) summarizes adjusted demand curtailment results obtained by using the developed tool for different amounts of demand curtailment (DC) ranging between 100-400 kW. From [TABLE XXIX](#), the strip mall’s contribution towards a load curtailment request of 100 kW should be 24.4 kW, however, at its highest temperature setpoint increment, the strip mall is only able to contribute 14.2 kW. Hence, excess demand is redistributed among remaining buildings in the same relative proportion, resulting in adjusted demand curtailment weights shown in [TABLE XXXIII](#).

TABLE XXXIII DEMAND CURTAILMENT ALLOCATION - ADJUSTED

DC	High-rise Office	Mid-rise Office	Middle School	Strip Mall	Hospital
100	27.4	16.8	21.6	14.2	20.0
150	44.6	27.4	31.2	14.2	32.6
200	66.0	40.5	31.2	14.2	48.1
250	71.6	80.6	31.2	14.2	52.4
300	121.6	80.6	31.2	14.2	52.4
350	171.6	80.6	31.2	14.2	52.4
400	221.6	80.6	31.2	14.2	52.4

[TABLE XXXIII](#) shows that the buildings reach their limiting conditions in the following order: strip mall, middle school, hospital, mid-rise office, and high-rise office. Since a conservative initial setpoint temperature of 70°F is assumed in our design, HVAC thermostat setpoint temperature increment bandwidth of +5°F serves

as the limiting constraint. In cases where a higher initial HVAC thermostat setpoint temperature is assumed, building indoor temperature is likely to be the limiting constraint.

Commercial building energy models developed in the first step are now utilized to translate the adjusted load curtailment to corresponding HVAC thermostat setpoint increments. The HVAC thermostat setpoint increments ( $\Delta T$ , °F) and corresponding load reduction ( $\Delta p$ , kW) are listed in [TABLE XXXIV](#). Additionally, the first, and last columns of [TABLE XXXIV](#) display requested and satisfied amounts of demand curtailment.

TABLE XXXIV DEMAND CURTAILMENT ALLOCATION - IMPLEMENTATION

DC required	High-rise Office		Mid-rise Office		Middle School		Strip Mall		Hospital		DC met
	$\Delta p$	$\Delta T$	$\Delta p$	$\Delta T$	$\Delta p$	$\Delta T$	$\Delta p$	$\Delta T$	$\Delta p$	$\Delta T$	
100	32.5	2	20.8	3	24.9	4	14.2	5	21.0	2	113.4
150	108.5	3	29.7	4	31.2	5	14.2	5	31.5	3	215.1
200	108.5	3	29.7	4	31.2	5	14.2	5	31.5	3	215.1
250	108.5	3	80.6	5	31.2	5	14.2	5	52.4	5	286.9
300	191.0	4	80.6	5	31.2	5	14.2	5	52.4	5	369.4
350	191.0	4	80.6	5	31.2	5	14.2	5	52.4	5	369.4
400	218.3	5	80.6	5	31.2	5	14.2	5	52.4	5	396.7

Demand curtailment requests of 150 kW and 200 kW appear the same, as both these cases result in a total demand curtailment of 215.1kW. This is because HVAC thermostat setpoint interventions are incremented in steps of 1°F. A similar

observation is made for curtailment requests of 300 kW and 350 kW. Also, note that demand curtailment has been executed optimistically. The only exception to this being the case of 400 kW curtailment request, where the system reaches its limiting conditions and is therefore able to honor only 396.7 kW. Note that demand curtailment limit for each building is defined based on indoor temperature of the building being within limits specified in [13]. Percentage contribution of each commercial building for various levels of demand curtailment request is depicted in [Fig. 26](#).

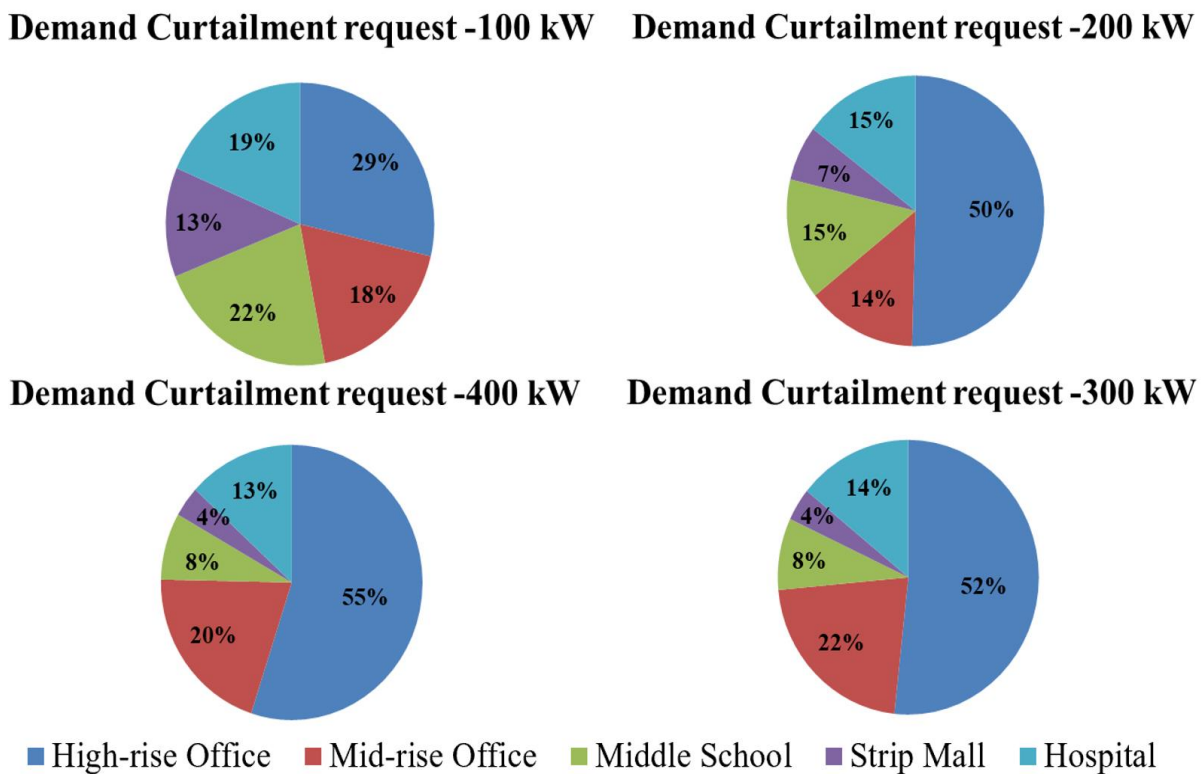


Fig. 26. Percentage of contribution to selected electric grid peak demand curtailment requests (100 - 400 kW)

As can be seen from [Fig. 26](#), the strip mall with least overall thermal capacity, contributes the lowest whereas the high-rise office building with highest overall thermal capacity has the highest contribution towards demand curtailment. Note that in this case study, the high-rise office building and hospital building have an area of 250,000 ft<sup>2</sup> and a comparable HVAC to peak load ratio of 31% and 25% respectively. As was shown in [TABLE XXVIII](#), high rise office building ranks 1 and hospital building ranks 3 with respect to amenability in varying the initial thermostat

setpoint temperature ( $T_o$ ). This shows that the high-rise office building is relatively less temperature sensitive compared to the hospital building and hence is far more amenable towards an HVAC thermostat setpoint variation. Individual demand curtailment contribution (kW) of each commercial building, for various levels of grid peak demand curtailment request, is shown in [Fig. 27](#).

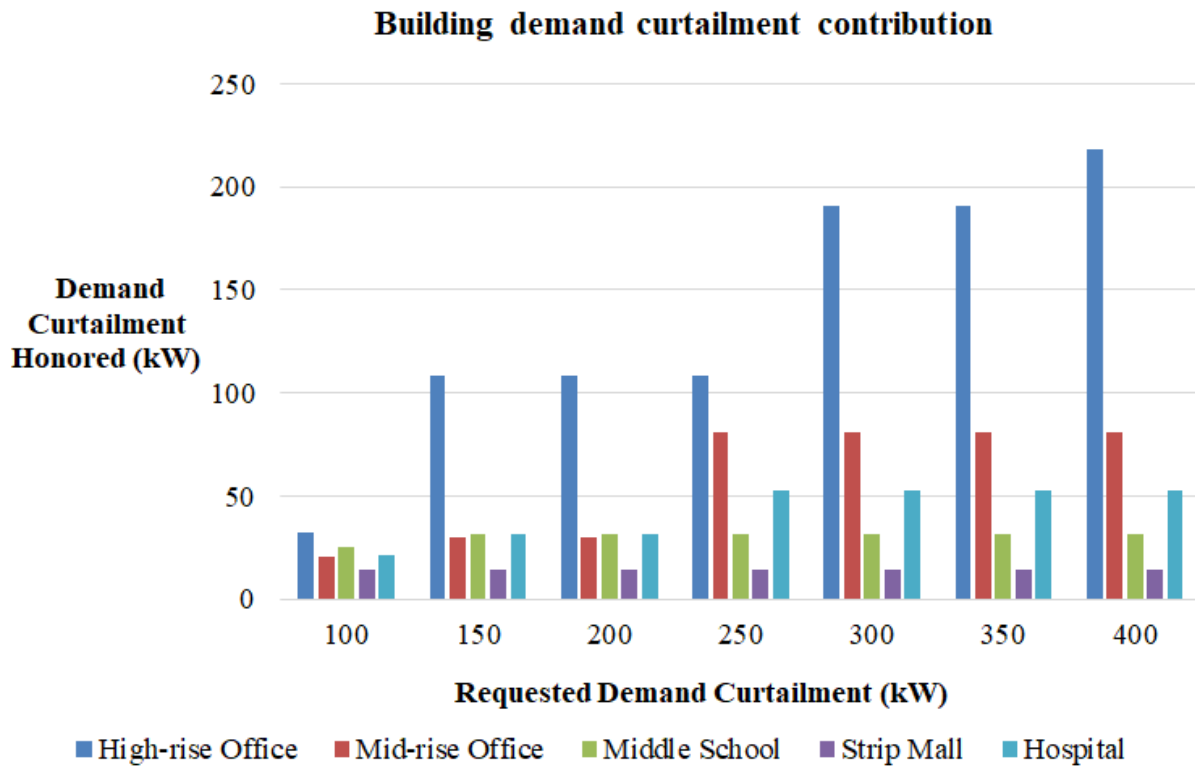


Fig. 27. Individual demand curtailment amount (kW) for each commercial building

As can be seen from [Fig. 27](#), the strip mall (in purple) reaches its demand curtailment limit first, followed by middle school (in green), hospital (in cyan), mid-rise office (in red), and high-rise office (in blue). The strip mall having the least area in the building portfolio has the least amount of thermal inertia and hence reaches saturation first, whereas the high-rise building having the largest area has the highest amount of thermal inertia and hence a greater ability to contribute towards demand curtailment. Therefore, it is the last building to reach saturation. The corresponding maximum indoor temperature ( $T_{max}$ , °F) during control period across all buildings, for various levels of demand curtailment is presented in [TABLE XXXV](#).

TABLE XXXV MAXIMUM INDOOR TEMPERATURE DURING THE CONTROL PERIOD  
[1-5 PM]

DC	High-rise Office	Mid-rise Office	Middle School	Strip Mall	Hospital
100	73.80	78.30	77.45	75.85	73.41
200	73.97	78.38	77.57	75.85	73.43
300	74.75	78.47	77.57	75.85	74.71
350	74.75	78.47	77.57	75.85	74.71
400	75.53	78.47	77.57	75.85	74.71

Note that maximum indoor temperature across buildings' ranges between 73.41-78.47°F, which is well within thermal comfort limit of 82°F, per ASHRAE standard 55. [Fig. 28](#) illustrates the profile of rise in maximum indoor temperature for each commercial building for different levels of demand curtailment request.

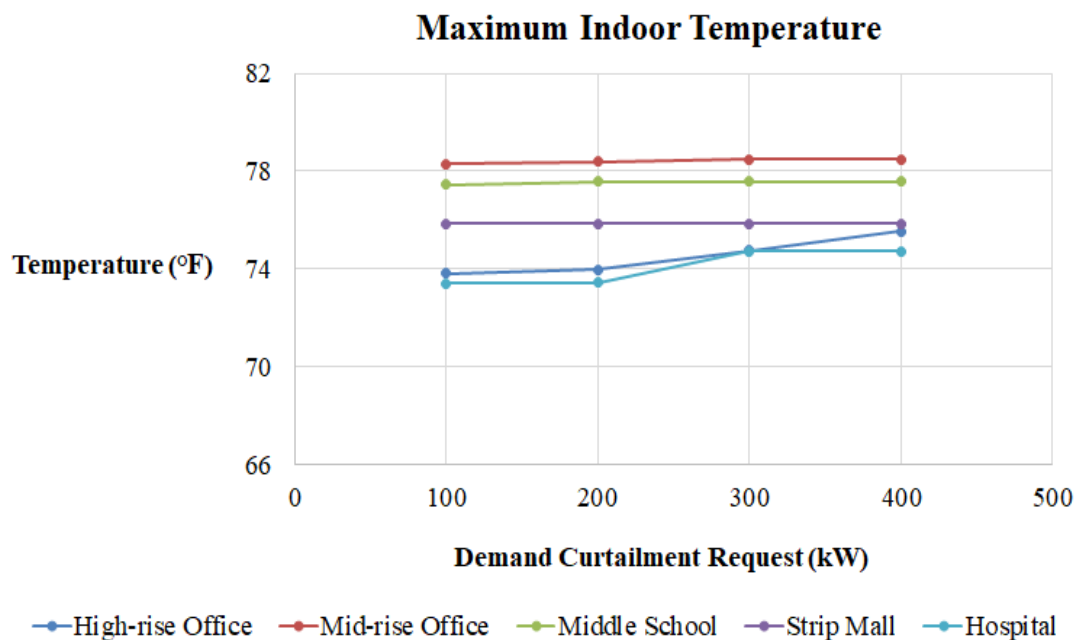


Fig. 28. Maximum indoor temperature in each building (°F) for various levels of demand curtailment request

The results show satisfactory performance for demand curtailment within the limit of the system. For these case studies the HVAC thermostat setpoint interventions were capped at +5°F increment, to ensure the required occupant thermal comfort level. Upon gradually raising the demand curtailment request, the temperature in the hottest area of each building was monitored. For example, the high-rise building showed the highest variation in indoor temperature from 73.8°F to 75.53°F by increment of 1.73°F. When the HVAC thermostat setpoint temperatures of all the buildings were raised by 5°F, the system (selected portfolio of commercial buildings) reached its limit at 396.7 kW. This implies that using the proposed expert-based scheme, we can mitigate the peak demand in the electric grid successfully within the system's limit. This was done to ascertain that all the buildings lie well within the thermal comfort range specified by the ASHRAE Standard 55.

## 5.7 Conclusion

Based on expert opinion, importance of each sub-goal and attributes of each building, a priority order of demand curtailment between participating commercial buildings, is obtained. Results indicate that change in thermostat setpoint temperature and occupancy in the building played a major role in determining which building must be prioritized for demand curtailment.

The execution of the algorithm always ensured that the requested demand curtailment was met. This was done to guarantee reliability in affecting grid peak demand mitigation. Case studies have been performed for different levels of demand curtailment and results show above-expected performance for demand curtailment within the limit of the system. The optimality is empirically proven. This AHP-based approach enabled us to design an extensive solution compared to our previous work in [120]. The solution incorporates several factors regarding buildings and considers the sensitivities of experts in a dynamic real-world scenario, hence making it widely applicable.

Further case studies using information from different buildings must be conducted to reveal the underlying factors and generalize the priority ranking order of demand curtailment in participating commercial buildings under various climatic conditions. A summary of results obtained by performing HVAC thermostat setpoint

interventions in commercial buildings is presented in Chapter 6. Further details regarding the performance of the proposed AHP-based demand curtailment tool under different loading conditions are also given.

## 6. RESULTS AND DISCUSSION

### 6.1 Introduction

This chapter summarizes results of the research presented in this dissertation using the proposed expert-based demand curtailment scheme. It also presents specific results of developing the building energy models presented in [Chapter 3](#). Further, the resulting peak demand reduction and energy savings obtained due to HVAC thermostat setpoint interventions are quantified. The key findings in this work are organized into three sections that correspond to specific chapter results:

- [Section 6.2.1](#) discusses overall results of using the proposed AHP-based demand curtailment scheme;
- [Section 6.2.2](#) discusses building energy modeling results; and
- [Section 6.2.3](#) quantifies the impacts of HVAC thermostat setpoint interventions on peak demand reduction and energy savings in commercial buildings.

### 6.2 Key Results

High fidelity building energy models have been developed in this dissertation. These models show accuracy of around 94% and hence serve as digital replicas of actual commercial buildings. Further, to improve scalability, minimum dataset models are constructed with relatively fewer input parameters and these revealed a promising accuracy of about 92%.

After constructing these digital replicas, parametric analysis is done to analyze the impact of HVAC thermostat setpoint interventions in commercial buildings. A 1°F-increment resulted in about a 3% peak demand reduction and 4.5% increase in energy savings across the participating commercial building portfolio. A similar observation made for a 5°F increment in setpoint temperature showed around a 14% reduction in peak demand and 15% in energy savings.

Based on these findings, an expert-based peak demand management tool was designed. The match between demand curtailment requested and demand

curtailment met during multiple case studies attests to the satisfactory performance of this tool across different scenarios. The illustrated case studies show that a maximum grid peak reduction of about 400 kW was obtained, solely through HVAC thermostat setpoint interventions in five participating commercial buildings.

### 6.2.1 Expert-based Grid Peak Demand Curtailment Scheme: Results and Discussion

This section presents an overview of results obtained by using the expert-based tool for curtailing grid peak demand on the hottest day of the year (1st, July 2019). Case studies for different levels of demand curtailment -- ranging from 100-400 kW -- are presented in [Chapter 5](#). The results show satisfactory performance for demand curtailment within the limit of the system. For these case studies, the HVAC thermostat setpoint interventions were capped at a +5°F increment, to ensure occupants' thermal comfort. Upon gradually raising the demand curtailment request, the temperature in the hottest area of each building was monitored. For example, the high-rise building showed the highest variation in indoor temperature from 73.8°F to 75.53°F by an increment of 1.73°F. When the HVAC thermostat setpoint temperatures of all the buildings were raised by 5°F, the system (selected portfolio of commercial buildings) reached its limit at 396.7 kW. This implies that using the proposed expert-based scheme, we can mitigate peak demand in the electric grid successfully within the system's limit. This was done to ascertain that all the buildings lie well within the thermal comfort range specified by the ASHRAE Standard 55.

The execution of the algorithm always ensured that requested demand curtailment was met. This was done to guarantee reliability in affecting grid peak demand mitigation. Because of choosing integral HVAC thermostat setpoint increments, the resulting demand curtailment was notably high in some cases.

This could be molded towards an optimal solution, enough to satisfy the requested demand curtailment by doing a fractional increment in HVAC thermostat setpoint temperature or doing a conservative HVAC thermostat setpoint increment together with a lighting control strategy. This now implies that by using the proposed expert-based scheme, we can mitigate the peak demand in the electric grid successfully.

Case studies have been performed for different levels of demand curtailment, and results show above-expected performance for demand curtailment within the limit of the system.

### 6.2.2 Building Energy Modeling: Results and Discussion

The models developed in eQUEST showed promising accuracy across different commercial building types and hence can serve as digital twins for the actual buildings. The results of HVAC thermostat setpoint interventions made on the digital twins can provide ballpark numbers for peak demand reduction and energy savings %, closely reflecting actual observations made in the respective buildings. A linear relationship is observed between peak demand reduction and HVAC-to-building peak load %; a similar observation is made in case of energy savings %.

#### **Observations:**

- The high accuracy shows that several important factors affecting building energy consumption and the interaction between them has been well accounted for.
- The sensitivity analysis reveals that models are robust with respect to thermostat setpoint temperature assumption.
- Modeling methodology is location-independent and can be extended to different types of buildings at different locations and climatic conditions.

While these serve as examples for ways in which the proposed methodology and simulator can be used, they also enable us to obtain deeper insights into the operation of transactive grid with active participation of commercial buildings. This helps in optimizing commercial building energy performance when participating in a transactive energy market. Further, the minimal input dataset models are reasonably accurate and enable mass-scaling of building energy model development process. Critical research areas leading to significant improvements in the field are also pointed out.

### 6.2.3 Impact of HVAC Thermostat Setpoint Intervention on Peak Demand Reduction and Energy Savings in Commercial Buildings: Results and Discussion

From Chapter 4, we infer that HVAC thermostat setpoint interventions have an impact on both peak demand reduction and energy savings. Analysis of experimental results provide two key insights: a.) medium hot days (when the average outdoor temperature is between 70 °F and 80 °F) yield maximum peak demand reduction and energy savings b.) larger commercial buildings with high HVAC-to-building peak load ratio can produce higher peak demand reduction and energy savings. This can be attributed to the high thermal load available for curtailment.

The promising results obtained as a part of this research pave way towards the development of a transactive energy grid with effective DR schemes that create favorable outcomes for all stakeholders involved. Chapter 7 concludes this dissertation and discusses the future work that needs to be done in this field of research.

## 7. CONCLUSION AND FUTURE WORK

This dissertation proposed an AHP-based scheme to mitigate the grid peak demand while inducing energy savings in participating commercial buildings. Numerical results testify to the effectiveness of the proposed scheme. One of the cornerstone contributions of this dissertation is also the development of high-fidelity building energy models which can be used to do a thorough impact analysis of different interventions. This chapter outlines the key conclusions from developing this AHP-based demand curtailment scheme to address grid peak reduction. Further, peak demand reduction potential and corresponding energy savings are also quantified. This is achieved by performing an impact analysis of HVAC thermostat setpoint interventions by using high fidelity building energy models.

### 7.1 Conclusion

As a part of this research, an expert opinion-based tool for demand curtailment via HVAC thermostat setpoint control has been constructed. The developed tool optimally allocates demand curtailment among participating commercial buildings and translates it into appropriate HVAC thermostat setpoint interventions. Case studies are performed by varying the load curtailment (100-400 kW) on the hottest day of the year, 1st July 2019, when the outdoor dry-bulb temperature reached a peak of 96°F. Results show good performance for different levels of demand curtailment. This demonstrates that the tool works under extreme conditions, thus validating its applicability in milder conditions. The developed tool is agile and robust and can be further extended to include other DSM strategies like control of lighting, battery, and electric vehicle charging.

This research provides an improved understanding of buildings' thermal flexibility for varying levels of demand curtailment requests. Additionally, it delivers insights to maximize buildings' economic benefits while being sensitive to occupant thermal comfort. A priority order of demand curtailment is obtained by considering experts' opinions, the weightage of each sub-goal, and the attributes of participating commercial buildings. Results indicate that change in thermostat setpoint temperature and occupancy in the buildings played a major role in determining which building must be prioritized for demand curtailment. The

knowledge gained through this research will be helpful in developing new and improved controls for reducing buildings' and distribution networks' peak demand. With these benefits, the designed strategy is successful and has large potential for applications across different electric distribution systems.

Accurate building energy models act as a cornerstone for understanding the realistic operation of the proposed AHP-based framework. As presented in [Chapter 3](#), a procedure for developing high-fidelity building energy models is outlined. In this method, the assumptions made are subject to various building energy codes and standards; for example, the assumptions in the thermal insulation category comply with IBC 2015 and ASHRAE standard 90.1 – 2016. The HVAC system is configured as per ASHRAE Standard 62.1 – 2016 for ventilation [11] and ASHRAE Standard 55 for thermal environmental conditions [13]. Through careful modeling, the error % range was minimized to 6.7%. The parametric analysis done for the initial HVAC thermostat setpoint showed an error variation ranging from 4.7-6.8%, which testifies to the robustness of the building energy modeling method. Furthermore, the reduced order models showed a promising result with error ranging between 7.6-8.8%, demonstrating high scalability in constructing accurate building energy models.

These high-fidelity building energy models are now used to analyze the impact of HVAC thermostat setpoint interventions in various commercial buildings. On hot days (when outdoor dry-bulb temperature is greater than 80°F), the HVAC system is continuously running and so reducing the thermostat setpoint results in relatively lesser change, whereas on medium-hot days (when the outdoor dry-bulb temperature is between 70°F and 80°F), raising the setpoint might result in the HVAC system turning off, causing significant peak demand reduction and energy savings. From [Chapter 4 \(TABLE IV\)](#), peak demand reduction potential during DR period ( $\Delta PR_{DR}\%$ ) ranges between 1.0-4.3% for the 1°F increment in HVAC thermostat setpoint temperature and between 8.1-20.1% for the 5°F increment across the selected building portfolio. Similarly, for a 1°F increment in HVAC thermostat setpoint temperature, energy savings range between 1.7-10.1% and 7.6-20.5% for a 5°F increment. It must also be noted that the buildings with the highest HVAC-to-peak load ratio offer the highest peak demand reduction and corresponding energy savings.

## 7.2 Future Work

While the AHP tool's usefulness for performing HVAC thermostat setpoint interventions has been established, its utility can be further extended to study other areas. Encouraging commercial buildings to transact with the electric grid involves several binding elements and multiple stakeholders. Due to the multivariate nature of this problem, there are several opportunities for expanding this dissertation work. These opportunities have been addressed in two parts - first, testing the performance and robustness of the AHP tool by varying different parameters and scenarios and, second, considering broader areas of investigations such as the impact of HVAC thermostat setpoint interventions on demand charge in buildings. Some specific questions to be answered in these regards include the following:

### **Future avenues to evaluate the proposed AHP tool:**

- How does the proposed scheme work under different climatic conditions?
- How does the AHP method perform when the participating buildings have different initial HVAC thermostat temperature setpoints?
- What happens if the priorities between different attributes at each level change?
- What is the outcome of incorporating precooling strategy into the proposed framework - how would it take care of demand restraints?
- How does the proposed AHP tool perform in different electricity markets?

### **Future avenues for overall investigation:**

- How much energy savings are obtained by using the proposed tool along with a precooling strategy in different electricity markets?
- How much more demand can be curtailed by varying the lighting load in the building?
- How does the proposed tool perform upon incorporation of rooftop solar PV and EVs into the system?

- What features need to be incorporated into the proposed tool to manage demand charge in commercial buildings across different seasons?
- What is the overall impact of using reduced order building energy models vs high fidelity building energy models, while implementing the proposed scheme?
- How to use machine learning techniques for model calibration, in order to automate development of high-fidelity building energy models?

Answering these questions will create a dynamic environment for commercial buildings to interact with the electric grid in a robust and reliable fashion, paving the way for a smarter grid.

## REFERENCES

- [1] “Smart Buildings Automation Systems Market”, Aug. 2019.  
<https://www.strategymrc.com/report/smart-building-automation-systems-market>.
- [2] Energy Information Administration, “Commercial Buildings Energy Consumption Survey (CBECS)”, Mar. 2015.  
<https://www.eia.gov/consumption/commercial/data/2012/>.
- [3] E. I. Administration, “Frequently Asked Questions: How much energy is consumed in U.S. residential and commercial buildings?”  
<https://www.eia.gov/tools/faqs/>.
- [4] S. Shao, M. Pipattanasomporn, and S. Rahman, “Demand response as a load shaping tool in an intelligent grid with electric vehicles,” *IEEE Trans Smart Grid*, vol. 2, no. 4, pp. 624-631, 2011.
- [5] “Demand Matters”, San Diego Gas and Electric.” [Online]. Available:  
<https://www.sdge.com/businesses/pricing-plans/understanding-demand>.
- [6] “Automated Demand Response for Smart Grid – Open ADR 2.0 Protocol”.
- [7] C. Soeiro, “9 strategies for businesses that want to take advantage of Auto Demand Response Savings” [Online]. Available:  
<https://www.pge.com/en/mybusiness/Save/smbblog/article/9-strategies-for-businesses-that-want-to-take-advantage-of-auto-demand-response-savings.page?redirect=yes>
- [8] T. Samad, E. Koch, and P. Stluka, “Automated Demand Response for Smart Buildings and Microgrids: The State of the Practice and Research Challenges,” *Proc. IEEE*, vol. 104, no. 4, pp. 726-744, Apr. 2016, doi: 10.1109/JPROC.2016.2520639.
- [9] R. Zimmer, “Intelligent Buildings and Cybersecurity”, in *Landmark Research Study*, Continental Automated Buildings Association (CABA, Germany, 2017.
- [10] “2018 INTERNATIONAL BUILDING CODE - ICC DIGITAL CODES.”  
<https://codes.iccsafe.org/content/IBC2018> (accessed Mar. 23, 2021).
- [11] ASHRAE Standard 62.1 – 2016, Ventilation for Acceptable Indoor Air-Quality (ANSI Approved. American Society of Heating, Refrigerating and Air-Conditioning Engineers, Inc. (ASHRAE).
- [12] ANSI/ASHRAE/IES Standard 90.1-2019 – Energy Standard for Buildings Except Low-Rise Residential Buildings.
- [13] ANSI/ASHRAE Standard 55-2013 – Thermal Environment Conditions for Human Occupancy. Inc.
- [14] V. S. K. V. Harish and A. Kumar, “A review on modeling and simulation of building energy systems”, *Renew. Sustain. Energy Rev.*, vol. 56, pp. 1272–1292, 2016.

- [15] Rallapalli, "A comparison of EnergyPlus and eQUEST Whole Building Energy Simulation Results for a Medium Sized Office building", Thesis, 2010.
- [16] M. T. Ke, C. H. Yeh, and J. T. Jian, "Analysis of building energy consumption parameters and energy savings measurement and verification by applying eQUEST software," *Energy Build.*, vol. 61, pp. 100-107, Feb. 2013.
- [17] G. Mustafaraj, D. Marini, A. Costa, and M. Keane, "Model calibration for building energy efficiency simulation," *Appl Energy*, vol. 130, pp. 72-85, 2014.
- [18] J. Zhuang, Y. Chen, and X. Chen, "A new simplified modeling method for model predictive control in a medium-sized commercial building: A case study," *Build Env.*, vol. 127, pp. 1-12, Jul. 2017.
- [19] "Building modeling as a crucial part for building predictive control," *Energy Build*, vol. 56, pp. 8-22, 2013.
- [20] M. Cai, S. Ramdasalli, M. Pipattanasomporn, S. Rahman, A. Malekpour, and S. R. Kothandaraman, "Impact of HVAC Set Point Adjustment on Energy Savings and Peak Load Reductions in Buildings," *IEEE Int Smart Cities Conf ISC2*, pp. 1-6, 2018.
- [21] C. Mehta and A. S. Fung, "A Case Study in Actual Building Performance and Energy Modeling with Real Weather Data," *eSIM*, 2014.
- [22] X. Li and J. Wen, "Review of building energy modeling for control and operation," *Renew Sustain Energy Rev*, vol. 37, pp. 517-537, 2014.
- [23] W. Li, "Modeling urban building energy use: A review of modeling approaches and procedures," *Energy*, vol. 141, pp. 2445-2457, 2017.
- [24] X. Shi, "Magnitude, Causes, and Solutions of the Performance Gap of Buildings: A Review," *Sustainability*, vol. 11, no. 3, p. 937, Feb. 2019.
- [25] P. Shiel, S. Tarantino, and M. Fischer, "Parametric analysis of design stage building energy performance simulation models," *Energy Build*, vol. 172, pp. 78-93, 2018.
- [26] M. Brøgger, P. Bacher, and K. B. Wittchen, "A hybrid modeling method for improving estimates of the average energy-saving potential of a building stock," *Energy Build*, vol. 199, pp. 287-296, 2019.
- [27] C. F. Reinhart and C. C. Davila, "Urban building energy modeling - A review of a nascent field," *Build Env.*, vol. 97, pp. 196-202, 2016.
- [28] T. A. Reddy, "Literature review on calibration of building energy simulation programs: Uses, problems, procedure, uncertainty, and tools," *ASHRAE Trans*, vol. 1, no. 4844, pp. 226-240, 2006.
- [29] I. A. Macdonald, J. A. Clarke, and P. A. Strachan, "Assessing Uncertainties in Building Simulation", in *Proceedings of Building Simulation 1999*, 1999, pp. 1-8.
- [30] D. R. Landsberg, *Measurement of Energy, Demand, and Water Savings*, vol. 2014. 2014.

- [31] M. Royapoor and T. Roskilly, "Building model calibration using energy and environmental data," *Energy Build*, vol. 94, pp. 109-120, 2015.
- [32] Z. Yang and B. Becerik-Gerber, "A model calibration framework for simultaneous multi-level building energy simulation," *Appl Energy*, vol. 149, pp. 415-431, 2015.
- [33] S. Asadi, E. Mostavi, D. Boussaa, and M. Indaganti, "Building energy model calibration using automated optimization-based algorithm," *Energy Build*, vol. 198, pp. 106-114, 2019.
- [34] P. Raftery, M. Keane, and J. O'Donnell, "Calibrating whole building energy models: An evidence-based methodology," *Energy Build*, vol. 43, no. 9, pp. 2356-2364, 2011.
- [35] G. Chaudhary, J. New, J. Sanyal, P. Im, Z. O'Neill, and V. Garg, "Evaluation of 'Autotune' calibration against manual calibration of building energy models," *Appl Energy*, vol. 182, pp. 115-134, 2016.
- [36] Y. Ji and P. Xu, "A bottom-up and procedural calibration method for building energy simulation models based on hourly electricity submetering data," *Energy*, vol. 93, pp. 2337-2350, 2015.
- [37] Y. S. Kim, M. Heidarinejad, M. Dahlhausen, and J. Srebric, "Building energy model calibration with schedules derived from electricity use data," *Appl Energy*, vol. 190, pp. 997-1007, 2017.
- [38] F. Oldewurtel, "Use of model predictive control and weather forecasts for energy efficient building climate control," *Energy Build*, vol. 45, pp. 15-27, 2012.
- [39] F. Ascione, N. Bianco, C. D. Stasio, G. M. Mauro, and G. P. Vanoli, "Simulation-based model predictive control by the multi-objective optimization of building energy performance and thermal comfort," *Energy Build*, vol. 111, pp. 131-144, 2016.
- [40] M. Maasoumy, M. Razmara, M. Shahbakhti, and A. S. Vincentelli, "Handling model uncertainty in model predictive control for energy efficient buildings," *Energy Build*, vol. 77, pp. 377-392, 2014.
- [41] E. Ž. S. Prívarová, Z. Váňa, and J. Cigler, "Building modeling: Selection of the most appropriate model for predictive control," *Energy Build*, vol. 55, pp. 341-350, 2012.
- [42] R. Sangi, A. Kümpel, and D. Müller, "Real-life implementation of a linear model predictive control in a building energy system," *J Build Eng*, vol. 22, no. January, pp. 451-463, 2019.
- [43] D. H. Blum, K. Arendt, L. Rivalin, M. A. Piette, M. Wetter, and C. T. Veje, "Practical factors of envelope model setup and their effects on the performance of model predictive control for building heating, ventilating, and air conditioning systems," *Appl Energy*, vol. 236, no. August 2018, pp. 410-425,

2019.

- [44] M. Killian and M. Kozek, “Ten questions concerning model predictive control for energy efficient buildings,” *Build Env.*, vol. 105, pp. 403-412, 2016.
- [45] Y. Kwak, J. H. Huh, and C. Jang, “Development of a model predictive control framework through real-time building energy management system data,” *Appl Energy*, vol. 155, pp. 1-13, 2015.
- [46] eQUEST – building energy simulation tool, DOE-2.
- [47] L. Sanhudo, “Building information modeling for energy retrofitting – A review,” *Renew Sustain Energy Rev*, vol. 89, no. March, pp. 249-260, 2018.
- [48] Department of Energy, “Demand Response.
- [49] A. R. Jordehi, “Optimisation of demand response in electric power systems, a review,” *Renew. Sustain. Energy Rev.*, vol. 103, pp. 308–319, Apr. 2019, doi: 10.1016/j.rser.2018.12.054.
- [50] S. Mohajeryami, P. Schwarz, and P. T. Baboli, “Including the behavioral aspects of customers in demand response model: real time pricing versus peak time rebate”, Charlotte, NC, USA.
- [51] H. Zhong, L. Xie, and Q. Xia, “Coupon incentive-based demand response: Theory and case study,” *IEEE Trans Power Syst*, vol. 28, no. 2, pp. 1266-1276, May 2013.
- [52] Z. Luo, S. Hong, and Y. Ding, “A data mining-driven incentive-based demand response scheme for a virtual power plant,” *Appl. Energy*, vol. 239, pp. 549–559, Apr. 2019, doi: 10.1016/j.apenergy.2019.01.142.
- [53] S. Davarzani, R. Granell, G. A. Taylor, and I. Pisica, “Implementation of a novel multi-agent system for demand response management in low-voltage distribution networks,” *Appl Energy*, vol. 253, no. July, p. 113516, 2019, doi: 10.1016/j.apenergy.2019.113516.
- [54] B. Chai, J. Chen, Z. Yang, and Y. Zhang, “Demand response management with multiple utility companies: A two-level game approach,” *IEEE Trans Smart Grid*, vol. 5, no. 2, pp. 722-731, Mar. 2014.
- [55] P. Huang, C. Fan, X. Zhang, and J. Wang, “A hierarchical coordinated demand response control for buildings with improved performances at building group,” *Appl. Energy*, vol. 242, pp. 684–694, May 2019, doi: 10.1016/j.apenergy.2019.03.148.
- [56] S. Werminski, M. Jarnut, G. Benysek, and J. Bojarski, “Demand side management using DADR automation in the peak load reduction,” *Renew. Sustain. Energy Rev.*, vol. 67, pp. 998–1007, Jan. 2017, doi: 10.1016/j.rser.2016.09.049.
- [57] S. Li, W. Zhang, J. Lian, and K. Kalsi, “Market-based coordination of thermostatically controlled loads – Part 1: A mechanism design formulation”, *IEEE Trans Power Syst.*, vol. 31, no. ue 2, pp. 1170-1178, Mar. 2016.

- [58] S. Li, W. Zhang, J. Lian, and K. Kalsi, "Market-based coordination of thermostatically controlled loads – Part 2: unknown parameters and case studies", *IEEE Trans Power Syst.*, vol. 31, no. ue 2, pp. 1179-1187, Mar. 2016.
- [59] N. E. W. S. "The Number of homes with smart thermostats grew rapidly in 2015".
- [60] C. L., "2018 roundup of internet of things forecasts and market estimates". 2018.
- [61] R. Plus, "Smart Thermostat Market 2018: Company Profiles, Segments, Landscape, Industry Growth and Demand by Forecast to 2022", November, 2018, [Online]. Available: <https://www.reuters.com/brandfeatures/venture-capital/article?id=61700>.
- [62] W. Mai and C. Y. Chung, "Economic MPC of aggregating commercial buildings for providing flexible power reserve", *IEEE Trans. Power Syst.*, vol. 30, no. ue 5, pp. 2685-2694, Sep. 2015.
- [63] M. Hu and F. Xiao, "Investigation of the Demand Response Potentials of Residential Air Conditioners Using Grey-box Room Thermal Model," *Energy Procedia*, vol. 105, pp. 2759-2765, 2017, doi: 10.1016/j.egypro.2017.03.594.
- [64] M. Dastbaz, C. Gorse, and A. Moncaster, *Building information modeling, building performance, design and smart construction*. Springer International Publishing, 2017.
- [65] M. P. Fanti, A. M. Mangini, and M. Roccotelli, "A simulation and control model for building energy management," *Control Eng Pr.*, vol. 72, pp. 192-205, Mar. 2017.
- [66] S. Tang and Y. Xu, "Distributed control of multi-zone commercial buildings for demand response," in *Proc, IEEE Conf. on Energy Internet and Energy Integration*, 2017.
- [67] M. Sullivan, J. Bode, B. Kellow, S. Woehleke, and J. Eto, "Using residential AC load control in grid operations: PG&E's ancillary service pilot," *IEEE Trans Smart Grid*, vol. 4, no. 2, pp. 1162-1170, Jun. 2013.
- [68] A. Rodler, S. Guernouti, M. Musy, and J. Bouyer, "Thermal behaviour of a building in its environment: Modeling, experimentation, and comparison," *Energy Build*, vol. 168, pp. 19-34, 2018.
- [69] B. Morille, N. Lauzet, and M. Musy, "SOLENE-microclimate: A tool to evaluate envelopes efficiency on energy consumption at district scale," *Energy Procedia*, vol. 78, pp. 1165-1170, 2015.
- [70] T. Alves, L. Machado, R. G. DeSouza, and P. DeWilde, "Assessing the energy saving potential of an existing high-rise office building stock", *Energy Build.*, vol. 173, pp. 547-561, Jun. 2018.
- [71] R. Kamal, F. Moloney, C. Wickramaratne, A. Narasimhan, and D. Y. Goswami, "Strategic control and cost optimization of thermal energy storage in

- buildings using EnergyPlus,” *Appl Energy*, vol. 246, no. August 2018, pp. 77-90, 2019.
- [72] G. Reynders, R. A. Lopes, A. Marszal-Pomianowska, D. Aelenei, J. Martins, and D. Saelens, “Energy flexible buildings: An evaluation of definitions and quantification methodologies applied to thermal storage”, *Energy Build.* Feb, vol. 166, pp. 372–390, 2018.
- [73] R. Yin et al., “Quantifying flexibility of commercial and residential loads for demand response using setpoint changes”, *Appl. Energy*, vol. 177, pp. 149–164, May 2016.
- [74] M. Luzzi, M. Vaccarini, and M. Lemma, “A tuning methodology of Model Predictive Control design for energy efficient building thermal control,” *J Build Eng*, vol. 21, pp. 28-36, Mar. 2018.
- [75] M. Maasoumy and A. Sangiovanni-Vincentelli, “Total and peak energy consumption minimization of building hvac systems using model predictive control,” *IEEE Test Comput*, vol. 29, no. 4, pp. 26-35, 2012.
- [76] M. F. Haniff, H. Selamat, R. Yusof, S. Buyamin, and F. S. Ismail, “Review of HVAC scheduling techniques for buildings towards energy-efficient and cost-effective operations”, *Renew. Sustain. Energy Rev.*, vol. 27, pp. 94–103, Nov. 2013.
- [77] F. Sehar, M. Pipattanasomporn, and S. Rahman, “A peak-load reduction computing tool sensitive to commercial building environmental preferences,” *Appl Energy*, vol. 161, pp. 279-289, 2016.
- [78] Y. Zhang and G. Augenbroe, “Optimal demand charge reduction for commercial buildings through a combination of efficiency and flexibility measures,” *Appl Energy*, vol. 221, no. April, pp. 180-194, 2018, doi: 10.1016/j.apenergy.2018.03.150.
- [79] Z. Liang, D. Bian, X. Zhang, D. Shi, R. Diao, and Z. Wang, “Optimal energy management for commercial buildings considering comprehensive comfort levels in a retail electricity market,” *Appl Energy*, vol. 236, no. August 2018, pp. 916-926, 2019, doi: 10.1016/j.apenergy.2018.12.048.
- [80] R. Tang, H. Li, and S. Wang, “A game theory-based decentralized control strategy for power demand management of building cluster using thermal mass and energy storage,” *Appl Energy*, vol. 242, no. March, pp. 809-820, 2019, doi: 10.1016/j.apenergy.2019.03.152.
- [81] M. Saffari, “Optimized demand side management (DSM) of peak electricity demand by coupling low temperature thermal energy storage (TES) and solar PV,” *Appl. Energy*, p. 13, 2018.
- [82] L. C. Hau, Y. S. Lim, and S. M. S. Liew, “A novel spontaneous self-adjusting controller of energy storage system for maximum demand reductions under penetration of photovoltaic system,” *Appl Energy*, vol. 260, no.

- November 2019, p. 114294, 2020, doi: 10.1016/j.apenergy.2019.114294.
- [83] I. E. S. Standard, *Energy Savings Analysis: ANSI/ASHRAE/IES Standard 90.1-2016*. 2017.
- [84] R. Chedwal, J. Mathur, G. D. Agarwal, and S. Dhaka, “Energy saving potential through Energy Conservation building code and advance energy efficiency measures in hotel buildings of Jaipur City, India”, *Energy Build.*, vol. 92, pp. 282-295, Feb. 2015.
- [85] K. Sun and T. Hong, “A framework for quantifying the impact of occupant behavior on energy savings of energy conservation measures,” *Energy Build*, vol. 146, pp. 383-396, 2017.
- [86] K. Sun and T. Hong, “A simulation approach to estimate energy savings potential of occupant behavior measures,” *Energy Build*, vol. 136, pp. 43-62, 2017.
- [87] T. Hoyt, E. Arens, and H. Zhang, “Extending air temperature setpoints: Simulated energy savings and design considerations for new and retrofit buildings”, *Build. Environ.*, vol. 88, pp. 89–96, Jun. 2015.
- [88] G. Ali, K. Zhang, K. Dutta, Z. Yang, and B. G. Burcin, “Energy savings from temperature setpoints and deadband: Quantifying the influence of building and system properties on savings”, *Appl. Energy Mar*, vol. 165, pp. 930–942, 2016.
- [89] I. Öhrlund, M. Schultzberg, and C. Bartusch, “Identifying and estimating the effects of a mandatory billing demand charge,” *Appl Energy*, vol. 237, no. January, pp. 885-895, 2019, doi: 10.1016/j.apenergy.2019.01.028.
- [90] L. Xu, S. Wang, and F. Xiao, “An adaptive optimal monthly peak building demand limiting strategy considering load uncertainty,” *Appl Energy*, vol. 253, no. January, p. 113582, 2019, doi: 10.1016/j.apenergy.2019.113582.
- [91] A. Malik, N. Haghdadi, I. MacGill, and J. Ravishankar, “Appliance level data analysis of summer demand reduction potential from residential air conditioner control,” *Appl. Energy*, vol. 235, pp. 776–785, Feb. 2019, doi: 10.1016/j.apenergy.2018.11.010.
- [92] C. J. Meinrenken and A. Mehmani, “Concurrent optimization of thermal and electric storage in commercial buildings to reduce operating cost and demand peaks under time-of-use tariffs,” *Appl Energy*, vol. 254, no. July, p. 113630, 2019, doi: 10.1016/j.apenergy.2019.113630.
- [93] H. Tanaka, S. Tsukao, D. Yamashita, T. Niimura, and R. Yokoyama, “Multiple Criteria Assessment of Substation Conditions by Pair-Wise Comparison of Analytic Hierarchy Process,” *IEEE Trans. Power Deliv.*, vol. 25, no. 4, pp. 3017–3023, Oct. 2010, doi: 10.1109/TPWRD.2010.2048437.
- [94] D. P. Bernardon, M. Sperandio, V. J. Garcia, L. N. Canha, A. da R. Abaide, and E. F. B. Daza, “AHP Decision-Making Algorithm to Allocate Remotely

- Controlled Switches in Distribution Networks,” IEEE Trans. Power Deliv., vol. 26, no. 3, pp. 1884–1892, Jul. 2011, doi: 10.1109/TPWRD.2011.2119498.
- [95] B. Lee, K. M. Kim, and Y. Goh, “Unified power quality index using ideal AHP,” in ICHQP 2008 13th Int. Conf. Harmon. Qual. Power, 2008, pp. 4-8,
- [96] S. Fattahi, S. Afsharnia, and M. H. Javidi, “A new AHP-Based reactive power valuation method,” in 2008 IEEE Canada Electric Power Conference, Vancouver, BC, Canada, Oct. 2008, pp. 1–7, doi: 10.1109/EPC.2008.4763359.
- [97] D. Bian, M. Pipattanasomporn, and S. Rahman, “A human expert-based approach to electrical peak demand management,” IEEE Trans Power Deliv, vol. 30, no. 3, pp. 1119-1127, 2015, doi: 10.1109/TPWRD.2014.2348495.
- [98] S. Shao, M. Pipattanasomporn, and S. Rahman, “An approach for demand response to alleviate power system stress conditions,” in 2011 IEEE Power and Energy Society General Meeting, Detroit, MI, USA, 2011, pp. 1-7, doi: 10.1109/PES.2011.6039852.
- [99] W. Underground, “Weather Underground.”  
<https://www.wunderground.com/>.
- [100] X. Zhou and T. Hong, “Comparison of Building Energy Modeling Programs: HVAC Systems,” LBNL, Aug. 2013. [Online]. Available: <https://www.osti.gov/servlets/purl/1165199>.
- [101] “DOE2.3 Dictionary,” vol. 2. Oct. 01, 2018, [Online]. Available: [https://doe2.com/Download/DOE-23/DOE23Vol2-Dictionary\\_50h.pdf](https://doe2.com/Download/DOE-23/DOE23Vol2-Dictionary_50h.pdf).
- [102] P. Sreedharan and P. Haves, “Comparison of Chiller Models for Use in Model-Based Fault Detection,” presented at the International Conference for Enhanced Building Operations, Austin, TX, Jul. 2001, [Online]. Available: <https://www.osti.gov/servlets/purl/829977>.
- [103] M. Hydeman, “Tools and Techniques to Calibrate Electric Chiller Component Models,” presented at the ASHRAE Conference, 2002, [Online]. Available: [http://www.taylor-engineering.com/wp-content/uploads/2020/04/ASHRAE\\_Symposium\\_AC-02-9-1\\_Electric\\_Chiller\\_Model.pdf](http://www.taylor-engineering.com/wp-content/uploads/2020/04/ASHRAE_Symposium_AC-02-9-1_Electric_Chiller_Model.pdf).
- [104] “2013 Building Energy Efficiency Standards - Reference Ace,” in Title 24, 2013.
- [105] D. of E. United States, “Commercial Reference Buildings.”  
<https://www.energy.gov/eere/buildings/commercial-reference-buildings>  
(accessed Apr. 24, 2021).
- [106] Z. Syafii, D. Juliandri, and Y. Akbar, “Design of PV System for Electricity Peak-Shaving: A Case Study of Faculty of Engineering, Andalas University,” in 2018 International Conference on Computing, Power and Communication Technologies (GUCON), Greater Noida, Uttar Pradesh, India, 2018, pp. 294-298, doi: 10.1109/GUCON.2018.8675096.

- [107] S. Park and W. Park, "CES peak demand shaving with energy storage system," in 2017 International Conference on Information and Communication Technology Convergence (ICTC), Jeju, 2017, pp. 1124-1126, doi: 10.1109/ICTC.2017.8190874.
- [108] T. Mao, Q. Xu, B. Zhou, R. Zhang, and J. Wang, "A Load-based Mechanism Supporting Peak Shaving for Energy Storage (ES): an Adaptive Method," in 2019 IEEE Sustainable Power and Energy Conference (iSPEC, Beijing, China, 2019, pp. 1648-1652, doi: 10.1109/iSPEC48194.2019.8975283.
- [109] K. Ananda-Rao, R. Ali, S. Tanisellam, and N. H. Baharudin, "Microcontroller based battery controller for peak shaving integrated with Solar Photovoltaic," in 4th IET Clean Energy and Technology Conference (CEAT 2016, 2016, pp. 1-6, doi: 10.1049/cp.2016.1262.
- [110] K. Mahmud, S. Morsalin, Y. R. Kafle, and G. E. Town, "Improved peak shaving in grid-connected domestic power systems combining photovoltaic generation, battery storage, and V2G-capable electric vehicle," in 2016 IEEE International Conference on Power System Technology (POWERCON, Wollongong, NSW, 2016, pp. 1-4, doi: 10.1109/POWERCON.2016.7753990.
- [111] "Smart Thermostat Market by Type, Application, and End Use: Global Opportunity Analysis and Industry Forecast, 2019-2026", Report Linker, [Online]. [Online]. Available: [https://www.reportlinker.com/p05844101/Smart-Thermostat-Market-by-Type-Application-and-End-Use-Global-Opportunity-Analysis-and-Industry-Forecast.html?utm\\_source=GNW](https://www.reportlinker.com/p05844101/Smart-Thermostat-Market-by-Type-Application-and-End-Use-Global-Opportunity-Analysis-and-Industry-Forecast.html?utm_source=GNW).
- [112] Y. Zhang and N. Lu, "Demand-side management of air conditioning cooling loads for intra-hour load balancing," in 2013 IEEE PES Innovative Smart Grid Technologies Conference (ISGT, Washington, DC, 2013, pp. 1-6, doi: 10.1109/ISGT.2013.6497905.
- [113] B. Sivaneasan, K. Thachinamoorthi, and K. P. Goh, "Interruptible load scheme: Demand response management for buildings," in 2016 IEEE Region 10 Conference (TENCON, Singapore, 2016, pp. 1716-1719, doi: 10.1109/TENCON.2016.7848311.
- [114] D. Ardiyanto, M. Pipattanasomporn, S. Rahman, N. Hariyanto, and Suwarno, "Occupant-based HVAC Set Point Interventions for Energy Savings in Buildings," in 2018 International Conference and Utility Exhibition on Green Energy for Sustainable Development (ICUE, Phuket, Thailand, 2018, pp. 1-6, doi: 10.23919/ICUE-GESD.2018.8635595.
- [115] D. Pamungkas, M. Pipattanasomporn, S. Rahman, N. Hariyanto, and Suwarno, "Impacts of Solar PV, Battery Storage and HVAC Set Point Adjustments on Energy Savings and Peak Demand Reduction Potentials in Buildings," in 2018 International Conference and Utility Exhibition on Green Energy for Sustainable Development (ICUE, Phuket, Thailand, 2018, pp. 1-8,

doi: 10.23919/ICUE-GESD.2018.8635736.

- [116] D. Cheng, W. Zhang, and M. Liu, "Modeling and Control of Central Air Conditioning Loads for Peak Shaving," in 2019 IEEE PES Asia-Pacific Power and Energy Engineering Conference (APPEEC), Macao, Macao, 2019, pp. 1-5, doi: 10.1109/APPEEC45492.2019.8994566.
- [117] S. T. L, Analytical hierarchy process: Planning, priority setting, resource allocation". New York: McGraw-Hill International Book Co, 1980.
- [118] "AHP Priority Calculator", 2020. <https://bpmsg.com/ahp/ahp-calc.php>.
- [119] "Markets and Operations – Demand Response", PJM, 2020.
- [120] S. Ramdasalli, M. Pipattanasomporn, M. Kuzlu and S. Rahman, "Transactive control for efficient operation of commercial buildings," 2016 IEEE PES Innovative Smart Grid Technologies Conference Europe (ISGT-Europe), 2016, pp. 1-5, doi: 10.1109/ISGTEurope.2016.7856173.